



BURIAL DIAGENESIS AND MISSISSIPPI VALLEY-TYPE
MINERALIZATION IN THE UPPER DEVONIAN REEF
COMPLEXES OF THE LENNARD SHELF,
CANNING BASIN, WESTERN AUSTRALIA.

ANDREW M^CMANUS

JULY, 1991

This thesis is submitted as a partial fulfilment of the requirements of the Master of Science (Petroleum Geology and Geophysics) Degree at the National Centre for Petroleum Geology and Geophysics, University of Adelaide.

To the best of this author's belief, this thesis contains no material which has been accepted for the award of any other degree or diploma in any University, and contains no material previously published or written by another person, except where due reference is made in the text of this thesis.

Andrew McManus

The author consents to the thesis being made available for photocopying and loan if applicable if accepted for the award of the degree.

ACKNOWLEDGEMENTS

I wish to express my gratitude to the following people for their assistance and encouragement over the last two years;

Firstly, to Dr Malcolm Wallace who instigated this research project and provided continuous encouragement and support. Malcolm always made himself available to discuss ideas and it was due to his enthusiasm that this project was a success.

Billiton Australia Ltd. for sponsoring this project and providing field support and airfares, as well as accommodation whilst in Perth. I would especially like to thank Rick Berg and Mike Clifford for their assistance during field trips and for the great interest they took in this project.

Dr Phil Playford for his advice and review of this thesis.

The staff at the NCPGG for their support and encouragement; Dr John Warren (for his assistance as supervisor), Dr Bill Stuart (for organising financial assistance) and Dr Nick Lemon.

The technical staff of the Geology Department at Adelaide University; Dr Keith Turnbull (isotope analysis), Wayne Mussared (fluid inclusions), and Geoff Trevelyan (thin sections).

My fellow students at the NCPGG (especially Eamonn, Coxy and Bruce), who helped make my time in Adelaide an enjoyable experience.

Finally, but most importantly, I would like to thank my family, to whom I dedicate this thesis. Without their unfailing support and their belief in me I would not have achieved as much as I have.

ABSTRACT

Mississippi Valley-type (MVT) lead/zinc mineralization has been discovered within the Late Devonian reef complexes of the Lennard Shelf, in the northern part of the Canning Basin. MVT deposits are carbonate hosted lead/zinc deposits formed from brines at temperatures of 80 to 120°C. A basin brine model is proposed for their development.

Cathodoluminescence (CL) was used to determine the cement stratigraphy of the burial cements. The generalised calcite cementation sequence from non-luminescent, bright-luminescent to dull-luminescent, represents a progression from oxidizing to reducing conditions for the carbonate pore fluids. This sequence represents cementation during Late Devonian- Early Carboniferous burial of the reef complexes. The mineralization event occurs within the bright-luminescent cement zone.

A regional dolomitization event occurred after the non-luminescent calcite cement zone. This dolomite is a burial dolomite and created secondary moldic and intercrystalline porosity. Saddle dolomites occur as pore filling cements and post-date mineralization. The saddle dolomite is closely associated with the mineralization event.

The MVT mineralization on the Lennard Shelf was formed during the early burial of the reef complexes (latest Devonian or Early Carboniferous). This period corresponds to rapid subsidence in the nearby Fitzroy Trough. Hot brines, driven by sediment compaction, migrated along aquifers into porous zones within the carbonates on the Lennard Shelf. Fracture porosity was generated by the mineralizing fluids and dissolution of the host carbonates also enhanced porosity. Fluid inclusions indicate temperatures of 90°C for pore fluids at the time of sulphide precipitation. The carbonates contain progressively more radiogenic strontium with younger generations, further supporting an evolving basinal derived fluid. The availability of reduced sulphur appears to be important to the formation of the MVT deposits.

TABLE OF CONTENTS

	<u>Page No.</u>
<u>INTRODUCTION</u>	1
Geological History of the Northern Canning Basin	2
Depositional Model	4
Previous Diagenetic Studies	7
Mississippi Valley-Type Deposits	11
MVT Deposits of the Canning Basin	14
Scope of this Study	18
<u>LABORATORY METHODS</u>	23
Staining and Cathodoluminescence	23
Isotopes	23
Fluid Inclusions	25
Microprobe	26
<u>CALCITE CEMENTS</u>	27
Marine Diagenesis	27
Burial Diagenesis	31
1) Non-luminescent cement zone	32
2) Bright-luminescent cement zone	36
3) Dull-luminescent cement zone	39
4) Late bright-luminescent cement zone	41
5) Late brightly banded-luminescent cement zone	42
6) Late ferroan dull-luminescent cement zone	44
<u>ORIGIN OF CLEAR EQUANT CALCITE CEMENTS</u>	46
Non-luminescent calcite	46
Bright-luminescent calcite	52
Dull-luminescent calcite	54
Late bright-luminescent cement	55
Late brightly banded-luminescent cement	56
Late ferroan dull-luminescent cement	56
<u>DOLOMITIZATION, MINERALIZATION AND KARSTIFICATION</u>	58
Dolomites	58
Synsedimentary dolomite	58
Regional dolomite	58
Saddle dolomite	64
Mineralization	68
Pyrite	70
Sphalerite	71
Galena	72
Marcasite	73
Possible barite pseudomorphs	74
Paragenesis of mineralization relative to host-carbonate diagenesis	74
Karstification and subaerial exposure	77

	<u>Page No.</u>
<u>ORIGIN OF DOLOMITES AND MINERALIZATION</u>	80
Synsedimentary dolomite	80
Regional dolomite	80
Saddle dolomite	85
Mineralization	89
<u>CONCLUSIONS</u>	93
<u>BIBLIOGRAPHY</u>	98
<u>APPENDICES A, B, C, D, and E.</u>	

LIST OF FIGURES

	<u>Page No.</u>
<u>Figure 1.</u> Generalized geological map of the Devonian reef complexes of the northern Canning Basin	2
<u>Figure 2.</u> Facies and subfacies nomenclature of the Devonian reef complexes	4
<u>Figure 3.</u> Generalized geological map of the Geikie Gorge area illustrating the outcropping reef atoll at Fossil Downs Station and Brooking Springs Station	6
<u>Figure 4.</u> Comparison of previous studies of the diagenetic phases and the timing of diagenetic events of the Devonian reef complexes of the Lennard Shelf	9
<u>Figure 5.</u> Distribution of surface samples and mineral exploration drill-holes in the Fossil Downs exploration lease area	20
<u>Figure 6.</u> Generalized geological map of the Horse Spring Range exploration lease	21
<u>Figure 7.</u> Generalized geological map of the northern Canning Basin illustrating the location of exploration leases of Billiton Australia	22
<u>Figure 8.</u> Thin section photomicrographs of marine and clear equant calcite cement generations in plane-polarized light and cathodoluminescence	
<u>Figure 9.</u> Thin section photomicrographs of clear equant calcite cement generations in plane-polarized light and cathodoluminescence	
<u>Figure 10.</u> Thin section photomicrographs of clear equant calcite cement generations in plane-polarized light and cathodoluminescence	
<u>Figure 11.</u> Distribution of pseudosecondary fluid inclusion final melt temperatures for the non-luminescent cement generation	48
<u>Figure 12.</u> Carbon and oxygen isotope results for marine and clear equant calcite cements	49
<u>Figure 13.</u> Strontium and oxygen isotope plot for calcite cements	51
<u>Figure 14.</u> Thin section photomicrographs and core samples illustrating calcite cementation, dolomitization, and mineralization paragenesis	
<u>Figure 15.</u> Thin section photomicrographs illustrating timing of mineralization and sulphide paragenesis	

	<u>Page No.</u>
<u>Figure 16.</u> Thin section photomicrographs and core samples illustrating sulphide paragenesis, Late Famennian ?karst, and ?barite pseudomorphs	
<u>Figure 17.</u> Thin section photomicrographs of sulphide mineralization within calcite cements in other areas of the Lennard Shelf	
<u>Figure 18.</u> Carbon and oxygen isotope compositions of regional dolomite, saddle dolomite and synsedimentary dolomite	81
<u>Figure 19.</u> Distribution of carbon isotope values of regional dolomites	83
<u>Figure 20.</u> Distribution of oxygen isotope values of regional dolomites	84
<u>Figure 21.</u> Strontium isotopic composition of calcite and dolomite diagenetic phases	87
<u>Figure 22.</u> Strontium and oxygen isotopic compositions of calcite and dolomite diagenetic phases	87
<u>Figure 23.</u> Fluid inclusion homogenization and last melt temperatures from sphalerite and diagenetic phases that are closely associated with sulphide mineralization	88
<u>Figure 24.</u> Sulphur isotope composition of sulphide mineralization from Cadjebut Mine and the Fossil Downs Prospect	91
<u>Figure 25.</u> Comparison of diagenetic studies of the Devonian reef complexes of the Lennard Shelf	94
<u>Figure 26.</u> Burial history of the Lennard Shelf reef complexes, illustrating the timing of the diagenetic phases	95

LIST OF TABLES

	<u>Page No.</u>
<u>Table 1.</u> Carbon and oxygen isotopic compositions of the calcite diagenetic phases	28
<u>Table 2.</u> Microprobe results for calcite cement generations	30
<u>Table 3.</u> Fluid inclusion results of burial calcite cement generations	34
<u>Table 4.</u> Strontium isotopic compositions of the calcite cements	39
<u>Table 5.</u> Summary of geochemical data for calcite cement zones	47
<u>Table 6.</u> Carbon and oxygen isotopic compositions of the synsedimentary, regional, and saddle dolomite generations	61
<u>Table 7.</u> Strontium isotopic values for the regional and saddle dolomite generations	62
<u>Table 8.</u> Homogenization and last melt temperatures of primary fluid inclusions from saddle dolomite and sphalerite	65
<u>Table 9.</u> Microprobe results of two samples of saddle dolomite	67
<u>Table 10.</u> Sulphur isotope compositions of sulphide phases	71

INTRODUCTION



Lead and zinc sulphide mineralization has been identified in the Late Devonian reef complexes on the Lennard Shelf, northern Canning Basin. The mineralization is considered to be of the Mississippi Valley - type (MVT). The approach of cathodoluminescence, fluid inclusion, and geochemical analysis, combined with the already well-defined stratigraphy and geological history of the Lennard Shelf, provides an insight into the timing, temperature, and chemistry of the diagenetic fluids (including Pb-Zn mineralization) that affected the Devonian reef complexes from the time of their deposition to the present.

Billiton Australia (the Metals Division of the Shell Company of Australia Limited) are actively exploring for MVT mineralization on the Lennard Shelf. The main region of interest for this study is centred on Billiton's Fossil Downs exploration license (Figure 1). However, analysis of carbonate samples from other areas on the Lennard Shelf have also been incorporated into this study.

The main objectives of this project were to;

- *Analyse the burial diagenetic history of the reef complexes in the Fossil Downs Station area, including calcite cementation, dolomitization and porosity and permeability evolution.

- *Determine the relationship between the porosity evolution/diagenetic history in the host carbonates and the MVT mineralization.

- *Determine the compositional character of the burial diagenetic phases (including the mineralization event) using cathodoluminescence, carbon, oxygen, sulphur and strontium isotope analysis, fluid inclusion microthermometry and microprobe analysis.

- *Determine the relationship between local and regional burial diagenetic events.

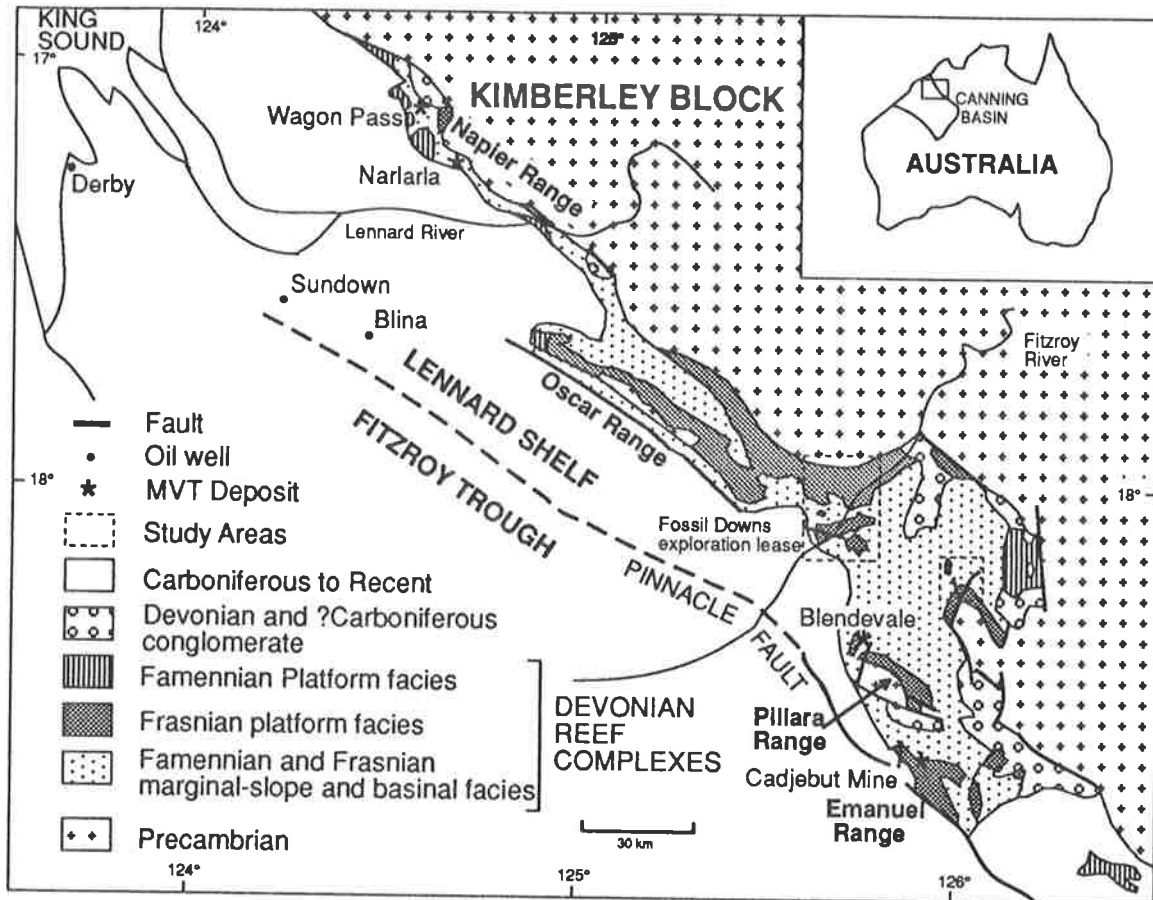


Figure 1.— Generalized geological map of the Devonian reef complexes of the northern Canning Basin (modified from Playford 1984). The dashed areas, indicating the main areas of study, appear in later figures.

Geological History of the Northern Canning Basin.

Regional summaries of the geology and evolution of the Canning Basin have been published by Forman and Wales (1981), Towner and Gibson (1983), Brown *et al.* (1984), and Yeates *et al.* (1984) and these form the basis of the following summary. The Canning Basin, a large (over 400 000 km²) intracratonic basin in the north-west of Australia (Figure 1), was initiated during the Early Ordovician and has accumulated over 10 000 m of Palaeozoic sediments (Brown *et al.* 1984). During the Middle Devonian to Early Carboniferous, tectonic events caused subsidence and development of a large, northwest-trending rift-graben in the north of the basin, known as the Fitzroy Trough (Yeates *et al.* 1984 and Brown *et al.* 1984). North of the Fitzroy Trough, reef complexes developed on the tilted

fault blocks of the Lennard Shelf in the Middle Devonian (Playford and Lowry 1966, Yeates *et al.* 1984 and Brown *et al.* 1984). Interfingering terrigenous conglomerates, derived from the Precambrian Kimberley Block, indicate fault movement continued through the Late Devonian (Playford and Lowry 1966, Yeates *et al.* 1984 and Botten 1984).

Shallow marine clastics and carbonates of the Fairfield Group were deposited over the reef complexes on the Lennard Shelf in the Late Devonian-Early Carboniferous. Rapid subsidence and infill of the Fitzroy Trough, between the Tournaisian and Namurian (Early Carboniferous), resulted in up to 2500 m of sediment deposited with only approximately 5 km of crustal extension (Brown *et al.* 1984). Brown *et al.* (1984) suggested that facies changes within the sediments indicate the existence of a large, northwest prograding delta within the Fitzroy Trough at this time.

The Middle Carboniferous to recent history of the Canning Basin is dominated by the passive margin breakup of Gondwana. Middle to Late Carboniferous uplift and erosion occurred basinwide and resulted in karstification of the Devonian reef complexes on the Lennard Shelf. On the Lennard Shelf, at least 1 kilometre (Forman and Wales 1981) of Late Carboniferous-Early Permian non-marine and marine glacial sediments (Towner and Gibson 1983) of the Grant Group were deposited on this unconformable surface. In the southeast Oscar Range, sandstones of the Grant Group have filled cavities within the Devonian carbonates to depths of 210 m (Hurley 1986).

Basinwide subsidence continued from the Early Permian until the Late Triassic. Uplift and folding during the Late Triassic/Early Jurassic Fitzroy Movement produced another regional unconformity. Although Jurassic and Cretaceous sediments are preserved in the southern portion of the Canning Basin, apatite fission track analysis (Arne *et al.* 1989) infers that the Lennard Shelf has undergone almost continuous erosion since the

Early Jurassic. The reef complexes of the Lennard Shelf have again been exhumed as a result of this erosion, with karstification presently continuing.

Depositional Model.

A barrier-reef system, ranging in age from Givetian through Famennian, developed predominantly as a series of reef-fringed platforms along a landmass of Precambrian metasediments (Kimberley Block) and around islands of Precambrian and Ordovician rocks (Playford 1980). Platforms of several hundreds of square kilometres developed, along with small platform atolls and pinnacle reefs. The reef complexes can be subdivided (Figure 2) into platform facies (consisting of back-reef, reef-flat, and reef-margin subfacies), marginal-slope facies (reefal-slope and fore-reef subfacies), and basinal facies (Playford 1980 and 1984).

Although the reefs grew close to sea-level, the only regression of major significance that has been identified was at the Frasnian-Famennian boundary. The Frasnian-Famennian boundary separates two cycles of platform development; the Givetian-Frasnian Pillara cycle and the Famennian Nullara

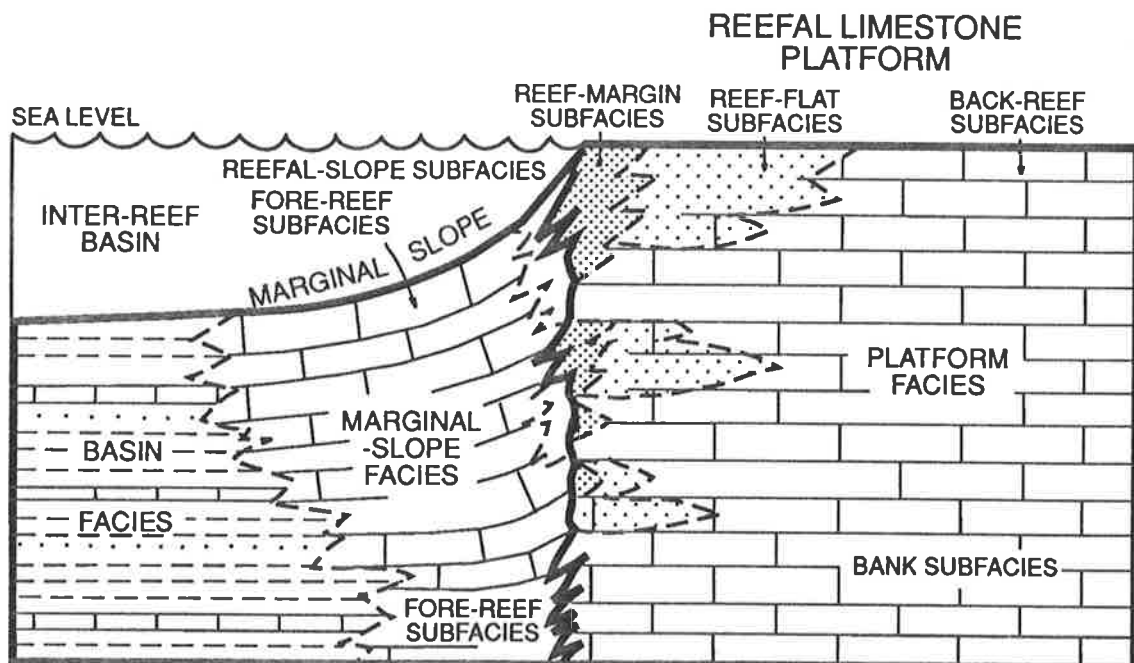


Figure 2.—Facies and subfacies nomenclature of the Devonian reef complexes (from Playford, 1984).

cycle. The regression is marked by a disconformity on the platforms while deposition was continuous in the deeper water marginal-slope and basin facies. The platforms are considered to have been emergent for not more than a few tens of metres above sea-level (Playford 1980; Hurley 1986).

The response of the reefs to the almost continuous relative sea-level rise, resulted in different platform development between the Pillara and Nullara cycles. The Pillara cycle is characterized by vertical platform growth (in response to an increased rate of relative rise in sea-level) followed by episodically abrupt sea-level rises that resulted in drowning of platforms and backstepping of platform margins (Playford *et al.* 1989). In contrast, the Nullara cycle was influenced by slow relative rise in sea-level that resulted in platforms advancing basinward, interfingering and overgrowing marginal-slope deposits.

The carbonates that crop out in the Fossil Downs Station area (Figure 3) represent an eroded section through a Frasnian/Famennian atoll. The Frasnian reef-flat and back-reef subfacies are exposed in the centre of the atoll. The relative fall in sea-level at the Frasnian-Famennian boundary produced erosion of the Frasnian platform margin. Deep water stromatolites colonized the scalloped-shaped eroded margins and the deeper, conformable marginal-slope facies (Wallace 1987). Preserved sections of Frasnian reef-margin subfacies are rare in outcrop in the Fossil Downs atoll. The atoll is surrounded by Famennian marginal-slope facies, although Frasnian marginal-slope facies occur at depth. The Frasnian platform developed with very steep margins. Backstepping of the atoll in the latest Frasnian was followed by an advancing platform during the Famennian. The Late Carboniferous and present day unconformities have eroded the reef platform below the level of the Frasnian-Famennian boundary.

Carbonates that crop out in the Brooking Springs Station area (Figure 3) are part of a large east-northeast trending atoll. This elongate atoll was separated from the main reef-fringed platform (that abuts the

Kimberley Block) by a narrow channel-way east of Sheep Camp Yard (Wallace 1987). The Frasnian platform cropping out in the Brooking Springs Station area displays a similar sequence of facies as that observed in the Fossil Downs atoll. However, in the northern and eastern regions of the atoll, the Frasnian platform margin was not eroded away by the relative sea-level fall at the Frasnian-Famennian boundary and Frasnian marginal-slope facies occur in contact with the Frasnian reef-margin facies.

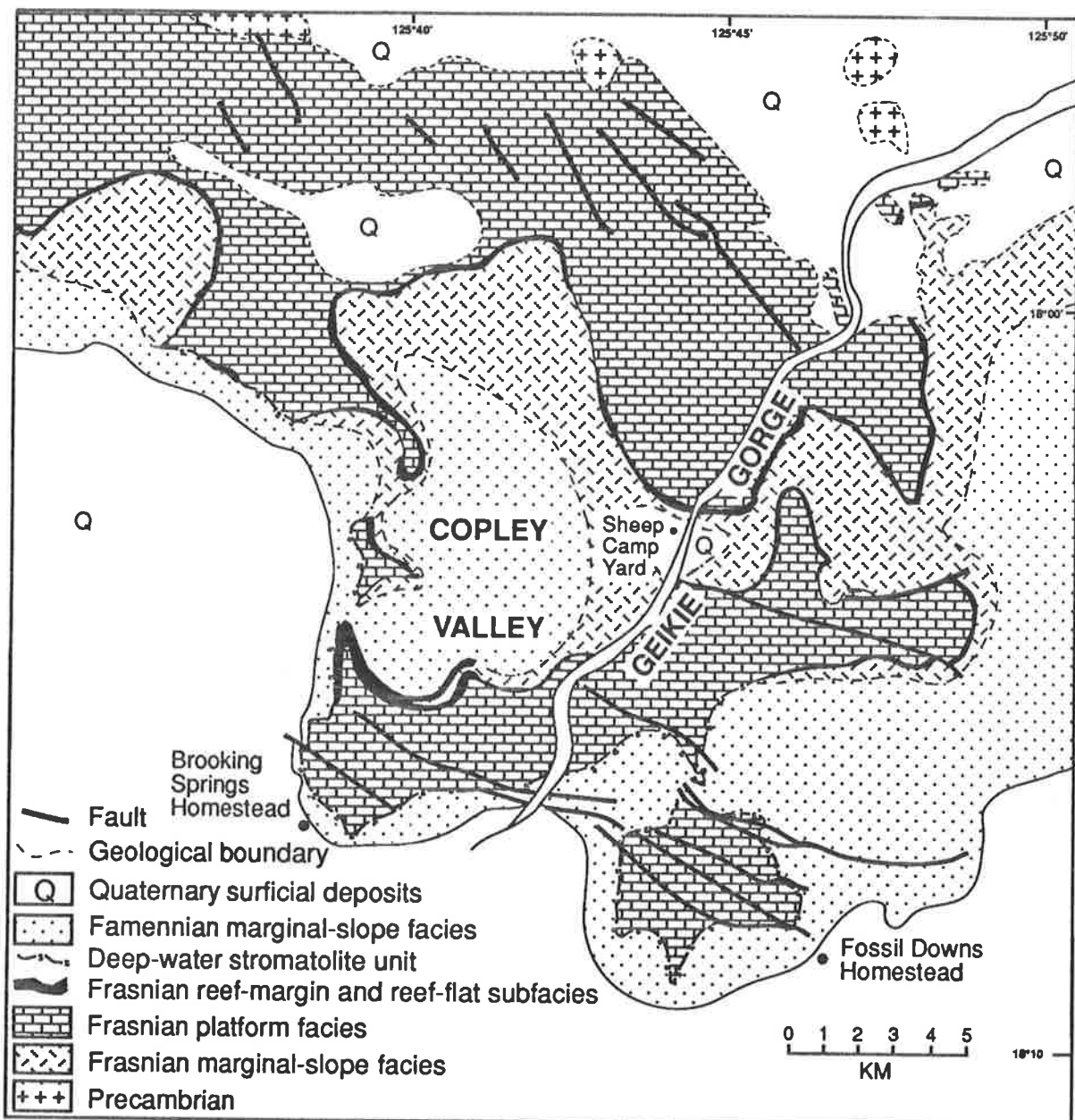


Figure 3.— Generalized geological map of the Geikie Gorge area illustrating the outcropping reef atoll at Fossil Downs Station and Brooking Springs Station (modified from Wallace 1987).

In outcropping carbonates of the northern Geikie Gorge region, the Frasnian back-reef deposits are dolomitized in part and composed of peloid, ooid and oncoid grainstone, skeletal wackestones, and lime mudstones (Wallace *et al.* in press). These well-bedded deposits grade into a narrow zone of thickly bedded fenestral peloidal or ooid grainstones of the reef-flat subfacies (Wallace *et al.* in press). Similar lithologies are encountered in drill-cores and outcrop of the Frasnian platform sequences in the Brooking Springs Station and Fossil Downs Station areas. However, in the Fossil Downs area, dolomite within the platform sequence is less common. Reef-margin subfacies consist of massive cyanobacterial-stomatopoid framestones that are strongly marine cemented. Early submarine cementation of the platform margin and reefal-slope helped produce steep margins on Frasnian and Famennian platforms (Playford 1980; Kerans *et al.* 1986).

Reefal-slope facies are composed of sponge bindstones and stromatactis structures and have depositional dips ranging from 30° to near vertical (Playford 1980; Wallace *et al.* in press). The reefal-slope subfacies interfingers down-dip with the well-bedded fore-reef subfacies. The fore-reef subfacies consist of peloidal grainstones and sedimentary breccias, with dips of up to 35°. Basinal deposits of calcareous shales and marls have been preferentially eroded and are poorly exposed.

Previous Diagenetic Studies.

The first regional petrographic and diagenetic analysis of the Devonian reef complexes in the Canning Basin was published by Kerans (1985). Apart from the depositional aspects of this study, Kerans also concentrated on the syndepositional through burial diagenetic history of the reefs and the associated porosity evolution. Using stratigraphic information, staining, cathodoluminescence, stable isotopes and petrographic techniques, Kerans

detailed nine major cement types, produced in four diagenetic environments. The three main diagenetic environments were marine, marine-burial, and burial. The fourth diagenetic environment, associated with later uplift and erosion during the Late Carboniferous, was confined to the section immediately below the resulting unconformity. The marine diagenetic environment includes micritic, microcrystalline, radiaxial, epitaxial and syntaxial cements. Kerans considered the scalenohedral cement to be transitional from marine to marine-burial. Marine-burial cements also included bladed cements and Frasnian non-ferroan (non-luminescent to banded-luminescent) blocky cements. Famennian non-ferroan (non-luminescent to banded-luminescent) blocky cements, dolomite and ferroan (homogenous-luminescent) blocky cements were considered to be of Late Devonian/Early Carboniferous burial origin. Poikilitic cements were related to Late Devonian/Early Carboniferous burial and karst processes along the Late Carboniferous unconformity. Kerans, in agreement with Playford (1980 and 1984), considered early cementation in the marine diagenetic environment to be the single most important diagenetic event in the diagenetic history of the reef complexes (Kerans *et al.* 1986).

The regional diagenetic and petrographic study by Kerans (1985) laid the foundation for more detailed diagenetic studies of the reef complexes of the Canning Basin. Two more recent studies, Hurley (1986) and Wallace (1987) concentrated on geographically more localized areas, the Oscar Range and Geikie Gorge respectively. These localized studies included detailed mapping, examination of the sedimentology and stratigraphy as well as analysis of the diagenetic history of the areas. Figure 4 provides a summary and comparison of previous studies on the timing of diagenetic phases of the reef complexes of the Lennard Shelf.

In the diagenetic analysis of the Oscar Range, Hurley (1986) and Hurley and Lohmann (1989) concentrated on five of the nine major cement types

recognized by Kerans (1985). These included: (1) microcrystalline calcite, (2) radial fibrous calcite, (3) scalenohedral calcite, (4) blocky calcite, and (5) poikilitic calcite. They concluded that the first three cement types were marine and the third cement type (scalenohedral calcite) extends into the marine-burial environment. These conclusions were in agreement with Kerans (1985). Hurley and Lohmann proposed a Late Devonian marine/eogenetic signature of $\delta^{18}\text{O} = -4.5 (\pm 0.5)\text{‰}$ (PDB) and $\delta^{13}\text{C} = +2.0 (\pm 0.5)\text{‰}$ (PDB) based on isotopic analyses of marine biota and these marine cements. This marine/eogenetic signature provides a reference point to compare isotopic results from later diagenetic phases.

DIAGENETIC ENVIRONMENT		Kerans (1985)	Hurley (1986) and Hurley and Lohmann (1989)	Wallace (1987) and Wallace <i>et al.</i> (in press)
MARINE-BURIAL	DEVONIAN	Scalenohedral and bladed (Non-luminescent)	Scalenohedral calcite	Scalenohedral calcite
		Dolomite	Non-ferroan blocky calcite (Banded bright luminescent)	Non-luminescent calcite
BURIAL	CARBONIFEROUS	(Frasnian carbonates) Non-ferroan blocky calcite (Non-luminescent to banded-luminescent)	Dolomite	Pressure solution
		(Famennian carbonates)	Pressure solution Non-ferroan blocky calcite (Non-luminescent)	Bright-luminescent calcite
UPLIFT-RELATED	PERMIAN	Ferroan blocky spar (Homogenous luminescence)	Non-ferroan blocky calcite (Moderate luminescent)	Dolomite
		Non-ferroan poikilitic calcite (Irregular, largely non-luminescent)	Dedolomite, poikilitic calcite	Dull-luminescent calcite
BURIAL	PERMIAN		Sinkholes Calcrete crusts Vertical solution tubes	Banded-luminescent calcite
			Pressure solution Non-ferroan blocky calcite (Bright or moderate luminescent)	Karstification
		Ferroan blocky calcite (Dull or non-luminescent)		Late dull-luminescent calcite
				Pressure solution

Figure 4. — Comparison of previous studies of the diagenetic phases and the timing of diagenetic events of the Devonian reef complexes of the Lennard Shelf.

The diagenetic history proposed by Hurley and Lohmann (1989) for the Oscar Range region incorporates six diagenetic events, of which Diagenetic Events II to VI are represented by blocky calcite cements and are distinguished by cathodoluminescence and carbon and oxygen isotopes. These diagenetic events from oldest to youngest include;

*Diagenetic Event I:—microcrystalline, radiaxial fibrous, and scalenohedral cements. These cements precipitated in the marine diagenetic environment and can generally be distinguished using transmitted light.

*Diagenetic Event II:—banded-luminescent, non-ferroan blocky calcite cements precipitated in marine-burial or meteoric-phreatic environment. Hurley and Lohmann considered the burial depths of several hundred metres required to explain the isotopic composition of these banded-luminescent cements, to be inconsistent with changing redox conditions of the pore waters from which they precipitated. However they agreed with Kerans (1985) in that there is a *lack of* evidence of prolonged exposure of the reefs to meteoric fluids.

*Diagenetic Event III:—non-luminescent, non-ferroan blocky calcite cements of Late Devonian/Early Carboniferous burial origin. The equivalent blocky calcite cements of Kerans (1985) were homogenous, dull-luminescent and ferroan.

*Diagenetic Event IV:—non-ferroan, irregularly banded, moderately luminescing blocky calcites represent uplift associated with the Late Carboniferous unconformity (equivalent to the poikilitic cements of Kerans 1985).

*Diagenetic Events V and VI:—bright-luminescent blocky calcite cements and ferroan dull- to non-luminescent blocky calcite cements precipitated in response to Late Carboniferous through Permian burial processes. Equivalent cements for these diagenetic events were not recorded by Kerans (1985).

Wallace (1987) examined and mapped in detail the sedimentology and stratigraphy of the Geikie Gorge region. Additionally, Wallace (1987) and Wallace *et al.* (in press) concentrated on the burial diagenetic history of the reef complexes of the Geikie Gorge area. The burial diagenetic events included clear equant (blocky) calcite cementation, pressure solution and dolomitization. With the aid of cathodoluminescence petrography, staining, and carbon and oxygen isotope analysis, Wallace (1987) and Wallace *et al.* (in press) described five major zones in the clear equant calcite cements. These included from oldest to youngest;

- 1) Non-luminescent calcite cement.
- 2) Bright-luminescent calcite cement.
- 3) Dull-luminescent calcite cement.
- 4) Late brightly banded-luminescent calcite cement.
- 5) Late dull-luminescent (ferroan) calcite cement.

The non-luminescent, bright-luminescent to dull-luminescent cements were considered to have formed during Late Devonian/Early Carboniferous burial of the reef complexes. During this Late Devonian/Early Carboniferous burial, almost all primary porosity was destroyed by these calcite cements. Wallace also provided evidence for the timing of burial dolomitization occurring between the non-luminescent and bright-luminescent calcite cement zones. The timing and sequence of these diagenetic events identified in the Geikie Gorge region are consistent with the events described by Kerans (1985) and are partially consistent with the diagenetic history of the Oscar Range (Hurley and Lohmann 1989).

Mississippi Valley - Type Deposits.

Mississippi Valley - type (MVT) deposits are the main source of lead and zinc mined in the United States of America. Individual deposits may not have large reserves, however districts commonly consist a number of deposits with

combined lead and zinc ore tonnage comparable to that of the McArthur River and Mt. Isa orebodies. Some of the distinctive features of MVT deposits include:

- * They are epigenetic, carbonate-hosted Pb-Zn sulphide deposits (Anderson 1978; Barnes 1983; Sverjensky 1986). Although there has been some support for syngeneses and consequent redistribution during diagenesis for some of the European deposits, Brown (1970) considers there is much more evidence to contradict the syngenetic-diagenetic model than there is in support of it.

- * They are generally tectonically little disturbed (although some districts occur in tectonically active areas) and occur towards the basin margins or above basement highs within basins (Heyl 1967; Anderson 1978).

- * Ore occurs predominantly as open-space filling rather than by replacement (Sangster 1983; Sangster 1988). Ore emplacement is often within solution collapse breccias (Sangster 1988; Ohle 1985).

- * An unconformity or disconformity surface is associated with all major MVT districts. In most cases this surface occurs immediately above the deposit and in some districts a karst morphology developed at the unconformity. However, one important exception is the southeast Missouri district where the major unconformity surface lies below the ore-bearing unit and there is no clear evidence for the existence of an unconformity above it (Sangster 1983 and 1988). In most MVT districts the ore consists of brecciated carbonate host rock cemented by sulphide and gangue minerals. In some of these districts there is evidence that ore solutions followed and enlarged pre-existing caves (Ohle 1985).

- * Mineralogy is generally simple and consists primarily of sphalerite, galena, pyrite, marcasite, calcite and dolomite (mostly copper-poor). However, individual deposits can vary in composition from lead dominant to zinc

dominant. Additionally fluorite and barite may be the dominant mineral in some deposits (Roedder 1984; Brown 1970; Sangster 1983 and 1988).

* Fluid inclusions indicate ore formation from highly saline brines (10 to 30 wt.% NaCl equivalent) at temperatures ranging from 70° to 150°C.

Pressures were above the vapour pressure of the brines but generally low. Immiscible oil droplets are sometimes observed in fluid inclusions in sphalerite. The highly saline brines consist mainly of Na and Ca chlorides (Roedder 1968, 1971 and 1984; Sangster 1983).

* Igneous activity is minor or lacking in most areas (Brown 1970).

The study of fluid inclusions in sphalerite have established that MVT ore-forming fluids have their closest affinities with oil-field brines (White 1968; Carpenter *et al.* 1974). The similarity between the ore-forming fluids (determined from fluid inclusion analysis) and deep basinal brines (in particular, oil-field brines) leads to the development of the basinal brine model. In this model, warm, saline brines migrated from the sedimentary basin along aquifers and formed ore deposits in carbonates tens to hundreds of kilometres from the basin. Despite the general support given to the basinal brine model there are a number of aspects of MVT deposits that remain unsolved. These include: timing of the ore formation; flow pathways and duration of flow; source and transport of metals and sulphides; and sulphide precipitation mechanism.

The time span between the host carbonate deposition and the emplacement of ore is not known for most MVT districts (Anderson 1978; Ohle 1980; Sangster 1983). This lack of knowledge regarding the timing of MVT mineralization has hindered the establishment of a single genetic model for MVT deposits. Three main techniques have been used in attempting to date the emplacement of MVT ores. These techniques are: palaeomagnetism, potassium-argon, and Pb-Pb isotopes. Conflicting results between the techniques, limitations of the techniques, and unrealistic age for the ores in relation to the host rock prove to be serious flaws in these dating techniques.

Three models have been proposed to explain the transportation and precipitation of base metals and sulphur in MVT deposits. The first model is a mixing model in which base metals were transported in one solution and sulphide was in a separate solution or as a sour gas. Ore precipitation occurred where the two solutions mixed (Anderson 1975 and 1983; Beales 1975). In the second model, a sulphate-reduction model, base metals and sulphur were transported together and precipitation resulted from the reduction of sulphate, possibly by oxidation of organic matter or methane (Barton 1967). The third model is a reduced sulphur model in which base metals and reduced sulphur were transported together at low and approximately equal concentrations, and precipitation was caused by pH increase, cooling, or dilution (Sverjensky 1981).

MVT Deposits of the Canning Basin.

The geology of a few lead-zinc prospects of the Lennard Shelf have been described by Ringrose (1989). These include the Wagon Pass and Blendevale prospects and the worked out Narlarla deposit. In addition to these prospects, BHP and Billiton Australia are currently mining the Cadjebut deposit. Exploration is continuing in other areas of the Lennard Shelf. The following summary of the lead and zinc mineralization of the Lennard Shelf incorporates the work of Ringrose (1984 and 1989), Lambert and Etminan (1987), and Etminan and Hoffmann (1989). Their information on the Wagon Pass and Blendevale prospects and the Cadjebut and Narlarla deposits is used to illustrate why the lead and zinc deposits of the Lennard Shelf are considered to be of the Mississippi Valley type.

The lead and zinc deposits at Narlarla, Wagon Pass, Blendevale and Cadjebut occur within the Devonian reef complexes of the Lennard Shelf. These reef complexes have undergone little tectonic deformation (Playford 1980). The deposits occur in a variety of facies and stratigraphic levels within

the reefs. The Cadjebut deposit occurs within Givetian platform facies, the Blendevale deposit occurs within Frasnian platform facies and the Narlarla and Wagon Pass deposits occur within Famennian marginal-slope facies. The host rock for the deposits range from totally dolomitized lithologies of the Cadjebut and Wagon Pass deposits, partially dolomitized lithologies of the Narlarla deposit, to undolomitized fenestral limestone of the Blendevale deposit (Lambert and Etminan 1987; Ringrose 1989). The zinc-to-lead ratio of the deposits is also variable. The Cadjebut and Blendevale deposits are zinc-rich while the Narlarla and Wagon Pass deposits have approximately equal amounts of zinc and lead. The Narlarla and Wagon Pass deposits are also significantly chloritized, unlike the other two deposits (Lambert and Etminan 1987; Ringrose 1989).

Mineralization of all the deposits occur mainly as open-space pore filling. Porosity hosting the sulphides includes primary fenestral porosity (Blendevale deposit), secondary intergranular and vuggy porosity created by dolomitization, and vein and fracture porosity. Ringrose (1989) suggested the mineralizing fluids were introduced episodically into the reefs and that they were active in the brecciation and fracturing of the host rock. Fault activity is also considered to have been active during mineralization. Ore textures (dendritic galena) indicate that some of the ore was precipitated rapidly. The main ore minerals are sphalerite, galena, pyrite and marcasite.

Fluid inclusion data from sphalerite and dolomite (closely associated with mineralization) from Cadjebut, Wagon Pass and Blendevale show homogenization temperatures ranging from 70° to 115°C and temperatures for the final melt of ice ranging from -32° to -15°C (Etminan and Hoffmann 1989). The solutes in the fluid inclusions consist of Na and Ca chlorides with low Mg (Lambert and Etminan 1987). These temperatures indicate mineralization occurred from warm saline brines. Significantly, liquid hydrocarbons were identified in fluid inclusions from all three deposits (Etminan and Hoffmann

1989). These temperatures and the occurrence of hydrocarbons within fluid inclusions are compatible with fluid inclusion data from MVT deposits in North America (Roedder 1968, 1971 and 1984).

Ringrose (1989) suggested the ore-forming processes, in the deposits of the Lennard Shelf, resulted from the semi-continuous passage of basinal brines, which became warmer and more metalliferous with time. Ringrose proposed that the genetic models, for the Wagon Pass, Narlarla and Blendevale deposits, involved transportation of metals in basin-derived brines and precipitation of sulphides on mixing with resident H₂S-bearing pore fluids. For the Wagon Pass and Narlarla deposits, Ringrose suggested that the warm basinal brines migrated from the Fitzroy Trough along aquifers during the Early Carboniferous. The carbonate host rocks were undergoing compaction stylolitization when they were dolomitized and chloritized by the basinal fluids. Mineralization occurred after dolomitization when the basinal brines became warmer and metalliferous. Basinal brines were introduced in pulses and mineralization occurred due to cooling or mixing with resident pore fluid. Ringrose considered mineralization to have occurred in the Early Carboniferous but indicated it was possible that the Narlarla No. 2 deposit formed within Late Carboniferous (pre-Grant Group) karst. He also noted it was possible that the precipitation mechanism for mineralization could have been the mixing of the karst-related meteoric fluids and basinal brines.

Ringrose proposed an earlier mineralization event for the Blendevale genetic model than for the Wagon Pass and Narlarla deposits. Between the Givetian and mid-Frasnian the Limestone Billy Hills limestone platform at Blendevale was covered by dark siltstone of the Gogo Formation. Sea-water sulphate was reduced by bacterial activity in the Gogo sediments and dispersed into the porous (and fractured) limestone by sediment compaction. Later warm metal-bearing brines migrated into the platform carbonates and

mixed with the reduced sulphate pore fluids, precipitating sulphides. The metal-bearing brines entered the limestone platform in pulses.

The principle similarities between MVT deposits of North America and the Lennard Shelf are that in both areas carbonate-hosted lead and zinc (copper-poor) deposits occur at the basin margin in relatively tectonically undisturbed rocks. Mineralizing fluids were warm, highly saline brines with closely associated liquid hydrocarbons, mineralization occurs predominantly as open-pore-space filling, and a major unconformity occurs above and resulted in karstification of the carbonate host sequence. Some aspects of the Lennard Shelf MVT deposits, like the North American examples, remain problematic. The range of sulphur isotope values, mineralogy of accessory minerals, differences in the zinc-to-lead ratios between deposits, and the differences between deposits of hydrocarbon biomarkers in fluid inclusions (Etminan and Hoffmann 1989) suggest that slightly different sources and processes are involved in the mineralization events in the deposits of the Lennard Shelf.

Two studies have attempted to constrain the timing of the sulphide deposits of the Lennard Shelf deposits. Ringrose (1989) proposed genetic models for individual deposits and suggested that the mineralization events ranged from Famennian (Blendevalle deposit) to possibly Late Carboniferous (Narlaria No.2 deposit). The genetic models and timing of mineralization were based on geological, geochemical, petrological and mineralogical data from selected deposits on the Lennard Shelf.

The other study concerning the timing of mineralization, by Arne *et al.* (1989), used apatite fission track analysis to reconstruct the regional thermal history of the Lennard Shelf. Their data consisted of samples from petroleum wells, outcropping carbonates in and near Pb-Zn mineralization, and the Precambrian basement. Apatite fission track ages for the Devonian carbonates indicated appreciable annealing of fission tracks in apatite had occurred in

post-Devonian times. They proposed the Devonian carbonates were buried in the Late Palaeozoic/Early Mesozoic, attaining peak temperatures of approximately 70° to 80°C, before uplift and cooling in the Late Triassic/Early Jurassic (Fitzroy Movement). Their studies of well sequences indicated *that rapid* uplift during the Fitzroy Movement resulted in erosion of approximately 1500 m of sediment (assuming a constant geothermal gradient of 30°C/km). The possibility of a phase of higher temperatures during the Late Devonian/Early Carboniferous is suggested by the apatite fission track results.

Arne *et al.* (1989) determined the thermal effects related to Miocene lamproite intrusions on the Lennard Shelf were restricted to less than 200 m of the contact zone. However, no enhanced annealing of apatite fission tracks was observed in relation to MVT mineralization. Arne *et al.* (1989) suggested two possibilities for the age of MVT deposits of the Lennard Shelf, in light of their apatite fission track data; 1) Mineralization preceded or accompanied peak regional temperatures suspected during the Late Devonian/Early Carboniferous. 2) Mineralization occurred in the Late Carboniferous/Late Triassic but the mineralization episodes were of too short a duration to significantly anneal fission tracks in apatite.

Scope of this study.

The aim of this study was to approach the problem of the timing of mineralization in MVT deposits in the context of the diagenetic evolution of the Devonian reef complexes of the Lennard Shelf. These carbonates were subject to two important burial diagenetic events, Late Devonian — Early Carboniferous and Permian — Cenozoic. The main products of these diagenetic events are equant calcite cementation, dolomitization, mineralization, pressure solution, karstification, dedolomitization and neomorphism. Cathodoluminescence, fluid inclusion, and geochemical techniques are useful tools in defining and characterizing the cement

stratigraphy and the porosity evolution of the carbonates. By determining the cement stratigraphy, constraining the possible diagenetic environments for the cements, and combining these with the stratigraphy and geological history of the Lennard Shelf, the timing of MVT mineralization may be inferred or determined directly. Knowledge of the diagenetic environments of the carbonates that predate and postdate the mineralization may also provide constraints on the MVT genetic models.

Cathodoluminescence is the main tool used in developing the cement stratigraphy. Cathodoluminescence is light emitted from a substance under electron bombardment. The intensity of cathodoluminescence is believed to be controlled by the presence of trace elements. In calcites and dolomites the principal trace elements responsible for the luminescence intensity are manganese (Mn^{2+}) and iron (Fe^{2+}) (Frank *et al.* 1982). These trace elements substitute for calcium and magnesium in calcite and dolomite, with manganese enhancing luminescence (an "activator") and iron quenching luminescence. The ratio of manganese to iron and the absolute quantity of iron, are the main factors determining luminescence intensity in carbonates (Grover and Read 1983 and Hemming *et al.* 1989). However, Pb^{2+} and several rare earth elements may also control luminescence in carbonates (Machel 1985).

If the luminescence intensity in carbonates is largely in response to iron and manganese, then the substitution of these elements into the calcite and dolomite lattice can be related to pore-fluid Eh/pH conditions (Frank *et al.* 1982). Under oxidizing conditions, both manganese and iron are in their oxidized state (Mn^{3+} and Fe^{3+}). Therefore there is no substitution and no luminescence. Under moderately reducing conditions, manganese substitution occurs and results in bright-luminescence. More strongly reducing conditions enable iron substitution and results in dull-luminescence as iron is a luminescence quencher.

The region of main interest in this study is Billiton's Fossil Downs exploration license in the Fossil Downs and Brooking Springs Station areas (Figure 5). Carbonate samples (calcites and dolomites) were selected from fully cored mineral exploration drill holes in platform and marginal-slope facies in these areas and from outcrop sampling. (Appendices A, B, C, and D illustrate cross sections and display sample localities in drill holes). Additional drill core samples were collected from Billiton's Horse Spring Range (Figure 6) and

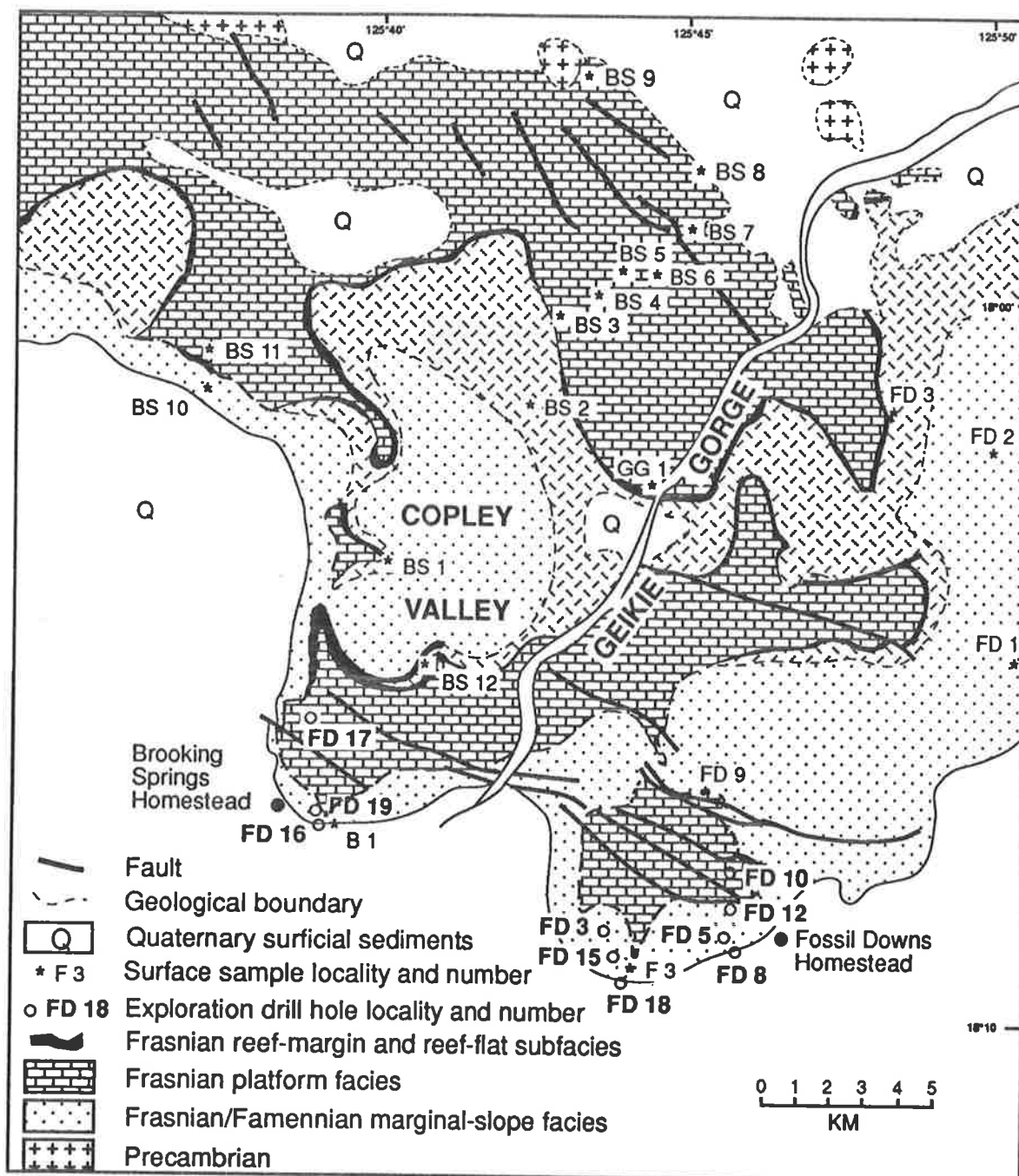


Figure 5.— Distribution of surface samples and mineral exploration drill-holes in the Fossil Downs exploration lease area (modified from Wallace 1987).

Napier Range exploration licenses. Surface samples were predominantly from these areas and the area north of Brooking Springs Homestead (including the Copley Valley and Sheep Camp Yard areas, and the area of limestone-basement contact further to the north). Additional surface samples were collected from across the Lennard Shelf, (Figure 7) from the Emanuel Range in the southeast to the Napier Range in the northwest. These samples included mineralized and unmineralized samples, as well as dolomite, partially dolomitized limestone, and limestone. (a table of all samples with location identification and sample number, is provided in appendix E).

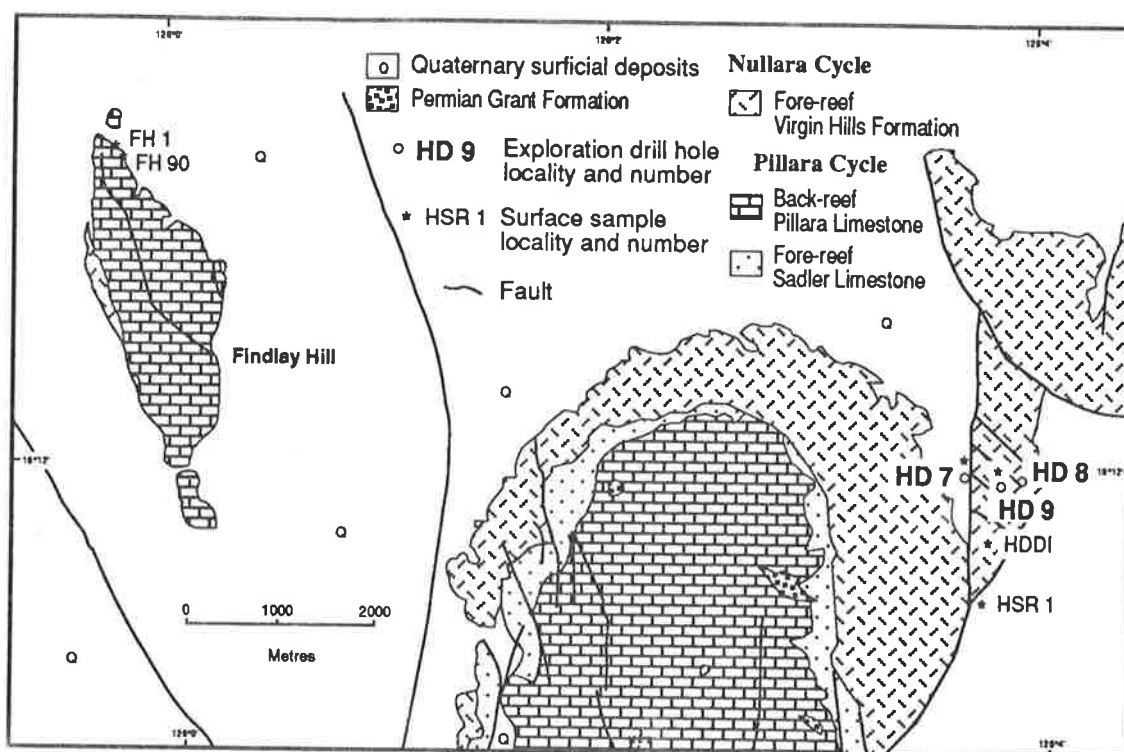


Figure 6.— Generalized geological map of the Horse Spring Range exploration lease (modified from Billiton Australia unpublished geological map P/SD85/041). Surface sample localities and mineral exploration drill-holes are indicated.

In selecting samples from both core and outcrop, primary pores were of greatest interest. Primary pores included marine-cement-lined pores and fractures, fenestral pores and shelter pores. These pores record the transition from near-surface diagenetic processes to the "subsurface burial-diagenetic realm" (Choquette and James 1987). Partially dolomitized and partially

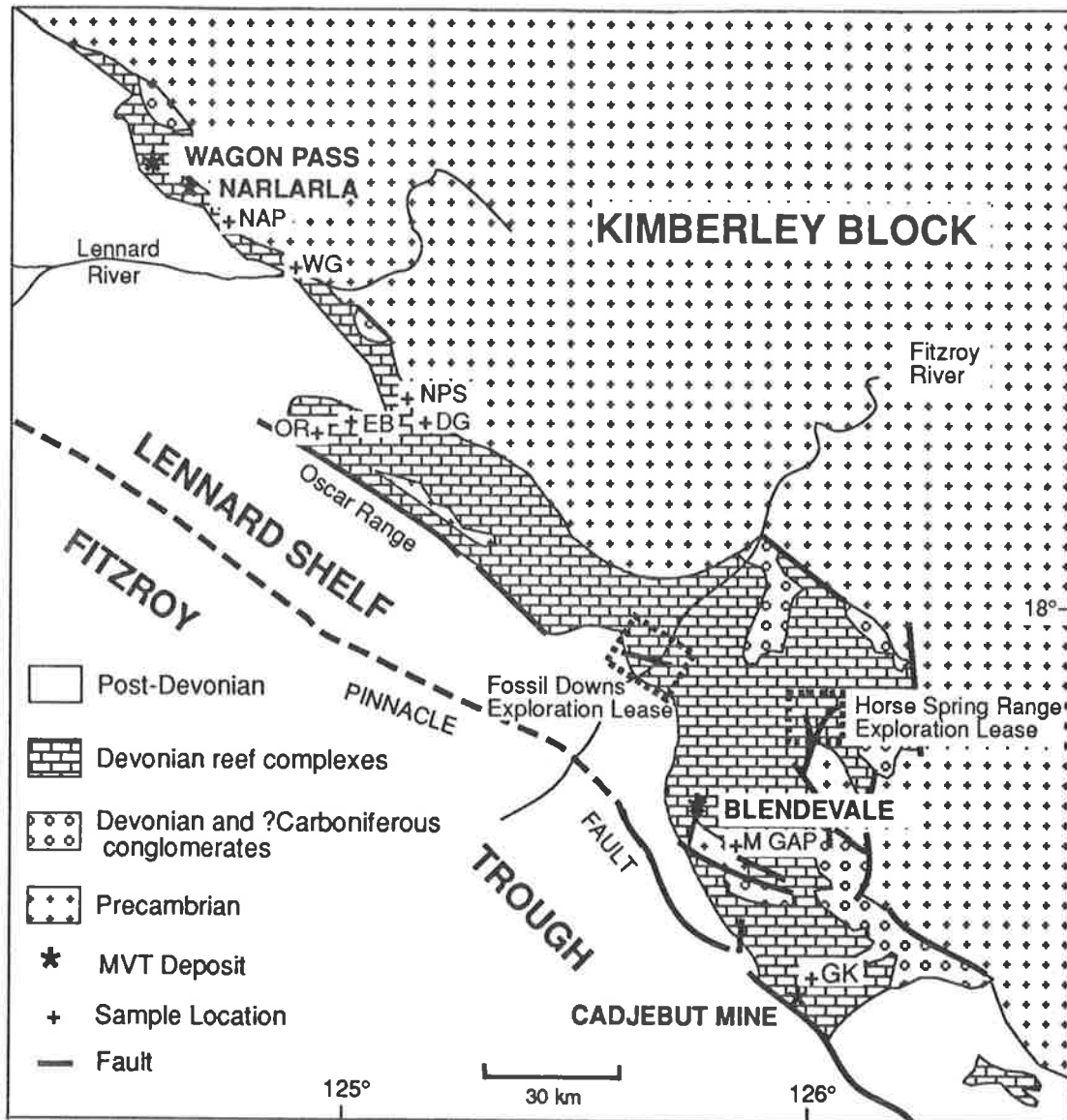


Figure 7.— Generalized map of the northern Canning Basin illustrating the location of exploration leases of Billiton Australia (modified from Playford 1984). Sampling localities outside these leases are also indicated (GK = Glenister Knoll; M Gap = Menyous Gap; OR = Oscar Range; EB = Elimberrie Bioherms; DG = Dingo Gap; NPS = North Pandanus Springs; WG = Windjana Gorge; Nap = Napier Downs Station).

mineralized limestone samples were collected to link the timing of dolomitization and mineralization with the diagenesis of the reef complexes. Marine diagenetic processes in the Devonian reef complexes of the Lennard Shelf have been described in detail (Kerans 1985; Kerans *et al.* 1986; Hurley 1986; Hurley and Lohmann 1989) and are outside the scope of this study. However, a few samples of marine cements were geochemically analyzed for comparison with later burial-diagenetic phases.

LABORATORY METHODS

Staining and Cathodoluminescence

Selected slabbed surface samples and drill-core samples were stained with Alizarin Red S and potassium ferricyanide (Dickson 1966). Alizarin Red differentiates calcite from dolomite while potassium ferricyanide determines ferroan from non-ferroan calcite and/or dolomite. Staining provides a quick method to differentiate certain carbonate phases. Upon treatment with potassium ferricyanide, the clear equant calcite cements were classified as non-ferroan (unstained), ferroan (stained pale blue) or strongly ferroan (stained azure).

Cathodoluminescence microscopy was used in evaluating the cement stratigraphy (Meyers 1974). For this study, 60 highly polished thin sections were examined using a Technosyn (8200 MK 11) Luminoscope. Operating conditions for cathodoluminescence microscopy and photomicroscopy (Kodak Ektapress 1600 ASA colour film) were 13 to 18 kV for beam energy and between 150 and 200 microamps for beam current.

Isotopes

Carbon and oxygen isotope analysis was used to characterize the diagenetic phases identified by cathodoluminescence and staining. The information obtained from these techniques is useful in attempting to differentiate between marine, meteoric and burial environments for the carbonate cement phases.

A dental drill was used to collect samples from individual carbonate diagenetic phases for carbon and oxygen isotope analysis. The width of the dental drill-bit (1 mm) and the amount of sample needed for analysis (15 mg), prevented some of the diagenetic phases from being sampled. Polished slabs, viewed under cathodoluminescence before and after drilling, were used for some samples to ensure that the correct zone had been sampled.

Drilled samples were immersed (overnight) in phosphoric acid in reaction vessels, with calcite phases at 25°C and dolomites reacted at 50°C. The reaction vessels were attached, in turn to a gas extraction system and CO₂ was collected and sealed in glass tubes. Stable-isotope analyses were run on a Micromass VG 602E ratio mass spectrometer. All analyses were converted to PDB values and corrected for ¹⁷O as described by Craig (1957). For this study, carbon and oxygen isotopic analysis was performed on 89 calcite and dolomite samples. Precision was determined by analysis and duplication of the calcite standards ANU-P3 (Australian National University standard No. 3), NBS-18 and NBS-19. The largest difference in values recorded for these standards was 0.07‰ for δ¹³C and 0.24‰ for δ¹⁸O. Accuracy was determined by comparison of the mean values for standards NBS-18 {δ¹³C = -5.00‰ (PDB) and δ¹⁸O = -22.98‰ (PDB)} and NBS-19 {δ¹³C = +1.99‰ (PDB) and δ¹⁸O = -2.20‰ (PDB)} with the corresponding values determined by Coplen *et al.* (1983). The maximum difference in values of these analyses were 0.09‰ for δ¹³C and 0.10‰ for δ¹⁸O.

Sulphur isotope analyses were performed on 11 sulphide samples. The samples were selected from mineralized zones in drill-cores from the Fossil Downs Station (6 iron sulphide samples and 1 galena sample) and the Cadjebut Mine (2 iron sulphide samples, 1 galena sample and 1 sphalerite sample). Samples (weighing approximately 10 mg, 15 mg, and 40 mg for pyrite, sphalerite and galena respectively) were roasted progressively in a furnace tube attached to a gas extraction system and SO₂ was collected and sealed in glass tubes. Sulphur isotope analyses were run on a Micromass VG 602E ratio mass spectrometer. All analyses are reported relative to CDT. Precision was determined by analysis and duplication of an internal galena standard (Jensen's Galena). The maximum difference in values recorded was δ³⁴S = 1.6‰. The internal galena standard has a set value of δ³⁴S = -6.7‰.

Comparison of this set value with the measured values of this study indicated a maximum difference of 2.5‰ (accuracy of $\delta^{34}\text{S}$ values).

Strontium isotope analysis was performed on nine selected carbonate phases on which carbon and oxygen isotope analysis had already been performed. Approximately 50-100 mg of unspiked sample was digested in a teflon beaker using 2-4 mls 6N HCl. This was then evaporated and then taken up in 1.5 mls 3N HCl and centrifuged at 3000 rpm for five minutes. Sr was then separated from the sample solution using standard cation exchange column procedures. The resulting Sr samples were loaded onto single tantalum filaments using H_3PO_4 and analyzed for their isotopic compositions, at the University of Adelaide Department of Geology and Geophysics, on a Finnigan Mat 261 thermal ion, solid source, mass spectrometer. Data blocks of ten scans each were run until acceptable in-run statistics were achieved (8-16 blocks for Sr using a double collector) and mass fractionation was corrected to $^{88}\text{Sr}/^{86}\text{Sr}=8.3752$. The average procedural blank during the course of isotopic analysis for Sr was ~1.1 ng. The following results have been obtained from multiple runs of standards in the lab (errors are 2 standard errors of the mean of in-run statistics):

<u>Standard</u>	<u>$^{87}\text{Sr}/^{86}\text{Sr}$ (measured) error</u>	<u>Number of runs</u>
E & A	0.708001 \pm 0.000037	1
NBS SRM 987	0.710234 \pm 0.000025	10

Fluid Inclusions

Fluid inclusion microthermometry was performed on selected samples to help establish formation temperatures and salinities for the individual diagenetic phases. Selected samples were prepared as doubly polished plates ranging in thickness from 50 to 200 μm . Dolomite samples were prepared much thinner than the calcite samples to improve the optical resolution of the inclusions within the dolomite samples. The samples were prepared under low temperature (<50°C) conditions to avoid possible

stretching or decrepitation of the inclusions. Primary fluid inclusions were of most interest as these inclusions are records of the pore fluids at the time when a particular cement phase was precipitated. However, when primary inclusions were too small or could not be identified with confidence, measurements on pseudosecondary inclusions were taken. Dual homogenization and last melt temperatures for individual inclusions was, in most cases, prevented because of decrepitation or stretching of inclusions on freezing.

Fluid inclusions were analyzed using a USGS-type gas-flow heating and freezing stage. Precision of freezing data is low due to the small inclusion size and the poor optical quality of some of the samples. In some of the optically poor samples, last melt temperatures were repeatable only to $\pm 2^{\circ}\text{C}$. However, most inclusions measured had last melt precisions of $\pm 0.2^{\circ}\text{C}$. Repeatability of homogenization temperatures indicate a precision of $\pm 3^{\circ}\text{C}$ for most of the inclusions measured.

Microprobe

Microprobe analyses were performed on a KEVEX 7000 Series energy dispersive system attached to a JEOL JCSA-733 analyzer. Analyzing conditions used were 15 kV accelerating voltage, 30 nA beam current, 30 μm beam diameter, and 200 second counting times. Silicate standards were used for daily calibration. Data was corrected on-line using modified JEOL software based on JASTRAN, employing full ZAF corrections. Detection limits for Mg, Ca, Sr, Mn, Fe, Na, and Zn were 40, 80, 90, 130, 110, 45, and 220 respectively.

Trace-element analyses of calcite and dolomite cement zones were performed on five highly polished thin sections. Normal transmitted light photos and cathodoluminescence photos were taken of the areas to be analyzed. Preselected points across the cathodoluminescent zoned calcite and dolomite cements were entered into the on-line computer and trace element analysis was then performed automatically.

CALCITE CEMENTS

MARINE DIAGENESIS (marine calcite cements)

Previous diagenetic investigations of the Devonian reef complexes of the Lennard Shelf (Playford 1984; Kerans 1985; Kerans *et al.* 1986; Hurley and Lohmann 1989) indicate that the marine diagenetic environment is the most important diagenetic environment controlling cementation of the carbonates. Marine cementation of the Devonian reefs has been summarized elsewhere (Kerans 1985; Kerans *et al.* 1986; Hurley 1986; Hurley and Lohmann 1989) and is outside the scope of this study. However, some general observations of the cathodoluminescence character of the marine cements, as well as some geochemical analyses of marine cements, were included to provide comparisons between the marine diagenetic and burial diagenetic environments.

Radiaxial and microcrystalline marine calcite cements display variable luminescence intensities. These range from non-luminescent to bright-luminescent and have a mottled texture. Primary marine components generally should not luminesce. Enrichment in the heavy rare-earth elements (enriched due to bacterial influence) may activate luminescence in marine carbonate cements (Machel 1985). However, the variable and mottled luminescence character of the Devonian marine cements on the Lennard Shelf is presumably due to neomorphism as well as microfracturing and infill by later cement generations. Sample FD 15 106.9m (Figures 8A, 8B) is an example in which microcrystalline marine cement displays a mottled non- and bright-luminescent texture. Microfractures of bright-luminescent cement are clearly observed in some areas of this sample and some of these microfractures extend into the younger non-luminescent cement generation (discussed later).

Figure 8. Thin section photomicrographs of marine and clear equant calcite cement generations in plane-polarized light and cathodoluminescence.

A) A large cement-filled cavity filled by an inclusion-rich microcrystalline marine (M) cement and clear equant calcite cement (plane-polarized light). Famennian marginal-slope facies, Fossil Downs Station drill-hole FD15 106.9 m. Scale bar = 0.5 mm. Billiton sample no. 106723

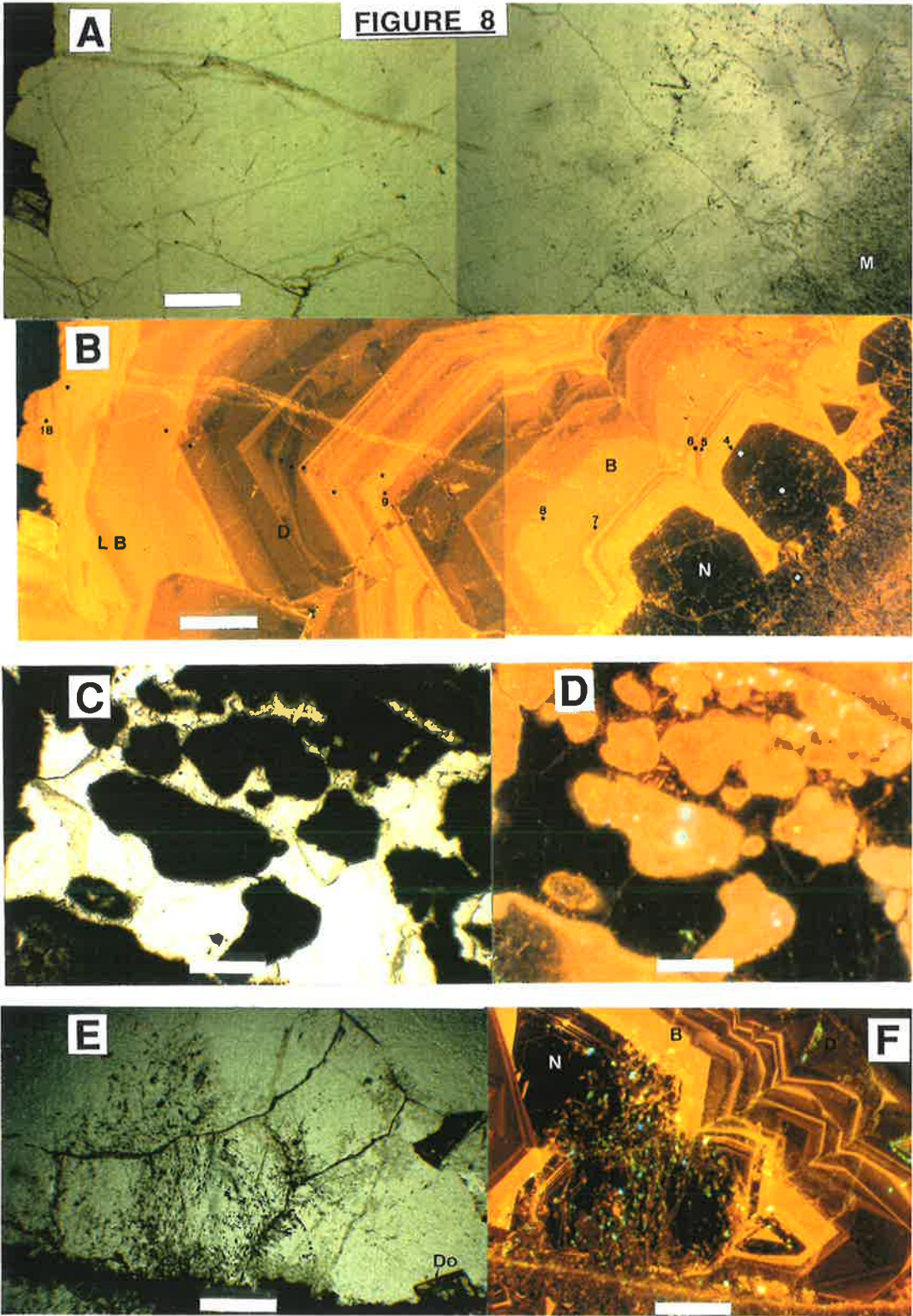
B) Same area in A under cathodoluminescence. The marine cement has a mottled bright- and non-luminescent character. Bright-luminescent filled microfractures (F) occur within the marine cement and to a lesser extent, within the non-luminescent cement zone (the first generation of the clear equant cement). The clear equant cement consists of non-luminescent (N) cement, overgrown by a bright-luminescent (B) cement (banded), overgrown by a dull-luminescent (D) cement (uniform), which is in turn overgrown by the late bright-luminescent (LB) cement. The dots indicate the positions of microprobe analyses.

C) Fenestral pores filled predominantly by clear equant cement, with only minor marine cementation (plane-polarized light). Frasnian back-reef subfacies, Fossil Downs Station drill-hole FD 10 113.3 m. Scale bar = 0.5 mm. Billiton sample no. 106768

D) Same area in C under cathodoluminescence. The clear equant cement is almost entirely non-luminescent.

E) A cement-filled intraparticle pore within a mollusc lined by microcrystalline marine cement and filled by clear equant cement (plane-polarized light). A dolomite (Do) rhomb precipitated on the base of the pore. Frasnian back-reef subfacies, Fossil Downs Station drill-hole FD 10 28.5 m. Scale bar = 0.5 mm. Billiton sample no. 106772

F) Same area in E under cathodoluminescence. The clear equant cement consists of non-luminescent (N) cement, overgrown by bright-luminescent (B) cement (younger bands duller than earlier bands), which is in turn overgrown by a dull-luminescent (D) cement (uniform). The non-luminescent cement contains thin bright-luminescent growth bands. The core of the non-luminescent cement has been recrystallized and now displays dull-luminescence.



Scaleno-hedral (Kerans 1985) marine cements are non-luminescent and inclusion poor.

Carbon and oxygen isotopes.—Stable isotope analysis was performed on a brachiopod shell and two marine cement samples from the Fossil Downs Station area. The $\delta^{13}\text{C}$ values averaged +1.7‰ and $\delta^{18}\text{O}$ values averaged -5.3‰ for the three samples (Table 1). The samples were not totally pristine (all displayed a variable mottled luminescence), and the oxygen isotope results are slightly more negative than the Devonian marine isotopic signature ($\delta^{13}\text{C} = +2.0 (\pm 0.5)\%$ and $\delta^{18}\text{O} = -4.5 (\pm 0.5)\%$) proposed by Hurley and Lohmann (1989).

Table 1.— Carbon and oxygen isotopic compositions of the calcite diagenetic phases.

Billiton number	$\delta^{18}\text{O}$ (PDB)	$\delta^{13}\text{C}$ (PDB)	LOCATION / DEPTH
Late Devonian Marine Signature (Hurley and Lohmann 1989)			
	-4.5	2.0	
Marine calcite cement			
106802	-4.7	1.8	Fossil Downs Station/Surface (F3)
106787	-5.6	2.4	FD 12 52.79-52.94m
106718	-5.7	0.8	FD 15 18.82-19.00m
Non-luminescent calcite cement			
106803	-5.7	1.7	Geikie Gorge/Surface (85.30)
106830	-6.8	0.9	Brooking Springs Station/Surface (BS4)
106833	-7.0	2.0	Brooking Springs Station/Surface (BS7)
Bright-luminescent and dull-luminescent calcite cements			
106719	-7.0	1.0	FD 15 38.10-38.20m
106726	-10.9	0.9	FD 15 171.40-172.00m
106723	-11.4	1.0	FD 15 106.90-107.00m
106734	-5.7	-0.6	FD 8 105.64-105.76m
Dull-luminescent calcite cement			
106734	-14.1	1.0	FD 8 105.64-105.76m
106734	-12.9	1.5	FD 8 105.64-105.76m
106735	-13.2	0.7	FD 8 68.72-68.84m
106801	-13.6	0.0	Geikie Gorge/Surface (MW 1)
106772	-11.5	-0.2	FD 10 28.50-28.60m
106828	-9.9	2.1	Brooking Springs Station/Surface (BS2)
106837	-10.6	0.3	Brooking Springs Station/Surface (BS11)
Late bright-luminescent calcite cement			
106723	-13	-3.3	FD 15 106.90-107.00m
Late brightly banded-luminescent calcite cement			
106721	-9.7	-5.4	FD 15 63.95-64.05m
106726	-9.5	-2.8	FD 15 171.40-172.00m
106719	-9.3	-4.0	FD 15 38.10-38.20m
Late ferroan dull-luminescent calcite cement			
106836	-16.4	-1.1	Brooking Springs Station/Surface (BS10)
106813	-15.6	-4.7	Dingo Gap/Surface (DG)
106825	-14.2	-2.4	Fossil Downs Station/Surface (FD2)

Strontium isotope analyses.—Strontium isotope analyses were performed on the brachiopod shell and a sample of marine cement. The brachiopod shell had a $^{87}\text{Sr}/^{86}\text{Sr}$ value of 0.70841 and the marine cement value was 0.70876.

Trace elements.—Two samples of scalenohedral marine cement and one sample of microcrystalline marine cement were analyzed for trace elements composition. These marine cements averaged 2757 ppm magnesium, 322 ppm strontium, 37 ppm manganese, 11 ppm iron, 75 ppm sodium, and 70 ppm zinc (Table 2).

Table 2.— Microprobe results for calcite cement generations.

Billiton sample number	Sample locality /microprobe data point	Trace element concentration							Calcite cement generation
		Mg ppm	Ca mole%	Sr ppm	Mn ppm	Fe ppm	Na ppm	Zn ppm	
106779	HD 9 270								
	1	4614	98.3	85	15	0	28	45	Scaleno-hedral marine
	2	3512	98.3	129	2101	0	10	82	Non-luminescent
	3	575	98.7	116	4389	1838	0	0	Bright-luminescent
	4	832	98.0	13	8019	1374	97	538	Bright-luminescent
	5	1167	99.4	364	544	323	62	160	Dull-luminescent
106734	FD 8 105								
	1	525	98.9	153	4790	829	8	80	Bright-luminescent
	2	198	99.6	169	1988	63	45	0	Bright-luminescent
	3	526	99.1	217	1676	2537	24	0	Bright-luminescent
	4	174	99.9	119	169	45	16	19	Bright-luminescent
	5	526	99.7	55	237	135	12	0	Bright-luminescent
	6	579	99.7	28	321	156	0	0	Dull-luminescent
	7	1225	99.5	516	20	20	72	127	Scaleno-hedral marine
	8	480	99.8	489	0	0	4	47	Non-luminescent
	9	1099	99.4	375	508	180	53	28	Bright-luminescent
	10	1462	99.0	152	2262	275	23	0	Bright-luminescent
	11	186	99.2	117	3825	537	0	0	Bright-luminescent
	12	1011	98.9	173	1723	2368	6	267	Bright-luminescent
	13	685	99.7	92	156	178	0	0	Bright-luminescent
	14	225	99.8	9	173	369	0	199	Dull-luminescent
106726	FD 15 171								
	1	2652	98.9	205	982	0	90	0	Bright-luminescent
	2	549	99.8	204	194	25	100	0	Bright-luminescent
	3	164	99.9	89	138	0	55	0	Dull-luminescent
	4	884	99.1	767	2911	173	138	130	Late bright-luminescent
	5	1884	99.3	103	56	0	188	481	Late brightly banded-lum
	6	650	99.2	164	2568	951	92	0	Late brightly banded-lum
106723	FD 15 107								
	1	2432	99.1	366	75	12	125	39	Microcrystalline marine
	2	3689	98.7	76	0	0	70	0	Non-luminescent
	3	3698	98.6	86	0	94	127	0	Non-luminescent
	4	3327	98.6	83	1245	51	26	0	Bright-luminescent
	5	1222	99.5	89	56	0	67	0	Bright-luminescent
	6	789	99.7	66	200	0	108	0	Bright-luminescent
	7	3383	98.6	172	496	354	115	0	Bright-luminescent
	8	2991	98.8	104	704	250	113	0	Bright-luminescent
	9	1103	99.4	225	44	0	55	0	Bright-luminescent
	10	974	99.5	151	249	146	170	50	Bright-luminescent
	11	697	99.6	137	841	105	114	0	Bright-luminescent
	12	1305	99.4	100	402	495	111	0	Bright-luminescent
	13	168	99.9	90	126	0	238	0	Dull-luminescent
	14	229	99.9	60	70	0	149	0	Dull-luminescent
	15	636	99.7	168	131	0	59	0	Dull-luminescent
	16	625	99.4	266	1619	880	91	0	Late bright-luminescent
	17	455	99.4	0	2647	28	89	0	Late bright-luminescent
	18	838	98.6	96	4937	1725	77	113	Late bright-luminescent

BURIAL DIAGENESIS (clear equant calcite cements)

Clear equant calcite cements occlude almost all of the porosity remaining after marine cementation. A paragenetic sequence of cementation was established for the clear equant calcite cements, principally by observations of superposition of cathodoluminescent zones in primary pores. Cross-cutting relationships of veins and fractures, as well as staining and oxygen and carbon isotope analysis, aided the identification and characterization of these cathodoluminescence zones. The early clear equant calcite cements are non-ferroan, while later generations display non-ferroan and ferroan banding and later strong ferroan character. Calcite cementation of secondary porosity developed in dolomites will be discussed in the section dealing with dolomite formation.

To compare porosity occlusion by the clear equant calcite cement phases (identified by cathodoluminescence) in different areas on the Lennard Shelf, visual estimates were made of the pore-filling cement zones. From initial observations of the cathodoluminescent zones and even of stained slabs, it was apparent that there were differences in the proportions in which the cement zones occluded porosity. These differences occurred on both local and regional scales. Visual estimation of the individual cement phases, although only semi-quantitative, provides an insight into porosity occlusion of the reefs on the Lennard Shelf.

A distinctive cathodoluminescence sequence was observed in the Fossil Downs Station area. This sequence was also observed in samples from other areas of the Lennard Shelf, although individual zones within the sequence displayed variable degrees of development across the Shelf. Six major zones were identified in this study and are described below. Five of these are the same as those proposed by Wallace *et al.* (in press), while a new zone is proposed in this study. The six zones from oldest to youngest are:

- 1) Non-luminescent cement.
- 2) Bright-luminescent cement.
- 3) Dull-luminescent cement.
- 4) Late bright-luminescent cement.
- 5) Late brightly banded-luminescent cement
- 6) Late ferroan dull-luminescent cement.

1) Non-luminescent cement zone.

Description.—The non-luminescent (non-ferroan) cements represent the first clear equant calcite cement phase after marine deposition and marine cementation (radial fibrous, microcrystalline and scalenohedral calcite cements). When the non-luminescent cement forms on microcrystalline or radial marine cements or on framework grains, it displays an equigranular crystal fabric. It may display either uniform non-luminescence (Figures 8B; 8C, 8D), non-luminescence with extremely fine (less than 10 μm) bright-luminescent banding (Figures 8E, 8F; 9A, 9B), or extremely faint, orange-red, banded-luminescence (Figures 9C, 9D). When scalenohedral marine cements are observed, the non-luminescent cement occurs as an overgrowth cement, retaining the morphology of the underlying scalenohedral cement. The occurrence of extremely fine bright-luminescent bands within the non-luminescent cement zone is the only distinguishing feature between these two cement generations when the non-luminescent cement overgrows the scalenohedral cement. The banding within the non-luminescent cement is generally conformable, but minor disruption due to corrosion has been observed. Scalenohedral cements (predating the non-luminescent cement) may display embayment and rounding from intermittent dissolution (Kerans 1985).

Where the non-luminescent cement is well preserved, it is inclusion poor. However, where the luminescence displays a mottled bright and dull-

Figure 9. Thin section photomicrographs of clear equant calcite cement generations in plane-polarized light and cathodoluminescence.

A) A clear equant cement-filled cavity which contains inclusion rich zones (plane-polarized light). Frasnian reef-margin subfacies, Copley Valley BS 3. Scale bar = 0.5 mm. Billiton sample no. 106829

B) Same area in A under cathodoluminescence. The clear equant cement consists of the following cement generations from oldest to youngest — non-luminescent (N), dull-luminescent (D), and late brightly banded-luminescent (BB). The non-luminescent cement contains very fine bright-luminescent banding. Recrystallization of the non-luminescent (RN) cement produced the inclusion-rich zonation observed in plane-polarized light. The recrystallized non-luminescent cement contains both bright- and dull-luminescent cement, resulting in a patchy luminescent character. The distinctive growth banding and truncation pattern (arrow) is characteristic of the late brightly banded-luminescent cement generation. A dull-luminescent zone occurs within the late bright-luminescent cement generation in this sample but was not observed in other samples of this generation.

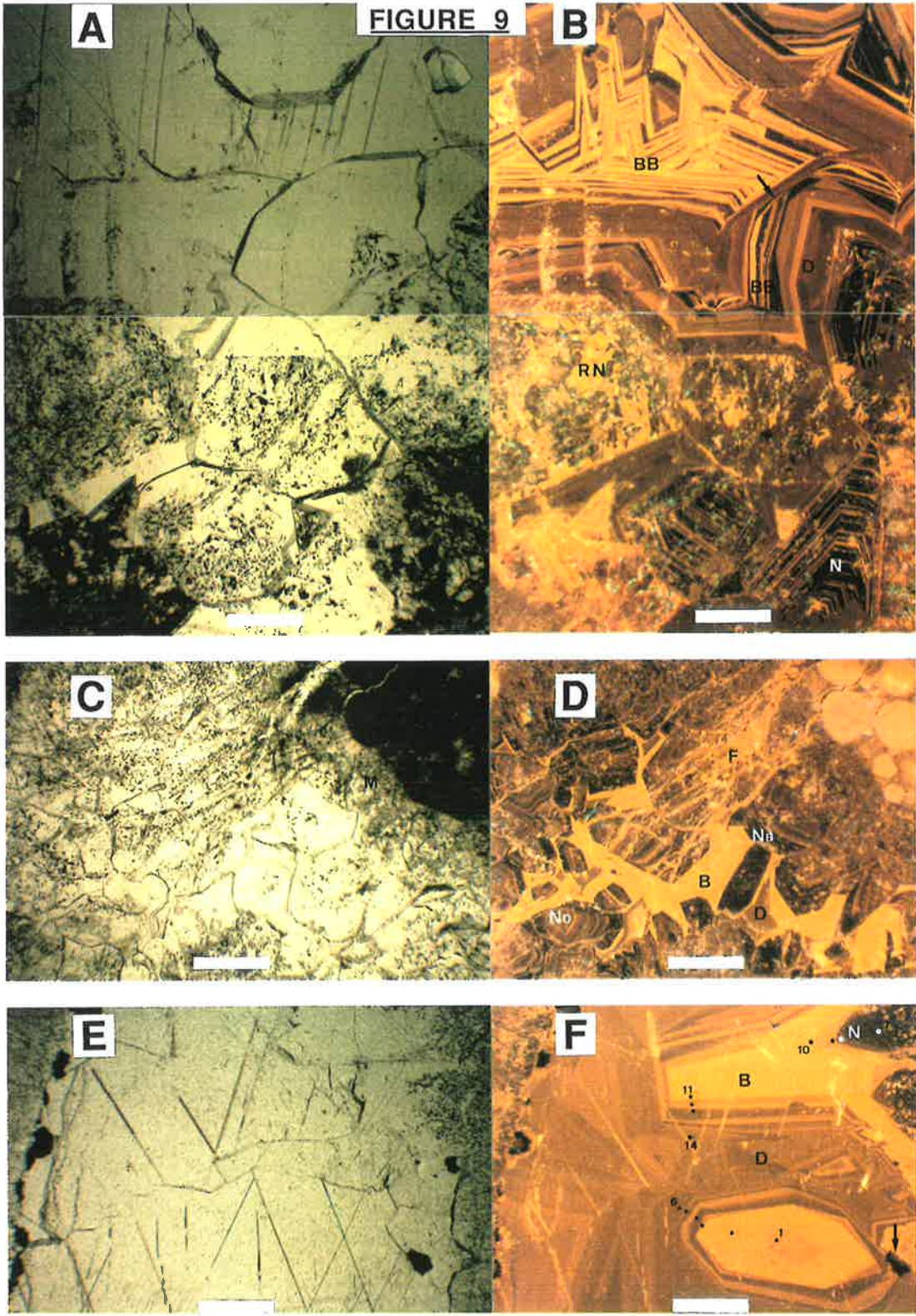
C) A cement-filled pore within an ooid grainstone filled by microcrystalline marine (M) cement and clear equant calcite cement (plane-polarized light). Frasnian back-reef subfacies, Brooking Springs Station drill-hole FD 17 17.0 m. Scale bar = 1 mm. Billiton no. 106764

D) Same area in C under cathodoluminescence. The microcrystalline marine cement is overgrown by the non-luminescent cement generation. The non-luminescent cement generation has a banded dull-luminescent core (ND) which is overgrown by a (black) non-luminescent (NB) rim. The non-luminescent cement is overgrown by a bright-luminescent (B) cement and this in turn is overgrown by a dull-luminescent (D) cement. The bright-luminescent cement fills microfractures in the older cement generations. The "horsetail" character of the bright-luminescent cement-filled microfractures (F) indicate probable hydraulic fracturing by the fluids that precipitated the bright-luminescent cement.

E) A microcrystalline marine cement-lined pore filled by clear equant calcite cement (plane-polarized light). The opaque mineral is sphalerite. Famennian marginal-slope facies, Fossil Downs Station drill-hole FD 8 105.7 m. Scale bar = 0.5 mm. Billiton sample no. 106734

F) Same area in E under cathodoluminescence. The microcrystalline marine cement has a mottled bright- and dull-luminescence. The clear equant cement consists of non-luminescent (N) cement, overgrown by bright-luminescent (B) cement, which in turn is overgrown by a uniform dull-luminescent (D) cement. The change from non-luminescent cement to bright-luminescent cement is gradational. Sphalerite occurs on the outer edge of the strongly bright-luminescent zone (arrow). The dots indicate the position of microprobe analyses.

FIGURE 9



luminescence, it is inclusion rich. This can be clearly seen in sample BS 3 (Figures 9A, 9B) where the non-luminescent cement has been partially replaced (mostly within the central area of the crystal) by the later dull- and bright-luminescent cements (also Figure 8E, 8F).

Carbon and oxygen isotopes.—Stable isotope analyses were performed on the non-luminescent cement drilled from three samples of Frasnian platform facies north of Copley Valley. Porosity was occluded almost entirely by the non-luminescent calcite cement in these three samples. The $\delta^{18}\text{O}$ values range from -6.9‰ to -5.7‰ (averaging -6.5‰) and $\delta^{13}\text{C}$ values range from +1.0‰ to +2.0‰ (averaging +1.6‰) (Table 1).

Strontium isotope analyses.—Strontium isotope analyses were performed on two samples of non-luminescent cement. The $^{87}\text{Sr}/^{86}\text{Sr}$ values were 0.70815 and 0.70825.

Fluid inclusions.—Within the non-luminescent calcite cement, fluid inclusions are small (less than 10 μm) and predominantly single phase. Conclusive evidence of primary origin for the fluid inclusions could not be established. However, most of the inclusions are probably of pseudosecondary origin as cathodoluminescence showed no significant microfractures (and infill by later cement phases) in the areas of interest. One pseudosecondary, two-phase fluid inclusion, had a homogenization temperature of 57.4°C. However most of the inclusions observed were single phase. Twelve inclusions from two samples (BS4 and BS7), of Frasnian platform facies north of Copley Valley, had last-melt temperatures for ice ranging from -4.2° to -0.1°C (averaging -2.5°C) (Table 3). These last-melt temperatures represent salinities ranging from 0 to 6.6 weight % NaCl equivalent. The eutectic temperature for these inclusions ranged from -40° to -21°C. One inclusion (not included in the averaging above) had a final melt temperature of -45.3°C. The homogenization temperature of this two-phased

inclusion was +27.2°C. The significance of this inclusion will be discussed later.

Table 3.— Fluid inclusion results of burial calcite cement generations.

Billiton sample no.	Sample locality	Mineral and inclusion type	Tm (°C)	Th (°C)	Te (°C)
Non-luminescent calcite cement					
106830	BS 4	Two phase, pseudo-secondary inclusion.	-2.8	—	-21
		Single phase, pseudo-secondary inclusion.	-3	—	-26
		Two phase, pseudo-secondary inclusion.	-0.1	—	—
		Single phase, pseudo-secondary inclusion.	-2	—	-40
		Single phase, pseudo-secondary inclusion.	-1.1	—	-40
		Single phase, pseudo-secondary inclusion.	-3.7	—	-40
		Single phase, pseudo-secondary inclusion.	-2.3	—	-40
		Single phase, pseudo-secondary inclusion.	-2.2	—	-40
		Single phase, pseudo-secondary inclusion.	-3.3	—	-40
		Two phase, pseudo-secondary inclusion.	-3	—	-30
		Single phase, pseudo-secondary inclusion.	-2.3	—	-28.4
106833	BS 7	Two phase, pseudo-secondary inclusion.	-4.2	—	-33
		Two phase, possibly primary inclusion. Liquid CO ₂	-45.3	27.2	—
		Two phase, possibly primary inclusion.	—	57.4	—
Bright-luminescent calcite cement					
106734	FD 8 105.6	Primary, two phase inclusion.	-13.4	—	-61.8
		Primary, two phase inclusion.	-14.3	—	-61.8
		Primary, two phase inclusion.	-15.3	—	-60.8
		Primary, two phase inclusion.	-13.7	—	-54.1
		Primary, two phase inclusion.	-13.8	79.4	-62
		Primary, two phase inclusion.	-15.1	74.1	-47.5
		Primary, two phase inclusion.	—	90.1	—
		Primary, two phase inclusion.	-12.9	66.2	-58
		Primary, two phase inclusion.	-8.2	—	-55
		Primary, two phase inclusion.	-7.9	53.9	-57
Late ferroan dull-luminescent calcite cement					
106836	BS 10	Large, two phase, primary inclusion.	-1.4	77.7	-23
		Large, two phase, primary inclusion.	—	77.5	—
		Large, two phase, primary inclusion.	0	79.1	—
		Large, two phase, primary inclusion.	—	75.5	—
		Large, two phase, primary inclusion.	—	75.4	—
		Large, two phase, primary inclusion.	—	82.2	—

Trace elements.—Four trace-element analyses were performed on non-luminescent cements from three samples. The non-luminescent cement averaged 2845 ppm magnesium, 195 ppm strontium, 53 ppm sodium, and 32 ppm zinc (Table 2). Concentrations of iron and manganese recorded 0 ppm for three analyses points. The remaining analysis point for manganese recorded 2101 ppm and the remaining analysis point for iron recorded 94 ppm.

Distribution.—The non-luminescent cement was observed in abundance in Frasnian platform facies north of the Copley Valley, at Menyous Gap in the Pillara Range, and within the Fossil Downs Station atoll. A sample from a drill-hole in the platform facies of the Fossil Downs Station area (FD10 113.30 m; Figures 8C, 8D), displayed non-luminescent cement that filled over 90% of the porosity that remained after marine cementation. Samples within the same drill-hole, but at shallower depths (FD 10 28.50 m; Figures 8E and 8F), had less than 60% of the porosity that remained after marine cementation filled by non-luminescent calcite. A sampling traverse was made north of the Copley Valley from the Frasnian reef-margin subfacies, across the Frasnian platform, to the basement contact (Figure 5). Within the reef-flat subfacies (Figures 9A, 9B), the non-luminescent cement occluded approximately 25% of the porosity (post-marine cementation). In the back-reef subfacies, the non-luminescent calcite cement filled from 60 to 100% of the porosity that remained after marine cementation. At Menyous Gap (Pillara Range), a single sample of fenestral limestone from Frasnian back-reef subfacies has clear equant calcite cement that is almost entirely non-luminescent.

The extremely dull, orange-red, banded-luminescent cements occur in the platform facies in the area north of Copley Valley and at Menyous Gap. The cement is non-ferroan (by staining) and the cause of this weak luminescence is unclear. Within the back-reef subfacies of the Brooking Springs Station area, the cement consists of an early phase of dull, orange-red, banded-luminescence (Figures 9C, 9D) and a later phase of uniform, non-luminescence (black). In other pores the non-luminescent cement contains extremely fine (less than 10 μm) bright-luminescent growth bands (Figures 9A, 9B). The non-luminescent cemented platform facies of the Fossil Downs atoll has clear equant cements that are a uniform black under cathodoluminescence. Within lesser non-luminescent cemented platform

facies of this area the non-luminescent cement contains thin bright-luminescent bands.

The non-luminescent cement also occurs in Famennian marginal-slope facies in the Fossil Downs Station area. In these marginal-slope deposits, the non-luminescent cement generally only occludes small pores (less than 1 mm). Large pores, generally have less than 25% of their porosity (post-marine cementation) occluded by the non-luminescent calcite cement.

In the northern Oscar Range, the non-luminescent cement is poorly developed. From the limited number of samples observed from this area, the non-luminescent cement accounts for less than 10% of the clear equant calcite cementation. When it occurs, it generally forms as overgrowths on the scalenohedral marine calcite cement. In the Horse Spring Range area, the non-luminescent cement fills 10% to 40% of the primary porosity (depending on pore size).

2) Bright-luminescent cement zone.

The non-luminescent cement is frequently overgrown by a banded, bright and dull-luminescent zone (bright-luminescent cement). The contact between the non-luminescent and bright-luminescent cement zones is predominantly sharp and conformable (Figures 8A, 8B). The bright-luminescent cement is generally non-ferroan but may contain ferroan zones.

Within the bright-luminescent cement, a distinct, bright-yellow luminescent band commonly occurs directly on the non-luminescent zone. In large pores (larger than 0.5 cm) from the Famennian marginal-slope facies of the Fossil Downs Station area, this bright-yellow luminescent band can be up to 200 μm thick (Figures 8A, 8B). A gradual change from non-luminescent to bright-luminescent cementation, represented by an intervening dull-luminescent band, is sometimes observed (Figures 9E, 9F).

There is a general progression towards duller luminescence in younger bands of the bright-luminescent zone (Figures 8E, 8F), however late bright banding does occur (Figures 8A, 8B). The dull- and bright-luminescent banding within the bright-luminescent zone is conformable and ranges from 10 to 400 μm in thickness (Figures 8A, 8B).

Carbon and oxygen isotopes.—Although the bright-luminescent cement is a common cement phase in the Fossil Downs Station area, it is mostly less than 1 mm thick and therefore could not be drilled as a pure, representative sample for isotope analysis. Four samples were drilled for isotopic analysis, but the samples included some of the dull-luminescent cement which overgrew the bright-luminescent cement zone. Stable isotope compositions for three of the samples have average $\delta^{13}\text{C}$ and $\delta^{18}\text{O}$ values of +1.0‰ (ranging +0.9 to +1.0‰) and -9.8‰ (ranging -11.4 to -7.0‰), respectively (Table 1). The fourth sample drilled for isotopic analysis has an anomalous value compared to the others and was therefore excluded from the averaging. This sample has a $\delta^{13}\text{C}$ value of -0.6‰ and a $\delta^{18}\text{O}$ value of -5.7‰. Although the early part of the bright-luminescent cement in this sample was well preserved, the area of contact with the dull-luminescent cement (which overgrows the bright-luminescent cement) shows disruption of the luminescent banding and has presumably undergone recrystallization to some degree.

Fluid inclusions.—Primary fluid inclusions from a sample (FD8 105.6 m) from the subsurface in the Fossil Downs Station area, are two-phase fluid inclusions (5 to 20 μm). Ten primary fluid inclusions were analyzed from the earlier part of this cement zone. Only four of these provided paired measurements for both homogenization and last-melt temperatures. Homogenization temperatures from five inclusions averaged +72.7°C (ranging +53.9° to +90.1°C). Last-melt temperatures for ice range from -15.3° to -7.9°C, averaging -12.7°C (Table 3). These last-melt temperatures represent salinities of approximately 11.6 to 19 weight % NaCl equivalent. Eutectic temperatures

between -62° and -48°C indicate that other ions besides Na and Cl are contained within these inclusion brines (most probably Ca).

Trace elements.—Four samples containing bright-luminescent calcite cement were analyzed for trace element compositions. For these samples, 23 points within the bright-luminescent cement zone were analyzed (Table 2). The points selected include both bright- and dull-luminescent bands within the zone. The bright-luminescent cement zone averaged 1165 ppm magnesium, 143 ppm strontium, 1528 ppm manganese, 512 ppm iron, and 59 ppm sodium. Two of the points analyzed recorded zinc concentrations above the detectable limit for this element. One of these points (point 3 in HD 9 270 m) recorded 538 ppm zinc in a homogeneous band of bright-luminescent cement. The analysis point was located immediately preceding sphalerite mineralization that coated (and therefore postdated) the homogeneous bright-luminescent cement. The second point (point 12 in FD 8 105 m), contains 267 ppm zinc in a band of dull-luminescent cement. Figure 9F illustrates a botryoid of sphalerite within the bright-luminescent cement in a luminescent band that is the lateral equivalent to the dull-luminescent band that recorded the 267 ppm zinc.

Distribution.—In the Fossil Downs Station area, the bright-luminescent cement is an important porosity-occluding cement in both the Famennian marginal-slope facies and the Frasnian platform facies. This cement accounts for 20 to 60% of the clear equant calcite cementation of primary pores in these limestones. In the northern Oscar Range, the bright-luminescent zone is not well developed and occludes less than 20% of the post-marine cemented porosity (Figures 10A, 10B and 10C, 10D).

In the Horse Spring Range area the bright-luminescent cement occurs as a uniform bright-luminescent cement zone. The bright-luminescent cement zone is up to 1 mm thick in large pores. However, this cement only accounts for approximately 10% of the clear equant calcite cement in these pores.

Figure 10. Thin section photomicrographs of clear equant calcite cement generations in plane-polarized light and cathodoluminescence.

A) A marine cement-lined pore filled by clear equant calcite cement (plane-polarized light). Famennian marginal-slope facies, Elimberrie Bioherm No.2 (EB 2). Scale bar = 0.5 mm. Billiton sample no. 106815

B) Same area in A under cathodoluminescence. The marine cement is overgrown by clear calcite cements. The clear cement consists of the following cement generations from oldest to youngest — non-luminescent scalenohedral (S) cement, thin bright-luminescent (B) equant, uniform dull-luminescent (D) equant, a thin late bright-luminescent (LB) equant, and a late brightly banded-luminescent (BB) equant cement. The arrows indicate the planar truncation surfaces within the late brightly banded-luminescent cement generation.

C) A marine cement-lined cavity filled with clear equant calcite cement (plane-polarized light). Frasnian back-reef subfacies, north-western Oscar Range (OR1). Scale = 0.5 mm. Billiton sample no. 106817

D) Same area in C under cathodoluminescence. The microcrystalline marine cement is overgrown by the non-luminescent scalenohedral (S) cement. The clear equant cement consists of the following cement generations from oldest to youngest — banded bright-luminescent (B), late non-luminescent (N), and late (ferroan) dull-luminescent (LD). The late dull-luminescent may be the correlative of the late brightly banded luminescent cement generation of this study. However, Hurley and Lohmann (1989) illustrated a non-luminescent cement that correlated with the dull-luminescent cement generation of Kerans (1985) (also with the dull-luminescent cement of this study).

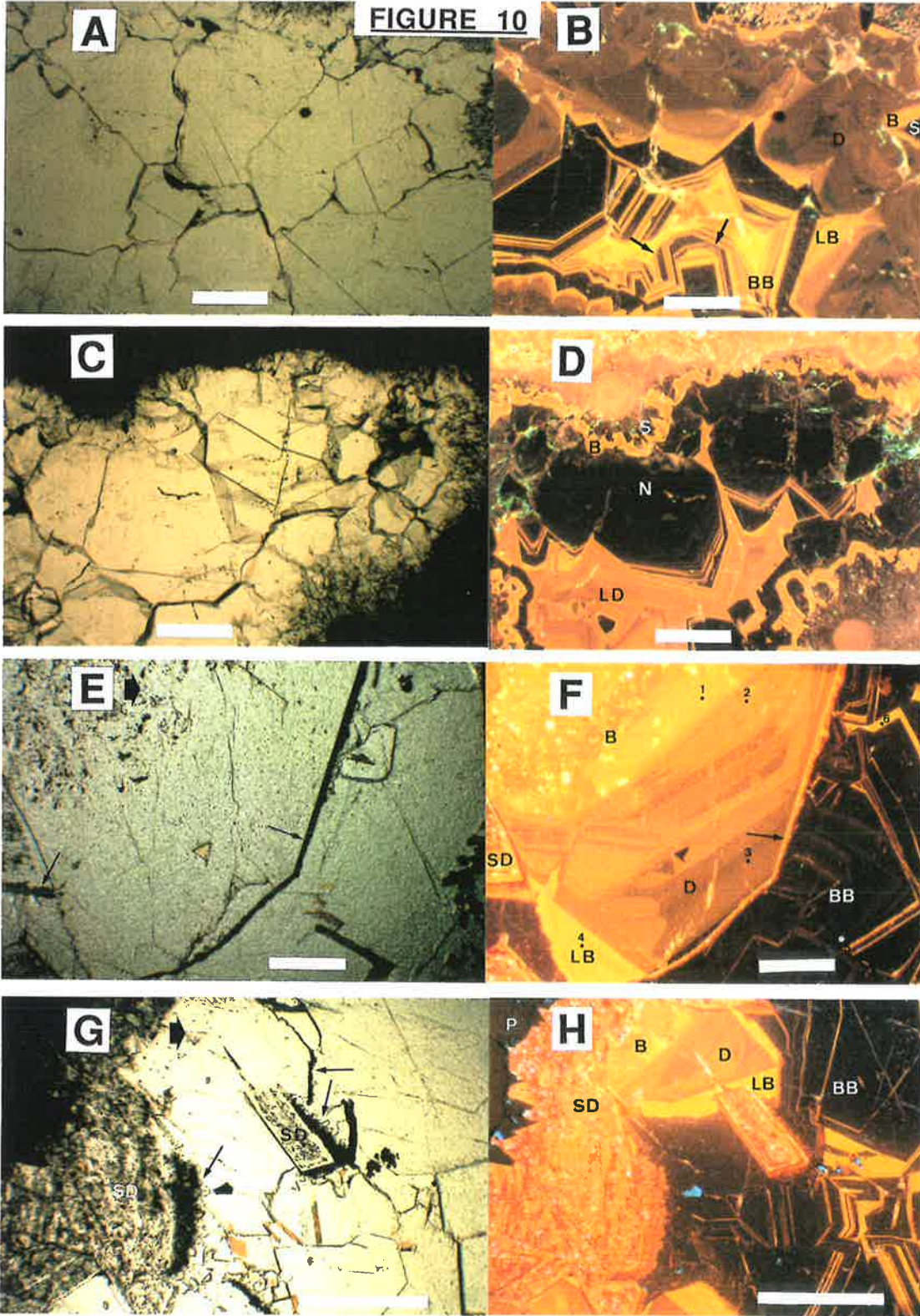
E) A marine cement-lined cavity partially filled by clear equant calcite cement and a red-brown stained calcite cement (plane-polarized light). The thick arrow indicates the upright direction. An opaque layer of iron oxide sediment (thin arrows) occurs within the clear equant calcite cement. Famennian marginal-slope facies, Fossil Downs Station drill-hole FD 15 171.4 m. Scale bar = 0.5 mm. Billiton sample no. 106726

F) Same area in E under cathodoluminescence. The edge of a saddle dolomite crystal is located at the left of the photo. The paragenetic sequence from oldest to youngest is, saddle dolomite (SD), bright-luminescent calcite (B), dull-luminescent calcite (D), late bright-luminescent calcite (LB), iron oxide sediment (arrow), and late brightly banded-luminescent calcite (BB). The dots indicate the positions of microprobe analyses.

G) A different part of the same cavity photographed in 10E and 10F. The thick arrow indicates the upright direction. Iron oxide sediment (thin arrows) covers the upward surfaces of the clear equant cement and the saddle dolomite (SD). Scale bar = 1 mm.

H) Same area in G under cathodoluminescence. Pyrite (P) occurs at the base of the cavity and is overgrown by saddle dolomite. The saddle dolomite (SD) is overgrown by bright-luminescent (B) cement, dull-luminescent (D) cement and late bright-luminescent (LB) cement. After the late bright-luminescent cement, iron oxide sediment was deposited on exposed, upward facing crystal surfaces. Late brightly banded-luminescent (BB) cement overgrew the iron oxide sediment.

FIGURE 10



3) Dull-luminescent cement zone.

Dull-luminescent cements overgrew bright-luminescent cements, non-luminescent cement and precipitated directly onto marine cements. The contact between the dull-luminescent cement and the underlying bright-luminescent cement is conformable and may be either sharp or gradational (Figures 8A, 8B; or Figures 8E, 8F). The dull-luminescent cement is characterized by a uniform, dull, orange-brown luminescence that may be banded, but the contrast in luminescence intensity between bands is small and therefore the banding is not always prominent. This dull-luminescent cement zone is commonly weakly-ferroan (staining pale blue).

Carbon and oxygen isotopes.—Stable-isotope analysis was performed on seven samples drilled from six specimens from the Fossil Downs Station and Brooking Springs Station areas. The isotope values for carbon ranged from -0.2‰ to +2.1‰ and averaged +0.8‰. Oxygen isotope values ranged from -14.1‰ to -9.9‰ and averaged -12.3‰ (Table 1).

Strontium isotope analyses.—Strontium isotope analyses were performed on three samples of dull-luminescent cement. The $^{87}\text{Sr}/^{86}\text{Sr}$ values ranged from 0.71462 to 0.71788 (averaging 0.71589) (Table 4).

Table 4.— Strontium isotopic compositions of the calcite cements.

Billiton sample no.	Sample locality	Calcite cement generation	$\delta^{18}\text{O}$	$\text{Sr}^{87}/\text{Sr}^{86}$	std dev	Sr (ppm)
	Upper Frasnian marine (Lohmann et al. 1989)		-4.5	0.70815	—	—
106802	F3	Brachiopod	-4.7	0.708411	0.000008	—
106787	FD 12 52.8	Marine	-5.6	0.708758	0.000018	—
106803	85.33	Non-luminescent	-5.7	0.708149	0.00001	—
106830	BS 4	Non-luminescent	-6.8	0.708254	0.000014	—
106734	FD 8 105.7	Dull-luminescent	-14.1	0.714621	0.00001	—
106772	FD 10 28.5	Dull-luminescent	-11.5	0.715168	0.000021	—
106735	FD 8 68.72	Dull-luminescent	-13.2	0.717883	0.00002	—
106836	BS 10	Late ferroan dull-lum.	-16.4	0.716663	0.000017	872.51
106825	FD 2	Late ferroan dull-lum.	-14.2	0.717703	0.000018	—

Fluid Inclusions.—Primary fluid inclusions were observed in the dull-luminescent cement. However these two-phase inclusions decrepitated on freezing.

Trace element.—Four samples containing dull-luminescent calcite cement were analyzed for trace-element compositions. For these samples, seven points within the dull-luminescent cement were analyzed (Table 2). The dull-luminescent cement zone averaged 453 ppm magnesium, 115 ppm strontium, 215 ppm manganese, 121 ppm iron, and 80 ppm sodium. Only two analyses points contained detectable zinc concentrations. These two points contained 199 and 160 ppm zinc.

Distribution.—The dull-luminescent zone is the final cement in most of the primary pores of the Fossil Downs Station area. In large pores it can account for over 50% of the clear equant calcite cementation of the pore. In the Fossil Downs Station, Brooking Springs Station and Horse Spring Range areas, most of the primary porosity within the limestones was occluded by the early clear equant cement phases (non-, bright-, and dull-luminescent cements). In the northern Oscar Range, the non-, bright-, and dull-luminescent cement zones only partly fill primary porosity and so are overgrown by younger cement generations. By the end of dull-luminescent cementation in the northern Oscar Range, large primary pores (greater than 0.5 mm in diameter) were generally less than 50% filled by clear equant calcite cements (Figures 10A, 10B; 10C, 10D). Most similar sized pores in the Fossil Downs Station, Brooking Springs Station and Horse Spring Range areas, were 95 to 100% filled by clear equant calcite cements by the end of the dull-luminescent cement phase (Figures 8C, 8D; 9C, 9D; and 9E, 9F). Smaller sized pores in all of these areas were generally totally cemented prior to the end of the dull-luminescent cement phase. Porosity and permeability of the limestone units of the Fossil Downs Station, Brooking Springs Station and Horse Spring Range areas, at this time, were extremely low.

4) Late bright-luminescent cement zone

The boundary between the dull-luminescent cement and the late bright-luminescent cement that overgrew it, may be gradational (Figures 10A, 10B), conformable but sharp (Figures 10E, 10F), or corrosive (Figures 8A, 8B). In sample, FD15 106.9 m (Figures 8A, 8B), basal and internal corrosion occurs and the younger generations of this zone display a progressive brightening in luminescence. In sample FD 15 171.4 m (Figures 10E, 10F), a thin layer of iron oxide sediment separates the late bright-luminescent cement generation from the late brightly banded-luminescent cement that overgrew it.

No fluid inclusion data was obtained from the late bright-luminescent cement.

Carbon and oxygen isotopes.—A single sample of the late bright-luminescent cement (FD15 106.9 m) was drilled for isotopic analysis. The carbon isotope value was -3.3‰ and the oxygen value was -13.0‰.

Trace elements.—Four points (from two samples) within the late bright-luminescent cement zone were analyzed for trace element composition (Table 2). This zone averaged 700 ppm magnesium, 282 ppm strontium, 3028 ppm manganese, 701 ppm iron, and 99 ppm sodium. Two analysis points contained zinc concentrations of 113 and 130 ppm.

Distribution.—The late bright-luminescent cement has not been recorded as a separate cement zone in the Geikie Gorge area (Wallace *et al.* in press) or in the Oscar Range (Hurley and Lohmann 1989). Volumetrically it is of minimal importance as a porosity occluding cement generation. However, the late bright-luminescent cement was observed in two samples, both from marginal-slope facies, in the Fossil Downs Station area. The limited number of samples taken from the northern Oscar Range indicate that this late bright-luminescent cement zone may occur in that area. A sample from Elimberrie Bioherm No. 2 (Figures 10A, 10B) displays a late bright-luminescent cement with a gradational base and internal zonation with progressive increases in

luminescence intensity, overgrown by the distinct late brightly banded-luminescent cement.

5) Late brightly banded-luminescent cement zone (non-ferroan)

The late brightly banded-luminescent cement is closely associated with dissolution cavities and iron oxide sediment in the Fossil Downs Station area. In normal light this cement zone may be clear, red or black calcite. Typically, the late brightly banded-luminescent cement is characterized by fine bright-luminescent bands (10 μm and less) in a predominantly non-luminescent cement (Figures 10E, 10F). The banded cement exhibits distinctive planar and non-planar truncations which are a growth feature that occurs at specific times during cementation (Figures 10A, 10B; 9A, 9B). During the cementation process, some growth surfaces of the pore-filling calcite were planes of little or no growth. Adjacent growth surfaces, in contrast, were planes of continuous growth. As a result of this growth pattern, the late brightly banded-luminescent cement zone sometimes appears to have developed a different crystal morphology to the older cements which it overgrew.

Late brightly banded-luminescent and younger cements are rare in the Fossil Downs Station area as almost all of the primary porosity was occluded by the older cements. One primary pore, that had not been totally cemented, shows the late brightly banded-luminescent cement overgrowing and therefore post-dating the late bright-luminescent cement zone (Figures 10E, 10F; 10G, 10H). A thin layer of iron oxide sediment is present between these two cement generations. This iron oxide sediment is only present on the upward-facing surfaces of the late bright-luminescent cement. Where the late bright-luminescent cement was absent, iron oxide sediment deposited on the older dull-luminescent cement and saddle dolomite. No data was obtained from fluid inclusions for this cement zone.

Carbon and oxygen isotopes.—Three samples of the late brightly banded-luminescent cement from the Fossil Downs Station area were drilled for isotope analysis. Of the three samples, only one (FD15 171.4 m) had the distinct non- and bright-luminescent banding that is characteristic of this zone. The other samples were black calcite spars {a patchy non-, bright- and dull-luminescent cement (FD15 38.20 m) and a predominantly bright-luminescent cement (FD15 63.95 m)}. The black spars occur in fractures and fill the base of karst caverns. The isotopic compositions of these three samples range from -5.4‰ to -2.8‰ (averaging -4.1‰) for carbon and for oxygen range from -9.7‰ to -9.3‰ (averaging -9.5‰) (Table 1).

Trace elements.—Sample FD 15 171.4 m was analyzed for trace-element compositions. Two points, within a non-luminescent band and a bright-luminescent band, were selected for analysis. The non-luminescent band contains 1884 ppm magnesium, 103 ppm strontium, 56 ppm manganese, 188 ppm sodium, and 481 ppm zinc. Iron concentrations were not detected. The bright-luminescent band contains 650 ppm magnesium, 164 ppm strontium, 2568 ppm manganese, 951 ppm iron, and 92 ppm sodium. Zinc concentrations were not detected (Table 2).

Distribution.—The brightly banded-luminescent cement zone is a rare cement generation in the Fossil Downs and Brooking Springs Station areas. In primary pores (marine-cement-lined pores), this cement zone is generally restricted to reef-margin and reefal-slope subfacies which were well cemented by marine cements (Wallace *et al.* in press). The brightly banded-luminescent cement zone is more commonly associated with karst-related dissolution cavities in these areas. In the northern Oscar Range, the brightly banded-luminescent cement is a common cement generation in large primary pores, as well as with karst-related dissolution cavities.

6) Late ferroan dull-luminescent cement zone

The late ferroan dull-luminescent zone was observed in only one primary pore (sample FD2) in the Fossil Downs Station area (within the Famennian marginal-slope facies north of the Fossil Downs atoll). Primary pores in the Fossil Downs Station area were generally filled by earlier cements. The late ferroan dull-luminescent cement was observed filling secondary porosity in dolomites and dissolution caverns in the Brooking Springs Station area. Wallace *et al.* (in press) observed the late ferroan dull-luminescent cement (their "late dull-luminescent cement"), in primary pores of the well-cemented platform margin, where it overgrew the late brightly banded-luminescent zone.

Late ferroan dull-luminescent cements were observed in primary pores in the northern Oscar Range. These ferroan calcite cements were the youngest generation of clear equant cements observed in these primary pores. This cement is a uniform, to weakly zoned, dull-luminescent cement, that is strongly ferroan (staining royal blue). The strong ferroan nature of this zone enables it to be identified in secondary porosity where relationships with earlier cement generations are not always clear. Secondary porosity created by dolomitization or karstification in the northern Oscar Range is commonly filled to some extent by late ferroan dull-luminescent cements. However, the calcite cements filling secondary porosity in the Fossil Downs Station area are rarely ferroan. In the Fossil Downs Station area the poikilitic cements filling such porosity display variable luminescence character and rarely show a strong ferroan nature on staining. Some karst cavities in the Brooking Springs area are filled with late ferroan dull-luminescent cement.

A large calcite-spar-filled cavern within marginal-slope facies in the Brooking Springs Station area contains calcite crystals more than 10 cm in size. A sample of this calcite (BS 10) proved to be strongly ferroan (by staining). The carbon isotope value for this ferroan calcite is -1.1‰ and the

oxygen value is -16.4‰. Six large (30 to 100 μm), two-phase, primary inclusions had homogenization temperatures that ranged from +74.5° to +82.2°C (averaging +77.8°C). Three last melt temperatures obtained from these inclusions were -1.4°, 0° and +1.2°C and a eutectic temperature of -23°C was recorded (Table 3). The last melt temperatures correspond to salinities from 0 to 2 wt.% NaCl equivalent. The positive last melt temperature possibly indicates that a metastable phase formed during freezing of the inclusion or that the inclusion is under negative pressure.

Two other late ferroan dull-luminescent cements were drilled for isotope analysis. These samples were from primary pores from Fossil Downs Station (sample FD 2) area and from Dingo Gap (northern Oscar Range). The carbon values for these samples were -2.4‰ and -4.7‰ respectively and the oxygen values were -14.2‰ and -15.6‰ respectively.

Strontium isotope analyses.—Strontium isotope analyses were performed on two samples of late ferroan dull-luminescent cement. The $^{87}\text{Sr}/^{86}\text{Sr}$ values were 0.71666 and 0.71770 (Table 4).

ORIGIN OF CLEAR EQUANT CALCITE CEMENTS

A summary of the results of the geochemical data for the marine calcite and clear equant calcite cements is presented in Table 5.

Non-luminescent cement.— Microprobe analyses of the non-luminescent cement indicate the iron and manganese concentrations are low (all analyses were below the detectable limits of the microprobe except for one anomolous manganese value). The scarcity of available Mn^{2+} may be due to the oxidized nature of the pore fluids (Frank *et al.* 1982) or a Mn^{2+} deficient source for the pore fluids (Meyers 1974).

Wallace *et al.* (in press) described two possible diagenetic models, based on the distribution, timing, and carbon and oxygen isotope data, for the non-luminescent cement. The first was the topography-driven, meteoric-water model whereby meteoric waters were driven into the carbonates, under shallow burial conditions, by a hydraulic gradient. The second diagenetic model was a marine-burial origin for the non-luminescent cement. This model proposes that the non-luminescent cement precipitated, under shallow burial conditions, from Devonian seawater at temperatures of approximately 25 to 40°C.

Fluid inclusion data indicate that the non-luminescent cement precipitated at temperatures generally less than 50°C, as there is a general lack of two-phase inclusions. Salinities, determined from last-melt temperatures in pseudosecondary inclusions in the non-luminescent cement (Figure 11), range from 0 to 6.6 wt. % NaCl equivalent (seawater ~ 3.5 wt % NaCl equivalent). The main group of salinity values correspond to pore fluids that were equivalent to, and slightly more saline than, seawater (Figure 11). These results, although based on a limited number of

			CALCITE CEMENT ZONES						
			Marine cement	Non luminescent	Bright luminescent	Dull luminescent	Late bright luminescent	Late brightly banded luminescent	Late ferroan dull luminescent
STABLE ISOTOPES	$\delta^{18}\text{O}$	N Range Mean	3 -5.3‰ -5.7‰ to -4.7‰	3 -6.5‰ -7.0‰ to -5.7‰	3 -9.8‰ -11.4‰ to -7.0‰	7 -12.3‰ -14.1‰ to -9.9‰	1 — -13.0‰	3 -9.5‰ -9.7‰ to -9.3‰	3 -15.4‰ -16.4‰ to -14.2‰
	$\delta^{13}\text{C}$	N Range Mean	3 +1.7‰ +0.8‰ to +2.4‰	3 +1.6‰ +0.9‰ to +2.0‰	3 +1.0‰ +0.9‰ to +1.0‰	7 +0.8‰ -0.2‰ to +2.1‰	1 — -3.3‰	3 -4.1‰ -5.4‰ to -2.8‰	3 -2.7‰ -4.7‰ to -1.1‰
STRONTIUM ISOTOPES	$^{87}\text{Sr}/^{86}\text{Sr}$		0.70841 0.70876	0.70815 0.70825	—	0.71462, 0.71517 0.71788	—	—	0.71666 0.71770
FLUID INCLUSIONS	T_E	N		13 -40° to -21°C	10 -62° to -48°C				6 -23°C
	T_{M-ICE} T_{HL-V}	WEIGHT % NaCl	—	-4.2° to -0.1°C (single phase) 0 to 6.6	-15.3° to -7.9°C +53.9° to +90.1°C 11.6 to 19	—	—	—	-1.4° & 0° 75.4° to 82.2°C 2 & 0
TRACE ELEMENTS	Mole % CaCO_3	N Range Mean	3 98.29 to 99.51% 98.95%	4 98.29 to 99.89% 98.9%	23 98.01 to 99.89% 99.28%	7 99.41 to 99.92% 99.75%	4 98.61 to 99.39% 99.13%	2 99.18 & 99.26%	
	Mg (ppm)	Range Mean	1225 to 4614 2757	480 to 3698 2845	174 to 3383 1165	164 to 1167 453	455 to 884 700	650 & 1884	
	Mn (ppm)	Range Mean	15 to 75 322	0 to 2101 525	44 to 8019 1528	70 to 544 215	1619 to 4937 3028	56 & 2568	
	Fe (ppm)	Range Mean	0 to 20 11	0 to 94 24	0 to 2537 512	0 to 369 121	28 to 1725 701	0 & 951	—
	Sr (ppm)	Range Mean	85 to 516 322	76 to 489 195	76 to 489 143	9 to 364 115	0 to 767 282	103 & 164	
	Na (ppm)	Range Mean	28 to 125 75	4 to 127 53	0 to 170 59	0 to 238 80	77 to 138 99	92 & 188	
	Zn (ppm)	Range Mean	39 to 127 70	0 to 82 32	0 to 538 43	0 to 199 51	0 to 130 61	0 & 481	
<p>Table 5.— Summary of Geochemical Data for Calcite Cement Zones</p> <p>N = number of analyses, TE = eutectic temperature, TM-ICE = melting temperature of ice, THL-V = homogenization temperature of liquid and vapour phases.</p>									

measurements, indicate that a simple diagenetic model based solely on marine or meteoric burial may not fully explain the origin of the non-luminescent cement generation.

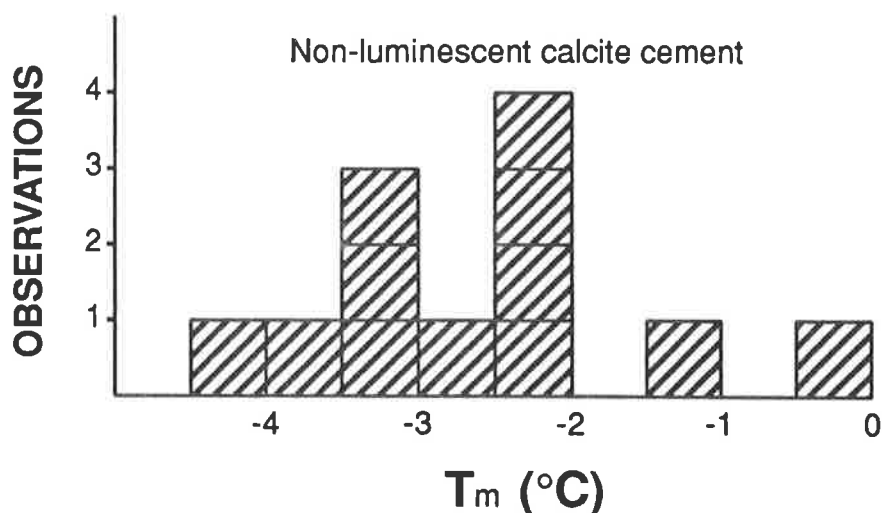


Figure 11.— Distribution of pseudosecondary fluid inclusion final melt temperatures (T_m) for the non-luminescent cement generation. Present day seawater would have a final melt temperature of approximately -2.1°C . The non-luminescent cement precipitated from pore fluids with salinities that were predominantly equal to or slightly more saline than seawater.

Wallace *et al.* (in press) noted that the non-luminescent cement was best developed in the coarse-grained back-reef lithologies that abut Precambrian basement in the Geikie Gorge region. This study has identified the non-luminescent cement as the dominant clear equant cement generation within the coarse-grained back-reef lithologies in the Pillara Range and at depth within the Fossil Downs atoll. However, the occurrence of non-luminescent cement is not solely controlled by the lithologies that maintained high porosities after marine cementation. In the northern Oscar Range, the non-luminescent cement is poorly developed, even within lithologies that had high porosities after marine cementation. The restricted access or distribution of flow paths for the non-luminescent cementing pore fluids may have controlled the occurrence of the non-luminescent cement.

The carbon and oxygen values of the non-luminescent cement, in this study, are consistent with the the data of Wallace *et al.* (in press). The average oxygen isotope value, for the three samples of non-luminescent cement analyzed (Figure 12), is 2‰ lighter than the Late Devonian marine oxygen isotope signature (Hurley and Lohmann 1989). Using the calcite-water oxygen isotope fractionation curve of Friedman and O'Neil (1977), this difference in oxygen isotope composition corresponds to the non-luminescent cement precipitating at an average 10°C higher than the marine cements.

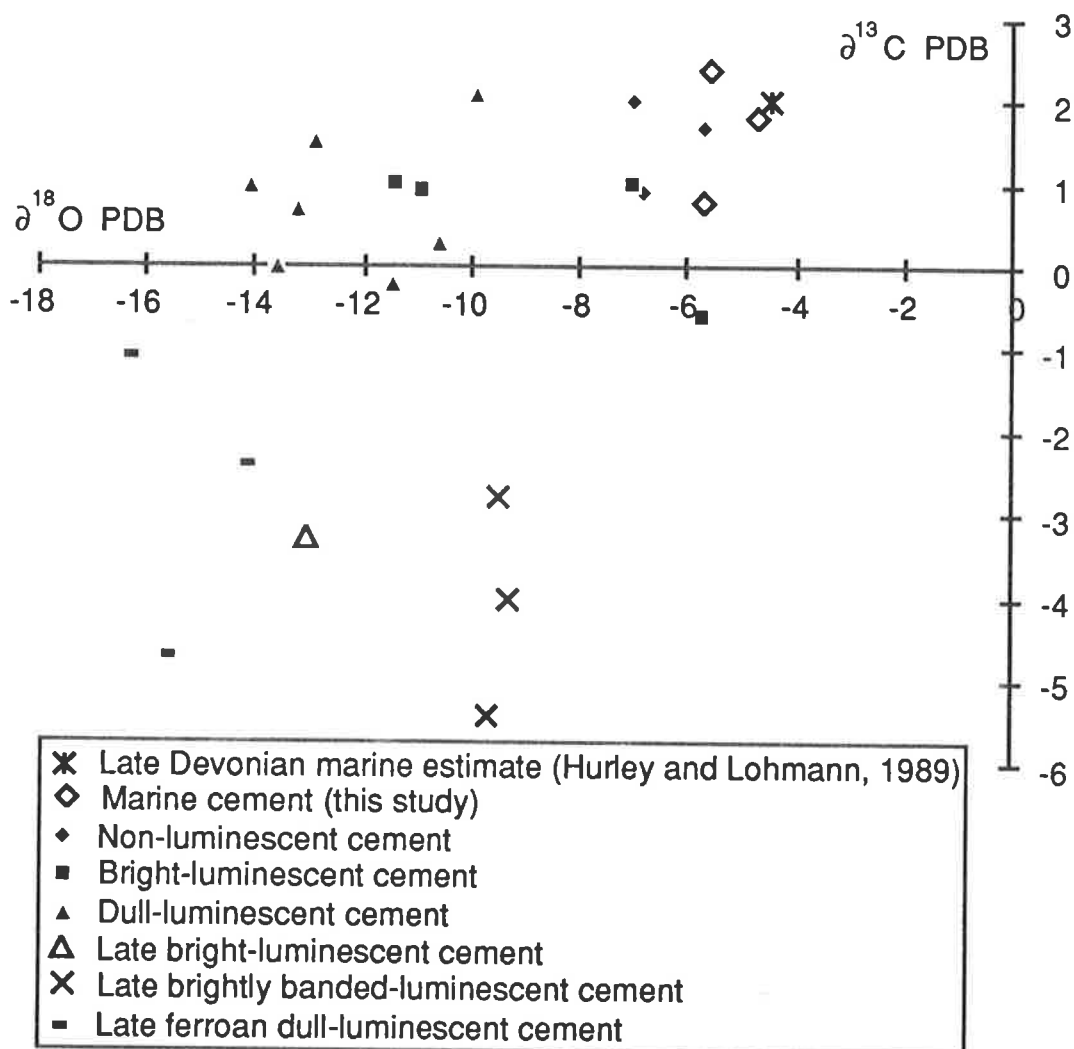


Figure 12.— Carbon and oxygen isotope results for marine and clear equant calcite cements.

The oxygen isotope values for the marine cements analyzed in this study (Figure 12) were slightly depleted compared to the Late Devonian marine value determined by Hurley and Lohmann (1989). This slightly depleted oxygen signature and the mottled luminescence character of these marine cements indicate they may have been recrystallized by later diagenetic processes. Figure 13 shows a plot of the $^{87}\text{Sr}/^{86}\text{Sr}$ ratios versus oxygen isotope values for the marine and non-luminescent cement generations. Also included in the plot is the value assigned to Late Frasnian seawater by Lohmann *et al.* (1989). The marine cements analyzed in this study are radiogenic and isotopically lighter in oxygen, relative to the values recorded for the Late Frasnian (Pillara Limestone) marine cements by Lohmann *et al.* (1989). The slightly higher strontium ratio for the marine cements of this study also suggests that diagenetic alteration has occurred. The $^{87}\text{Sr}/^{86}\text{Sr}$ ratio for the non-luminescent cement averaged 0.70820 and is similar to the Late Frasnian marine strontium value of Lohmann *et al.* (1989). Although the non-luminescent cement precipitated at 10° to 20°C more than the marine cements, the pore fluids were similar in regard to their strontium isotopic signatures.

Based on the fluid inclusion and geochemistry data, as well as the distribution of the non-luminescent cement, a diagenetic model involving precipitation of the non-luminescent cement under shallow burial conditions, from predominantly marine connate fluids, is proposed. Meteoric fluids may have been involved in the non-luminescent cementation but their contribution appears to be much less significant than the connate marine fluids. Terrigenous sandstones and conglomerates interfinger with the Frasnian and Famennian reef complexes and extended from the Kimberley Block into the deep water of the adjoining basins (Playford *et al.* 1989). The non-luminescent cement may have precipitated from the "connate" waters as they were driven, by sediment compaction, from the basinal sediments

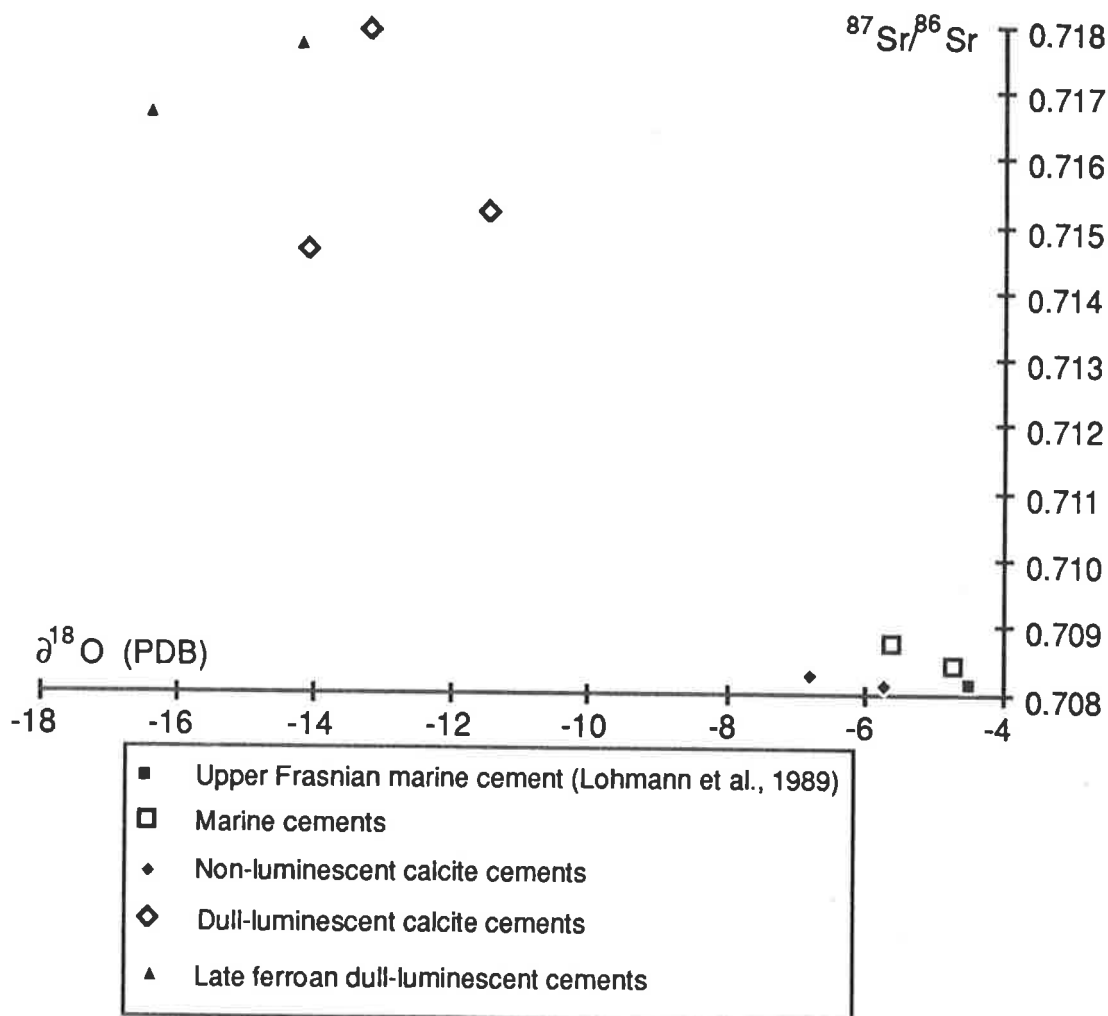


Figure 13.— Strontium and oxygen isotope plot for calcite cements. The Upper Frasnian marine value of Lohmann et al. (1989) is from the Pillara Limestone.

into the more porous and permeable limestone lithologies. The pore fluids were probably predominantly Devonian seawater, held within the pores of limestones and in the adjacent, shallow buried, basinal shales. As the fluids moved from the basinal sediments, the terrigenous sediments may have acted as conduits and focused the fluids through certain areas of the reef complexes (during the Late Devonian/Early Carboniferous). The interstitial meteoric water in the buried terrigenous sediments may have mixed with and diluted the marine fluids during the fluid migration. Terrigenous sandstones and conglomerates interfinger with the marginal-slope deposits in the Fossil Downs Station area. In the Pillara Range, conglomerates and sandstones occur in proximity to the reef platform (Figure 1). In contrast, in

the northern Oscar Range, where the non-luminescent cement is poorly developed, no conglomerates are linked to the reef platform.

Bright-luminescent cement.—The bright- and dull-luminescent bands of the bright-luminescent cement generation have variable and sometimes high concentrations of iron and manganese. The variable luminescence, which is reflected in the iron and manganese concentrations, may have been produced by fluctuating pore fluid redox potentials. As the pore fluids became reduced, manganese existed in solution in its reduced (2+) valence state, and when incorporated into the calcite, produced the bright-luminescence (Frank *et al.* 1982). Stronger reducing pore fluids enable iron to exist in its reduced (2+) valence state and when iron is incorporated into calcite it quenches luminescence, producing dull-luminescence.

Primary, two-phase fluid inclusions analysed in this study indicate the bright-luminescent cement precipitated from moderate to strongly saline (11.6 to 19 wt.% NaCl equivalent) pore fluids, at temperatures at least 53.9° to 90.1°C (not pressure corrected). These temperatures and salinities are inconsistent with an evolving, burial meteoric model.

The $\delta^{18}\text{O}$ values (Figure 12) for the bright-luminescent cement ($\sim -10\text{‰}$ for 3 analyzed samples) are significantly lighter than the Late Devonian oxygen signature (-4.5‰). Using similar $\delta^{18}\text{O}$ values for the bright-luminescent cement and Friedman and O'Neil's (1977) calcite-water oxygen isotope fractionation curve, the bright-luminescent cement would have precipitated at approximately 55-60°C. This temperature is less than most of the homogenization temperatures for the bright-luminescent cement. The following possibilities may explain this result:

(1) The fluid inclusion homogenization temperatures were reset to temperatures and pressures greater than those at the time of entrapment. The primary inclusions in the bright-luminescent cement were selected

because they lacked evidence for stretching or necking. The salinity data are probably reliable, as there is no evidence that the inclusions have leaked. The four inclusions that provide both homogenization and last-melt temperatures show a possible relationship between lower salinities, at lower trapping temperatures. This relationship would not be expected if the inclusions were reset to temperatures and pressures greater than those at the time of entrapment.

(2) The fluid inclusions reflect the trapping conditions of pore fluids when the bright-luminescent cement precipitated. The range of homogenization temperatures recorded for this cement suggest precipitation of the bright-luminescent cement occurred over a range of temperatures. The stable isotope analyses represent a bulk sampling of the bright-luminescent cement.

(3) The moderately high salinities and temperatures suggest that the pore fluids that precipitated the bright-luminescent cement may have been derived from deeply buried basinal brines. If this were the case, the fluids that precipitated the bright-luminescent cement, may have been sourced by fluids with $\delta^{18}\text{O}$ values heavier than the Late Devonian seawater signature.

A basin expulsion model can be used to explain the warm, saline pore fluids from which the bright-luminescent cements precipitated. During Late Devonian/Early Carboniferous burial of the reef complexes, pore fluids were expelled from compacting sediments in the Fitzroy Trough (at depths in the range of 3 to 5 km). The high salinities of the pore fluids may have been produced by shale membrane filtration (Cathles and Smith 1983) or by dissolution of evaporites. The changing redox potential of the pore fluids, as indicated by microprobe analysis and cathodoluminescence, could be the result of episodic pulses of the geopressured brines.

Dull-luminescent cement.— The relatively uniform dull-luminescent cement contains moderate to low concentrations of iron and manganese. The dull-luminescence is due to the low manganese concentrations and the relatively higher iron/manganese ratio of this cement generation compared to the bright-luminescent cement. The higher iron/manganese ratio of the dull-luminescent cement, compared to the bright-luminescent cement, is probably due to the more strongly reducing pore fluid nature of the dull-luminescent cement. The comparative low concentrations of manganese and iron in the dull-luminescent cement, compared to the bright-luminescent cement, may indicate that the pore fluids were "spent" after the mineralization event (discussed later).

Fluid inclusions in the dull-luminescent cement are two-phased but no homogenization or salinity measurements were obtained. The dull-luminescent cement has lower $\delta^{18}\text{O}$ values and higher $^{87}\text{Sr}/^{86}\text{Sr}$ ratios than the earlier cement generations of the reef complexes (Figure 13). The reef complexes inherited the strontium isotopic composition of Late Devonian seawater. The pore fluids must have been sourced from highly radiogenic sediments.

Stueber *et al.* (1984) illustrated a similar situation for the Upper Jurassic Smackover Formation. They suggested that the radiogenic strontium was released from detrital clay minerals and potassium feldspar during compaction and expulsion of interstitial pore fluids in shales. The dull-luminescent cement, of this study, may be the product of the continued evolution of basinal derived fluids flowing into the carbonates during Early Carboniferous burial. As the basinal fluids evolve, the interaction of the pore fluids with the detrital sediments results in the fluids becoming more radiogenic with time.

Late bright-luminescent cement.— The change from dull-luminescent back to bright-luminescent cementation can occur as a result of both an increase or a decrease in Eh conditions of the pore fluids (Frank et. al 1982). In environments where sulphate reduction produces reduced sulphur species, FeS₂ may precipitate with a Fe²⁺-poor calcite, which would display bright-luminescence. However, the late bright-luminescent cement did not contain coeval FeS₂ in the samples from Fossil Downs Station. In contrast, an increase in Eh of the pore fluids would result in the precipitation of bright-luminescent cement and, if Eh increased sufficiently, co-precipitation of calcite and iron oxide would occur. One sample from the Fossil Downs Station area displayed a cementation sequence in which the late bright-luminescent cement was postdated by non-luminescent calcite that was coeval with iron oxide.

The sequence of cementation from dull-luminescent, through bright-luminescent, to non-luminescent cementation (with iron oxide) may be explained by a change from burial conditions to exposure of the reef complexes to meteoric (oxidizing) waters. The late bright-luminescent cement would therefore represent the intermediate or uplift stage of this sequence. The late bright-luminescent cement has a negative carbon isotope signature relative to the earlier cement generations (Figure 12). The light carbon isotope ratio for the late bright-luminescent cement probably resulted from incorporation of organic carbon. The origin of the organic carbon is not known, but it is possible that the fluids that produced the higher Eh conditions (precipitating the late bright-luminescent cement) were derived from deeply penetrating karst fluids. These karst fluids may have incorporated light soil carbon.

Microprobe analyses display an increase in both iron and manganese content from dull-luminescent cementation to late bright-luminescent cementation. The Eh model predicts a decrease in iron content

during over this transition as iron converts to its oxidized valence state (Fe^{3+}). The increase in the manganese and iron concentration, from the dull-luminescent cement to the late bright-luminescent cement, reflects a change in the source, as well as Eh, of pore fluids.

Late brightly banded-luminescent cement.— The non- and bright-luminescent banding and coeval iron oxide precipitation, indicates oxidizing conditions of the pore fluids when this cement was precipitated. The relatively uniform $\delta^{18}\text{O}$ values (-9.5‰) and the variable $\delta^{13}\text{C}$ values (ranging from -5.4‰ to -2.8‰) (Figure 12) indicates that the cement was precipitated from meteoric fluids. This cement postdates the late bright-luminescent cement that is interpreted to be of Late Carboniferous uplift origin. The late brightly banded-luminescent cement is overgrown by cements of burial origin (late ferroan dull-luminescent cement) and is therefore considered to be related to the Late Carboniferous karst event. A microprobe analysis point in the late brightly banded-luminescent cement contained zinc in concentrations above the detectable limit. Zinc was probably derived from dissolution of sphalerite by the meteoric fluids. Field observations confirm the remobilization of sulphide mineralization by the Late Carboniferous meteoric fluids.

Late ferroan dull-luminescent cement.— The late ferroan dull-luminescent cement is the youngest cement generation (of significance) observed in the Devonian reef complexes on the Lennard Shelf. Primary fluid inclusions indicate this cement generation was precipitated from almost fresh water at temperatures at least 75.4° to 82.2°C. Hurley and Lohmann (1989) proposed that this cement generation may have been derived from hot basinal fluids. Wallace *et al.* (in press) suggested the low

$\delta^{18}\text{O}$ values may reflect high temperatures of precipitation and/or a meteoric water contribution.

A burial depth of 2500 m would be needed to account for the homogenization temperatures of the late ferroan dull-luminescent cement. A pressure correction (Potter 1977) of 30°C (25 MPa) would also need to be applied to the homogenization temperatures to obtain the temperature at which the late ferroan dull-luminescent cement precipitated.

Based on apatite fission track analysis, Arne *et al.* (1989) proposed that the Devonian carbonates were buried (1500 m) in the Late Palaeozoic/Early Mesozoic and attained maximum temperatures of 70° to 80°C. These values are significantly less than the 110°C and corresponding burial depth of 2500 m indicated by fluid inclusions in the late ferroan dull-luminescent cement.

The late ferroan dull-luminescent cement has extremely light carbon and oxygen isotopic ratios compared to the other calcite cement generations (Figure 12). The late ferroan dull-luminescent cement also has a high $^{87}\text{Sr}/^{86}\text{Sr}$ ratio. These results are consistent with precipitation of this cement generation in the deep burial diagenetic environment. Meteoric connate fluids within terrigenous sediments of the Grant Group may have supplied some of the pore fluids for the precipitation of the late ferroan dull-luminescent cement. The interaction of the fluids with the Grant Group sediments, over the relatively long period of burial (Permian to Triassic), may have provided the radiogenic strontium.

DOLOMITIZATION, MINERALIZATION AND KARSTIFICATION

DOLOMITES

At least three distinct generations of dolomite have been formed within the Devonian reef complexes of the Lennard Shelf. These have been termed synsedimentary (fabric-mimicking) dolomite, regional (fabric-destructive dolomite plus fine grained dolomite cement) dolomite, and saddle dolomite. On a regional scale, the reef complexes of the Lennard Shelf have not been extensively dolomitized. However on a local scale, totally dolomitized lithologies, tens of metres in thickness and lateral extent, do occur.

Synsedimentary Dolomite

Very fine grained ($\leq 10 \mu\text{m}$), fabric-mimicking, peritidal dolomite occurs in basal Pillara Limestone (Givetian-Lower Frasnian) in the Emanuel Range. Fabric mimicking dolomites were not observed in the Fossil Downs Station, Brooking Springs Station, or Horse Spring Range areas. A single sample of fabric-mimicking dolomite was analyzed to compare the carbon and oxygen isotope values for this type of dolomite with isotope values of coarser grained dolomites from the Fossil Downs Station and Brooking Springs Station areas. The synsedimentary dolomite from the Cadjebut Mine area (Emanuel Range) had a carbon isotope signature of $+0.2\text{‰}$ (PDB) and an oxygen isotope signature of -0.5‰ (PDB).

Regional Dolomite

The regional dolomite is volumetrically the most important dolomite generation observed in the outcropping limestones of the Lennard Shelf, from the Emanuel Range to the Napier Range. This dolomite is predominantly a replacement dolomite (fabric-destructive), although it sometimes occurs as a cement in primary pores in partially dolomitized lithologies. The crystals range from 80 to 200 μm in size. Euhedral crystals of regional dolomite are observed when lithologies have been only partially dolomitized and when the dolomite

occurs as a pore-lining cement. In pervasively dolomitized lithologies, dolomite crystals are subhedral to anhedral .

The regional dolomites are characterized by an inclusion-rich core and a clear rim when observed in transmitted light. In cathodoluminescence, the regional dolomites have a non-luminescent core (corresponding to the inclusion rich core) and a thin, bright orange-red luminescent (inclusion poor) rim. In the Fossil Downs atoll the regional dolomite generally does not display this clear cathodoluminescence zonation. These regional dolomites have a patchy, mostly bright-luminescent character, but often show well-banded overgrowths. This patchy bright-luminescence may be due to neomorphism by the later diagenetic fluids.

The regional dolomite preferentially replaces some limestone components while others remain undolomitized. The susceptibility of components to dolomitization, from most to least susceptible are: geopetal micrite; micritic matrix; ooids and peloids; skeletal components; and marine and blocky cements (Kerans 1985). The order of susceptibility to dolomitization is due to permeability as well as crystal size (Wallace *et al.* in press).

Dolomite cements occur in moldic pores in dolomite, in fractures, and in primary pores in partially dolomitized limestone. In many of the partially dolomitized limestones, the geopetal sediments in primary pores are often the only component replaced by dolomite. As well as the replacement dolomite of the geopetal sediment, dolomite cements may also occur and form as a thin pore-lining cement and/or grow directly on the upper surface of the dolomitized geopetal sediments. The dolomite cement crystals are fine grained, but within the size range of the regional dolomite. They also have the same luminescence zonation as the regional dolomite, indicating they were probably precipitated from the same generation of pore fluids.

The occurrence of dolomite cements in primary pores enables the relative timing, between the clear equant calcite cement zones and the

regional dolomite, to be established. In the Brooking Springs Station/Geikie Gorge area, superposition relationships are clear. The non-luminescent core of the regional dolomite is often observed in direct contact with the outer edge of the non-luminescent calcite cement (Figures 14A, 14B). Obstruction to the growth of the non-luminescent calcite cement, by the regional dolomite, was not observed. However, the growth of the regional dolomite was obstructed, as it abuts obliquely against the non-luminescent calcite cement. These relationships are evidence that the main stage of regional dolomitization (non-luminescent dolomite) postdated the non-luminescent calcite cement generation. The brightly banded-luminescent calcite cement (that postdates the non-luminescent calcite) abuts obliquely against the non-luminescent regional dolomite core, indicating the brightly banded-luminescent calcite cement generation postdated the main stage of regional dolomitization (Figures 14A, 14B). However there was some overlap between the later stages of regional dolomitization (banded-luminescent dolomite rim) and the earliest part of the brightly banded-luminescent calcite cement. The bright-luminescent rim of the regional dolomite and the bright-luminescent calcite cement display an alternation in growth and where these two zones were in direct contact a "stepped" growth pattern developed (Figures 14A, 14B).

Within partially dolomitized limestones, dolomite is often observed along stylolites. The dolomite along the stylolites has the same luminescence character as the regional dolomite. Pores that are near the stylolite are often lined with a thin zone of dolomite while pores further away from the stylolite may not contain any dolomite. This indicates that the stylolites acted as conduits for the dolomitizing fluids.

No fluid inclusion data was obtained from the regional dolomites due to their turbid nature and small size of the inclusions.

Carbon and oxygen isotope analysis.—Stable isotope analyses were performed on 39 samples of regional dolomite and include 24 surface samples

Figure 14. Thin-section photomicrographs and core samples illustrating calcite cementation, dolomitization and mineralization paragenesis.

A) A cement-filled pore within fenestral limestone filled by clear equant cement and two regional dolomite (D) rhombs (plane-polarized light). Note the jagged or stepped (arrow) contact of the dolomite with the clear equant calcite. Frasnian back-reef subfacies, Copley Valley (BS 6). Scale bar = 0.1 mm. Billiton sample no. 106832

B) Same area in A under cathodoluminescence. Non-luminescent (NC) calcite cement is the first clear equant cement generation. The non-luminescent (ND) core of the regional dolomite rhomb was obstructed during its growth by the non-luminescent calcite and therefore the regional dolomite post-dates the non-luminescent calcite cement. The paragenetic sequence following the non-luminescent dolomite core is from oldest to youngest, bright-luminescent dolomite (D1), bright-luminescent calcite, duller-luminescent dolomite (D2), remainder of the bright-luminescent (B2) calcite, and dull-luminescent (DC) calcite. The black lines indicate the boundaries between the cement generations.

C) A cavity with pyrite (P) at the base and filled with inclusion-rich saddle dolomite (SD) and clear equant calcite cement (plane-polarized light). Arrow indicates upright direction. Famennian marginal-slope facies, Fossil Downs Station drill-hole FD 15 171.4 m. Scale bar = 0.5 mm. Billiton sample no. 106726

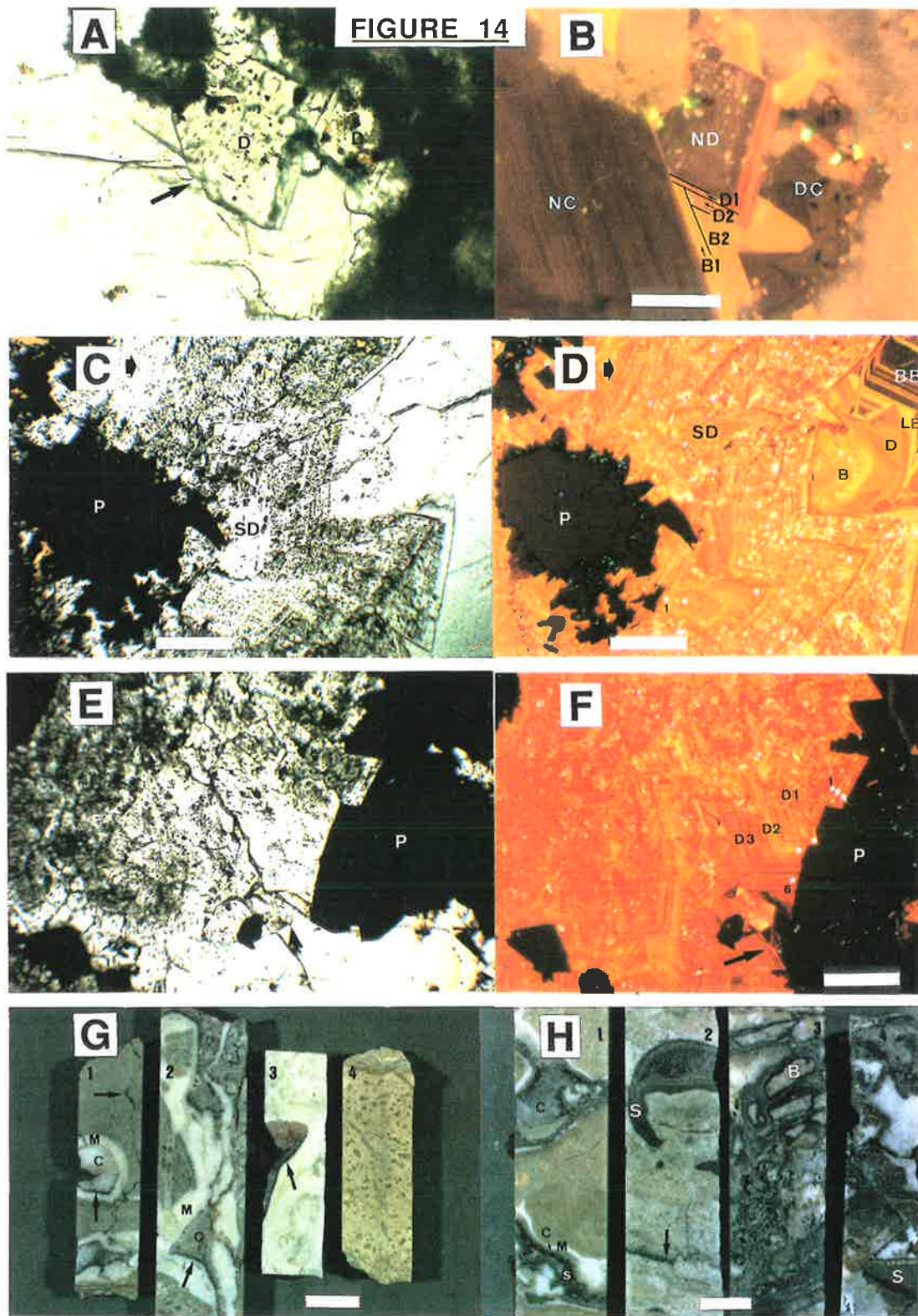
D) Same area in C under cathodoluminescence. The paragenetic sequence of this pore consists of the following — pyrite (P), saddle dolomite (SD), bright-luminescent calcite (B), dull-luminescent calcite (D), late bright-luminescent calcite (LB), and late brightly banded luminescent calcite (BB). The saddle dolomite displays banded luminescent zonation. The dots indicate the position of microprobe analyses points.

E) Dolomite with inclusion-rich cores and clear rims (plane-polarized light). The opaque mineral is pyrite (P). Famennian marginal slope facies, Fossil Downs Station drill-hole FD 8 274.9 m. Scale bar = 0.5 mm. Billiton sample no. 106781

F) Same area in E under cathodoluminescence. The inclusion-rich cores of the regional dolomite (D1) have a patchy non- and bright-luminescent character as a result of recrystallization. After the regional dolomite, an early bright-luminescent dolomite (D2) cement and a later banded dull- and bright-luminescent dolomite (D3) cement were precipitated. The dolomite cements have curved crystal faces (arrow). Pyrite (P) occurs early within the early bright-luminescent dolomite (D2) cement generation. The dots indicate the location of microprobe analyses points.

G) Core samples displaying porosity types and the occurrence of mineralization. Core samples 1, 2, and 3 illustrate sulphide mineralization (arrows) in primary, marine cement-lined (M) pores from Famennian marginal-slope facies. The sulphides occur after marine cementation and before the majority of the clear equant calcite cement (C). Mineralization occurs predominantly at the base of the pores but also in fractures. {1. Fossil Downs Station drill-hole FD 8 105.6 m (106734). 2. Fossil Downs Station drill-hole FD 18.8 m (106718). 3. Fossil Downs drill-hole FD 8 68.7m (106735)}. Core sample 4 is fenestral limestone from Frasnian platform facies. The sample does not contain any sulphides. {4. Brooking Springs Station drill-hole FD 17 66.5 m.(106760)}. Scale bar = 1 cm

H) Mineralized core samples. 1. Marine cement forms a thin pore-lining on a synsedimentary breccia in Famennian marginal slope facies. A thin clear calcite cement zone (C arrow) overgrew the marine cement before sphalerite (S) precipitated. The remainder of the porosity was filled by clear calcite (C). {1. Horse Spring Range drill-hole HD 9 270.6 m (106779)}. 2. Intraparticle pore of a mollusc lined by sphalerite (S) and filled by later clear calcite. Mineralization also occurs along the stylolite (arrow). {2. Fossil Downs drill-hole FD 8 179.2 m (106737)}. 3. Sulphides coating breccia clasts (B). The breccia clasts are not lined by marine cement, suggesting brecciation occurred outside the marine diagenetic environment. {3. Fossil Downs drill-hole FD 5 116.9 m (106790)}. 4. Dolomitized and mineralized core sample. Mineralization occurs predominantly around breccia clasts but intercrystalline mineralization also occurs. The sulphides at the base of the pore (S) are stratified. {4. Fossil Downs FD 18 272.4 m (106707)}. Scale bar = 1 cm.



from locations across the Lennard Shelf. The remaining 15 regional dolomite samples are from exploration drill cores in the Fossil Downs Station, Brooking Springs Station and Horse Spring Range areas. The average $\delta^{13}\text{C}$ and $\delta^{18}\text{O}$ compositions for all the regional dolomites were +1.9‰ (ranging +0.5‰ to +2.9‰) and -4.5‰ (ranging -2.4‰ to -8.4‰) respectively (Table 6).

Table 6.—Carbon and oxygen isotopic compositions of the synsedimentary, regional, and saddle dolomite generations.

Billiton number	$\delta^{18}\text{O}$ (PDB)	$\delta^{13}\text{C}$ (PDB)	LOCATION / DEPTH	Billiton number	$\delta^{18}\text{O}$ (PDB)	$\delta^{13}\text{C}$ (PDB)	LOCATION / DEPTH
Regional Dolomite							
106804	-4.7	2	Fossil Downs (F9A)	106823	-2.4	2.1	Horse Spring Rng (HD7)
106708	-5.9	1.8	FD 18 276.6-276.9	106829	-3.4	1.9	Brooking Springs (BS3)
106795	-2.9	2	Horse Spring Rng (HSR1)	106807	-4.2	1.4	Glenister Knolls (GK)
106706	-5.7	2.5	FD 18 240.95-241.50	106819	-4.6	2.4	Windjana Gorge (WG)
106729	-5.9	1.5	FD15 220.00-220.14	106821	-3.1	1.6	Horse Spring Rng (HDD1)
106782	-7.2	2.5	FD 19 55.90-56.05	106814	-4.8	1.8	Elimberrie Bioherm (EB1)
106744	-7.7	2.2	FD 16 271.85-272.07	106840	-3.1	1.5	Geikie Gorge (GG1)
106707	-5.1	1.8	FD 18 272.40-272.50	106830	-5.0	0.9	Brooking Springs (BS4)
106799	-3.7	2.1	Geikie Gorge (85.53A)	106834	-3.5	2.7	Brooking Springs (BS8)
106803	-3.1	1.8	Geikie Gorge (85-112)	106854	-4.4	1.8	FD8 231.8
106801	-6.5	0.6	Geikie Gorge (MW1A)	106839	-2.8	2.3	Nth Pandanus Springs (NPS)
106827	-3.8	2.6	Brooking Springs (BS1)	106857	-5.2	1.1	FD3 29.40
106843	-3.8	2.3	Napier Downs (NDS)	106784	-6.8	2.4	FD3 200.66
106842	-3.6	1.9	Narlarla Deposit (ND)	106728	-5.3	1.4	FD15 223.49
106838	-3.5	2.7	Brooking Springs (BS12)	106751	-8.4	2.0	FD16 166.88
106824	-3.6	1.4	Fossil Downs (FD1)	106747	-6.0	1.6	FD16 241.43
106825	-4.4	0.5	Fossil Downs (FD2)	106747	-6.0	1.7	FD16 241.43
106828	-3.6	2.9	Brooking Springs (BS2)	106775	-3.7	1.6	HD7 109.10
106831	-2.9	2.1	Brooking Springs (BS5)	106779	-2.9	2.2	HD8 44.12
106826	-3.9	1.7	Fossil Downs (FD3)	106777	-3.5	1.8	HD9 50.7
Syn depositional dolomite							
106858	-0.5	0.2	"No Way Gossan" (NWG)				
Dolomite with saddle dolomite overgrowths							
106701	-8.5	2.6	Findlay Hill (FH1A)	106740	-9.6	2.7	Brooking Springs (B1)
106701	-4.4	2.4	Findlay Hill (FH1B)	106820	-3.5	2.0	Findlay Hill (FH90F)
106793	-7.6	2.1	Brooking Springs (B1A)	106820	-7.6	2.6	Findlay Hill (FH90D)
Saddle Dolomite							
106725	-8	1.8	FD 15 225.86-225.92	106781	-5.9	1.5	FD 8 274.90-275.00
106705	-8.4	1.5	FD 18 228.4-228.55	106744	-9.5	2.4	FD 16 271.85
106752	-9.4	2.3	FD 16 203.15-203.25	106855	-5.5	1.1	FD8 271.1
106708	-6.6	1.5	FD 18 276.60-276.90	106856	-5.5	1.5	FD3 26.00
106722	-7.8	2.3	FD 15 168.40-168.50				

The exploration drill cores are biased to areas where mineralization has been or occurring in the subsurface. A comparison between surface and subsurface regional dolomite was made to determine if there was any significant difference in their isotopic compositions. The average $\delta^{13}\text{C}$ value for both surface and core samples was the same, +1.9‰ (ranging +0.5‰ to +2.9‰ and +1.1 to +2.5‰ respectively). The average $\delta^{18}\text{O}$ values were different with surface

were different with surface samples averaging -3.8‰ (ranging -2.4‰ to -6.5‰) and core samples averaging -5.6‰ (ranging -2.9‰ to -8.4‰).

The regional dolomites display weakly to strongly ferroan characteristics when treated with potassium ferricyanide. Surface samples were mainly weak to moderately ferroan while subsurface samples were generally strongly ferroan. In some of the strongly ferroan dolomites, the regional dolomite cathodoluminescence zonation has been overprinted so that the dolomite now displays bright-luminescence. These dolomites may also have significant amounts of banded-luminescent dolomite overgrowths filling intercrystalline pores. These bright-luminescent (neomorphosed) dolomites, with banded-luminescent overgrowths, have lighter oxygen isotope values compared to the regional dolomite. However, when the luminescence zonation of the regional dolomite is the same for both strongly ferroan and weakly ferroan dolomite, there is no correlation between lighter oxygen isotope values and the more ferroan dolomite. Present-day weathering processes may be responsible for extracting iron from the regional dolomite without dedolomitization occurring. This could explain why surface dolomites are generally weakly ferroan while subsurface dolomite (protected from weathering processes) are ferroan.

Strontium isotope analyses.—Strontium isotope analyses were performed on five samples of regional dolomite (Table 7). The $^{87}\text{Sr}/^{86}\text{Sr}$ values range from 0.708857 to 0.713755 (averaging 0.711615).

Table 7.—Strontium isotope values for the regional and saddle dolomite generations.

Billiton sample no.	Sample locality	Dolomite generation	$\delta^{18}\text{O}$	$\text{Sr}^{87}/\text{Sr}^{86}$	std dev	Sr (ppm)
Upper Frasnian marine (Lohmann et al., 1989)			-4.5	0.70815	—	—
106826	FD 3	Regional dolomite	-3.9	0.708857	0.000018	—
106831	BS 5	Regional dolomite	-2.9	0.709778	0.000026	—
106795	HSR	Regional dolomite	-2.9	0.712192	0.000015	—
106779	HD 8 44.12	Regional dolomite	-2.9	0.713493	0.000014	—
106854	FD 8 231.8	Regional dolomite	-4.4	0.713755	0.000011	—
106855	FD 8 271.1	Saddle dolomite	-5.5	0.711133	0.000014	91.38
106705	FD 18 228.4	Saddle dolomite	-8.4	0.712794	0.00001	—
106722	FD 15 168.4	Saddle dolomite	-7.8	0.713294	0.000014	—
106752	FD 16 203.2	Saddle dolomite	-9.4	0.71328	0.000026	—
106725	FD 15 225.9	Saddle dolomite	-8	0.714028	0.000012	—

Distribution.—Regional dolomite was observed in both Frasnian and Famennian carbonates on the Lennard Shelf. Frasnian back-reef subfacies immediately adjoining the reef-flat subfacies is strongly dolomitized in the Geikie Gorge region (Wallace *et al.* in press). Marginal-slope facies may or may not be dolomitized. A dolomite-sampling traverse was made across Frasnian and Famennian marginal-slope facies east of Geikie Gorge (Figure 5). The distal (Famennian) marginal-slope facies is partially (fabric selective) dolomitized. Marginal-slope facies is more dolomitized towards the west, where Frasnian distal fore-reef and proximal fore-reef subfacies is totally dolomitized. The Frasnian reef-flat subfacies has not been dolomitized but the back-reef subfacies immediately adjoining it is totally dolomitized.

The marginal-slope facies of the Fossil Downs atoll is strongly dolomitized in part. Drill-cores indicate that the dolomite may occur as a non-strata-bound unit in the marginal-slope facies of the Fossil Downs atoll. Drill-cores from marginal-slope facies near Brooking Springs Station homestead display variable degrees of dolomitization, but the dolomite appears to be more strata-bound than in the Fossil Downs atoll. North-northwest of Brooking Springs homestead, no dolomite was observed in any of the outcropping platform or marginal-slope limestones.

Elsewhere on the Lennard Shelf regional dolomite occurrence is also variable in quantity and distribution. At Windjana Gorge, in the Napier Range, vertical sections are well exposed through the Pillara Limestone. Beds up to one metre in thickness are totally dolomitized over lateral distances of tens of metres. These dolomitized beds are bounded above and below by undolomitized limestone beds of similar thicknesses. The vertical transition from totally dolomitized to undolomitized beds is gradational and the dolomite is predominantly restricted to individual beds. The beds that were dolomitized were the more porous and permeable Amphipora-rich carbonates.

Saddle Dolomite

Saddle dolomite (as defined by Radke and Mathis 1980) is a variety of dolomite characterized by curved cleavage and crystal faces, and sweeping extinction. This distinctive form of dolomite is almost invariably accompanied by adjacent sulphides in the carbonates of the Lennard Shelf (Figures 14C, 14D). Volumetrically, this saddle dolomite is considerably less important than the regional dolomite generation. Individual crystals may be up to 0.5 cm in diameter and display undulose extinction in cross-polarized light.

Saddle dolomite occurs almost exclusively as a void-filling cement (rather than as a replacement dolomite) in carbonates in the Fossil Downs Station and Brooking Springs Station areas. Saddle dolomite cementation occurs as an overgrowth on the regional dolomite (filling intercrystalline pores, fractures, and solution vugs) as well as lining fractures and marine cemented pores in undolomitized lithologies. Additionally, saddle dolomite sometimes occurs as an intergranular cement in coarse grainstones.

When saddle dolomite occurs as overgrowths on the regional dolomite, the contact between the two generations is conformable (Figures 14E, 14F). The regional dolomite phase is generally more inclusion rich than the saddle dolomite phase. Growth bands in the saddle dolomite are enhanced by changes in the density of inclusions. Cathodoluminescence of the saddle dolomite overgrowths is characterized by bright- and dull-luminescent banding (orange-red luminescence). The earlier luminescent bands tend to be dominated by brighter luminescing dolomite compared to the later dull-luminescent bands. The regional dolomites, on which the saddle dolomites overgrow, have a patchy bright and dull-luminescent character. This is in contrast to the well-developed non-luminescent core, with a thin banded-luminescent rim, observed in regional dolomites in areas where saddle dolomites do not occur. The patchy luminescence of the

regional dolomites is probably due to re-equilibration in the fluids that precipitated the saddle dolomite generation.

Saddle dolomite crystals lining fractures and marine cemented pores in undolomitized lithologies are generally large and more inclusion-rich than the saddle dolomite overgrowths on the regional dolomite. These large saddle dolomites also tend to have thicker luminescent bands than the overgrowth saddle dolomite. In undolomitized lithologies the saddle dolomite preferentially grows on geopetal sediment and sulphides, occasionally precipitating on marine cements and later sparry calcite.

When saddle dolomites occur with clear equant calcite, the bright-luminescent calcite cement both predates and postdates the saddle dolomite, but most postdate the saddle dolomite. This relationship indicates that the saddle dolomite formed at a time equivalent to the early part of the bright-luminescent calcite cement. The outer zones of the saddle dolomite sometimes exhibit an alternation in growth with calcite cementation. Saddle dolomites were precipitated soon after the regional dolomitization event.

Potassium ferricyanide staining indicates that large saddle dolomites are generally non-ferroan or low-ferroan while the overgrowth saddle dolomites range from non- to strongly ferroan. Saddle dolomite cement within intergranular porosity in grainstones (from surface samples at Findlay Hill and Brooking Springs Station) may be strongly-ferroan. Trace-element analysis also distinguishes significant differences in the iron content of zones within the saddle dolomite.

Fluid Inclusions.—Primary fluid inclusions in the saddle dolomites are large (5 to 10 μm) compared to the inclusions in the regional dolomites. The fluid inclusions are two-phased and occur randomly orientated or aligned with cleavage. The randomly orientated inclusions occur in inclusion-rich zones that delineate growth zones. These inclusions are considered to be of primary origin, and nine inclusions (Table 8) provided

homogenization temperatures ranging from 75.8° to 89.1°C (averaging 82.2°C). No freezing temperatures were obtained from the saddle dolomite inclusions.

Table 8.—Homogenization (Th) and last melt (Tm) temperatures of primary fluid inclusions from saddle dolomite and sphalerite.

Billiton sample no.	Sample Locality	Mineral and inclusion type	Th (°C)	Tm (°C)
106707	FD 18 272.41	Saddle Dolomite		
		Primary, two phase inclusion.	82.4	—
		Primary, two phase inclusion.	86.5	—
		Primary, two phase inclusion.	86.5	—
		Primary, two phase inclusion.	89.1	—
		Primary, two phase inclusion.	75.8	—
		Primary, two phase inclusion.	76	—
		Primary, two phase inclusion.	87.2	—
		Primary, two phase inclusion.	80.1	—
		Primary, two phase inclusion.	78.9	—
Primary, two phase inclusion.	77.2	—		
106707	FD 18 272.41	Sphalerite		
		Primary, two phase inclusion.	73.7	—
		Primary, two phase inclusion.	90.9	-17.1

Carbon and oxygen isotopes.—Carbon and oxygen isotope analyses were performed on nine samples of saddle dolomite drilled from core samples from the Fossil Downs Station and Brooking Springs Station areas (Table 6). Average $\delta^{13}\text{C}$ and $\delta^{18}\text{O}$ compositions for these saddle dolomites were +1.8‰ (ranging +1.1‰ to +2.4‰) and -7.4‰ (ranging -9.5‰ to -5.5‰) respectively. Isotope analyses were also performed on coarse grained saddle dolomite cements that fill intergranular pores in grainstones. These saddle dolomite cements were from surface samples from Findlay Hill and Brooking Springs Station. Average $\delta^{13}\text{C}$ and $\delta^{18}\text{O}$ compositions for six samples of saddle dolomite cement were +2.4‰ (ranging +2.0‰ to +2.7‰) and -6.9‰ (ranging -9.6‰ to -3.5‰) respectively.

Strontium isotope analyses.—Strontium isotope analyses were performed on five samples of saddle dolomite (Table 7). The $^{87}\text{Sr}/^{86}\text{Sr}$ values range from 0.711133 to 0.714028 (averaging 0.712906).

Trace-element analysis.—Trace-element analysis was performed on two samples of saddle dolomite. The first sample was a large saddle

dolomite crystal that overgrew mineralization in a primary pore. A trace element traverse of six analysis points was performed from the core to the outer edge of the crystal (Table 9). This saddle dolomite contained 44.04-55.76 mole% magnesium (averaging 47.39 mole%), 44.16-55.76 mole% calcium (averaging 52.13 mole%), 78-464 ppm strontium (averaging 220 ppm), 328-2611 ppm manganese (averaging 1283 ppm), 131-3774 ppm iron (averaging 1639 ppm), 15-1329 ppm sodium (averaging 373 ppm), and 0-113 ppm zinc (averaging 52 ppm).

Table 9.—Microprobe results of two samples of saddle dolomite.

Billiton sample number	Sample locality/ microprobe analysis point	Trace element concentration						
		Mg mole%	Ca mole%	Sr ppm	Mn ppm	Fe ppm	Na ppm	Zn ppm
106726	FD 15 171.4m	Saddle dolomite						
	1	46.38	53.13	211	2611	306	61	75
	2	44.04	55.42	128	1716	1554	138	33
	3	47.77	51.62	464	1382	2238	1329	47
	4	44.1	55.48	78	692	1830	171	0
	5	55.76	44.16	245	328	131	524	47
106781	FD 8 274.9m	Saddle dolomite and recrystallized regional dolomite						
	1	45.66	53.89	261	1933	946	66	135
	2	44.55	53.88	59	3215	7233	63	0
	3	45.38	52.5	101	2676	11336	80	43
	4	43.86	54.11	144	2733	10332	0	39
	5	44.72	54.13	79	2170	5019	0	200
	6	45.19	53.31	80	591	2628	153	228

The second sample is a saddle dolomite overgrowth on regional dolomite. The sample contains pyrite and sphalerite mineralization. The pyrite occurs just above the regional dolomite/saddle dolomite contact while the sphalerite occurs within the later part of the saddle dolomite generation. The six points analyzed include two points within the recrystallized regional dolomite (Table 9). The saddle dolomite contains 43.86-45.66 mole% magnesium (averaging 44.86 mole%), 52.5-54.13 mole% calcium (averaging 53.64 mole%), 79-261 ppm strontium (averaging 120 ppm), 591-3215 ppm manganese (averaging 2220 ppm), 946-11336 ppm iron (averaging 6249 ppm), 0-153 ppm sodium (averaging 60 ppm), and 0-228 ppm zinc (averaging 108). The analysis point that contained relatively high zinc

zinc concentration was in a cathodoluminescence zone that correlates to zones in which sphalerite occurs in the same sample.

Distribution.—Saddle dolomites are most commonly observed in drill-core samples in marginal-slope deposits of the Fossil Downs Station and Brooking Springs Station areas. The saddle dolomites are commonly associated with mineralization, either growing directly on the sulphides or with sulphides occurring nearby. Although saddle dolomite sometimes occurs in undolomitized lithologies, it was not observed in areas that are devoid of regional dolomite.

Saddle dolomite cements within grainstones were observed in outcrop samples from the Brooking Springs Station and Findlay Hill areas. In both of these areas, gossanous limestone and dolomites also occur. Kerans (1985) reported saddle dolomites from other areas of the Lennard Shelf and also noted the possible association of this type of dolomite with sulphide mineralization.

MINERALIZATION

The mineralization within the carbonates of the Fossil Downs Station, Brooking Springs Station, and Horse Spring Range areas occurs predominantly as cavity-filling sulphides. The main sulphide phases (in order of abundance) are pyrite, sphalerite, marcasite and galena. Very minor amounts of chalcopyrite occur in some samples.

Sulphide mineralization occurs in primary pores in limestone, moldic and intercrystalline porosity in dolomites, and fracture porosity (Figures 14G, 14H). The most important host for sulphides is in fracture porosity where mineralization occurs as the first generation lining the fractured surface or the breccia clasts (Figure 14H). The primary pores in limestone include grainstones and fenestral limestones of the platform facies, marine

cement-lined pores of marginal-slope deposits, and shelter pores and bioclast molds in both platform and marginal-slope facies. Within the larger primary pores, the mineralization precipitated as a pore lining (Figure 14G). In dolomitized lithologies, the mineralization occurs within secondary intercrystalline and moldic porosity that developed during the regional dolomitizing event.

Sulphides also occur lining fractures in both dolomitized and undolomitized lithologies. Breccia fabrics are observed in both outcrop and drill core. The breccias are of syn- and post-sedimentary origin. Mineralization within the synsedimentary breccias (Figure 14G) is generally restricted to the lithologies that retained significant primary porosity after marine cementation.

Post-depositional breccias are recognized by the absence of marine cement lining the fracture surfaces. The breccias are lined by different cement generations, reflecting the different times in which fracturing and brecciation occurred. In many of these mineralized fractures and breccias, it is often possible to match features across clasts indicating that little displacement or rotation of the clasts occurred during brecciation. This type of brecciation is consistent with an origin by hydraulic fracturing. Sulphides (mainly pyrite but occasionally sphalerite) also occur along stylolites, together with chlorite and regional dolomite. The occurrence of mineralization along stylolites indicates that some stylolitization occurred prior to sulphide precipitation and provided a conduit for the mineralizing fluids.

Pyrite.

Pyrite is the most abundant sulphide phase and when it occurs, is the first sulphide in the mineralization event. Within large (larger than 2 cm) marine-cement-lined pores, pyrite (as the first phase of the mineralization event) generally forms a deposit at the base of the pore. The tendency of pyrite to line the base of these pores rather than forming as a lining, suggests that pyrite initially precipitated relatively quickly from solution and settled on the base of the pore (Figure 14G). This initial pyrite precipitation provided nucleation points for later pyrite. Pyrite occurs as cubes disseminated in interparticle pores in grainstones and intercrystalline pores in dolomite. The most common form of pyrite is massive, coalesced grains, generally as deposits on the base of pores but also occurring in veins and fractures. Framboidal pyrite sometimes occurs as the final stage of the pyrite generation.

Pyrite mineralization often occurs by partial and localized replacement of the underlying host limestone and calcite cements. When pyrite occurs on clear equant calcite cements, cathodoluminescence zonations are truncated, indicating replacement of the calcite cement on which the pyrite formed (Figures 15A, 15B). This truncation of the cathodoluminescence zones during pyrite precipitation is generally restricted to the areas where pyrite is in direct contact with the calcite cement. Away from this pyrite/calcite contact, cathodoluminescence zonation is not disrupted and corrosion of the calcite is not observed. Pyrite replacement of dolomite is much less pronounced than pyrite replacement of calcite (Figure 14E, 14F).

Sulphur Isotopes.—Sulphur isotope analyses were performed on eight samples of pyrite (Table 10). Five pyrite samples from the Fossil Downs Station area have $\delta^{34}\text{S}$ values that range -2‰ to +2‰. A single

Figure 15. Thin-section photomicrographs illustrating timing of mineralization and sulphide paragenesis.

A) A cement-filled cavity filled with clear equant calcite and containing pyrite (P) (plane-polarized light). Frasnian back-reef subfacies, Fossil Downs Station FD 10 75.3 m. Scale bar = 0.5 mm. Billiton sample no. 106767

B) Same area in A under cathodoluminescence. The non-luminescent (N) calcite is the first clear equant cement generation. The non-luminescent cement contains very thin bright-luminescent bands and is overgrown by the bright-luminescent cement generation (B). Where the pyrite occurs, the bright-luminescent cement has been prevented from growing. The final pore-filling cement is the dull-luminescent (D) calcite generation.

C) The top of a microcrystalline (M) marine cement-lined pore filled with clear equant calcite and colloform sphalerite (S) (plane-polarized light). The base of the pore contains sediment produced during mineralization. A dolomite (D) rhomb grew on the surface of the sediment. Famennian marginal-slope facies, Horse Spring Range drill-hole HD 9 270.6 m. Scale bar = 1 mm. Billiton no. 106779

D) Same area in C under cathodoluminescence. The microcrystalline (M) marine cement has a mottled bright- and dull-luminescence. Non-luminescent scalenohedral (S) calcite cement overgrew the microcrystalline marine cement. A uniform zone of bright-luminescent (B) cement overgrew the scalenohedral cement. Colloform sphalerite (CS) coated the bright-luminescent cement and the pore was finally filled with dull-luminescent (D) cement. The dots indicate the location of microprobe analyses points.

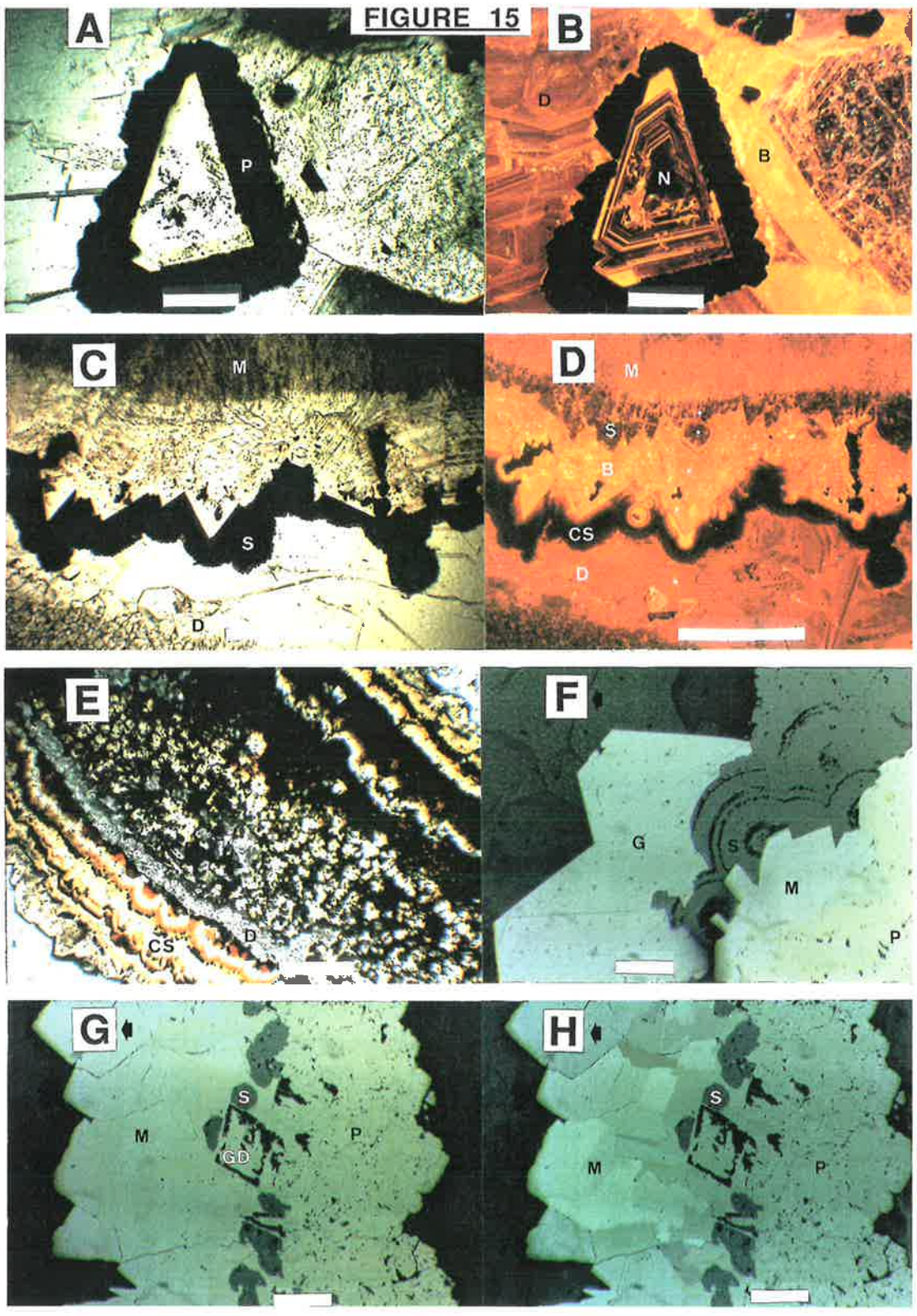
E) Zoned colloform sphalerite (CS) coating a dolomite (D) clast (plane-polarized light). Sphalerite also occurs disseminated in the intercrystalline porosity in the dolomite. Famennian marginal-slope facies, Fossil Downs Station drill-hole FD 18 272.4 m. Scale bar = 0.5 mm. Billiton no. 106707

F) Paragenetic sequence of pore -filling sulphides (reflected light). The paragenetic sequence from oldest to youngest is — pyrite (P), marcasite (M), colloform sphalerite (S), and galena (G). Calcite cement fills the remaining pore space. Famennian marginal-slope facies, Horse Spring Range drill-hole HD 9 270.6. Scale bar = 0.1 mm. Billiton no. 106779

G) Pore lining sulphide generations (reflected light). Large arrow indicates upright direction. The paragenetic sequence from oldest to youngest is — pyrite (P), framboidal sphalerite (S), and marcasite (M). A ghost dolomite (GD) rhomb is observed within the mineralization. Famennian marginal-slope facies, Fossil Downs Station drill-hole FD 18 305.2 m. Scale bar = 0.1 mm. Billiton sample no. 106709

H) Same area in G with polars slightly uncrossed. The anisotropy of marcasite is clearly illustrated.

FIGURE 15



sample from Brooking Springs Station has a $\delta^{34}\text{S}$ value of -12‰. Two samples of from the Cadjebut Mine have $\delta^{34}\text{S}$ values of +12‰ and +18‰.

Table 10.—Sulphur isotope composition of sulphide phases.

Billiton sample	Sample locality	$\delta^{34}\text{S}$ (CDT)
		SPHALERITE
106797	CADJEBUT MINE	13
		GALENA
106781	FD 8 274.90 (Fossil Downs)	6
106796	CADJEBUT MINE	9
		PYRITE
106798	CADJEBUT MINE	12
106797	CADJEBUT MINE	18
106707	FD 18 272.40 (Fossil Downs)	-2
106742	FD 8 269.54 (Fossil Downs)	2
106713	FD 18 44.80 (Fossil Downs)	0
106729	FD 15 220.00 (Fossil Downs)	1
106725	FD 15 225.86 (Fossil Downs)	1
106754	FD 16 153.15 (Brooking Springs)	-12

Sphalerite.

Sphalerite occurs in variable amounts, postdating (but slightly overlapping) the pyrite generation. Fine, granular sphalerite occurs disseminated in grainstones and dolomites. In large pores, the sphalerite forms laminated "colloform" and botryoidal textures lining the pore (Figures 15C, 15D, 15E, 15F). The "colloform" sphalerite is finely zoned (as observed in transmitted light), ranging in colour from pale-yellow to black and sometimes containing purple-coloured zones. When the sphalerite does not totally coat the pore, sphalerite may occur as isolated botryoids between the iron sulphide phases (Figures 15G, 15H) or within calcite or dolomite cement. There is no evidence of replacement of the carbonate host during sphalerite precipitation.

Sulphur Isotopes.—Sulphur isotope analysis was performed on one sample of sphalerite from the Cadjebut Mine (Table 10). This sphalerite sample has a $\delta^{34}\text{S}$ value of +13‰.

Fluid Inclusions.—Fluid inclusion analysis was performed on two primary, two-phased fluid inclusions (Table 8) from a single sample of sphalerite (FD 18 272.40 m). The first inclusion was from an early zone of honey-yellow sphalerite. This inclusion had a first melt temperature of -38.1°C and a final melt temperature of -17.1°C (~ 20 wt% NaCl equivalent). The homogenization temperature for this inclusion was $+90.9^{\circ}\text{C}$. The second inclusion was from the youngest zone in the sphalerite. No freezing data was obtained from this inclusion but the homogenization temperature was $+73.7^{\circ}\text{C}$.

Galena.

Galena is a minor sulphide phase relative to sphalerite in the Fossil Downs Station, Brooking Springs Station, and Horse Spring Range areas. Galena occurs as a replacement of sphalerite or as a pore cement generation after sphalerite. When galena forms a cement after sphalerite, the galena crystals usually have an octahedral form (Figure 15F). Replacement galena (within sphalerite) occurs as inclusions with irregular grain shapes when they are small but generally develop euhedral forms when they are large (Figure 16A). The small inclusions of galena have a skeletal form with a radial-like alignment within the sphalerite. The galena in sample FD 8 179.24 m displays a typical sequence of textures. The central region contains irregular shaped, small galena inclusions. Outside the central region the inclusions become aligned (in a radiating form), with medium sized inclusions being elongate. Further from the centre, the elongate inclusions form irregular edged large galena crystals with the faces furthest from the centre tending towards euhedral crystal development. Ringrose (1989) illustrated similar textures of galena within sphalerite in samples from the Narlarla deposit (Ringrose Plate 7C, 7D, and 7E).

Figure 16. Thin-section photomicrographs and core samples illustrating sulphide paragenesis, Late Famennian karst, and barite pseudomorphs.

A) Pore-filling sulphides in an intraparticle mollusc pore (reflected light). Large arrow indicates upright direction. Colloform sphalerite (S) was the first sulphide generation, followed by galena (G) and marcasite (M). The galena occurs inclusions within the sphalerite and has a skeletal texture. Famennian marginal-slope facies, Fossil Downs Station drill-hole FD 8 179.2 m. Scale bar = 0.1 mm. Billiton sample no. 106737

B) Core samples from the Wagon Pass prospect (large arrow indicates upright direction). The top sample illustrates the possible Late Famennian karst in the Windjana Limestone. The dissolution (thin arrow) cavity is filled with brown sediments containing a spore assemblage that is similar to the lower Fairfield Formation. Drill-hole NRD 91 25.5 m. Scale bar = 1 cm. Billiton sample no. 106845

C) Banded and spherulitic growth of sphalerite (S) within partially dolomitized limestone (plane-polarized light). Clear calcite fills lath-shaped pseudomorphs of barite (B). Famennian marginal-slope facies, Horse Spring Range drill-hole HD 7 63.5 m. Scale bar = 0.5 mm. Billiton sample no. 106776

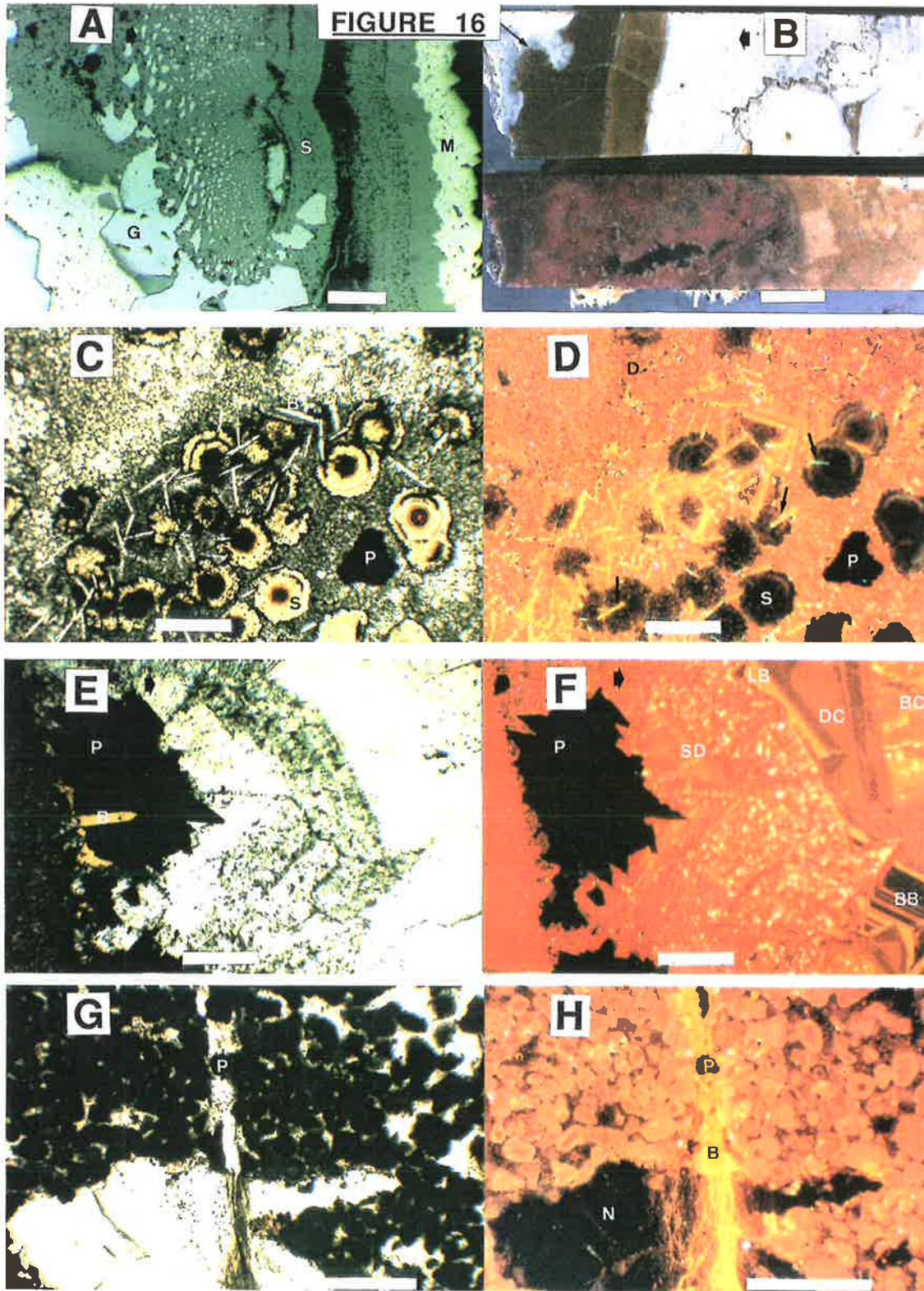
D) Same area in C under cathodoluminescence. The barite (B) pseudomorphs are filled with bright-luminescent calcite cement. The sphalerite (S) precipitated after the barite and, in some cases, appears to have nucleated on the barite (large arrows). The dolomite (D) rhombs have the characteristic non-luminescent core and bright-luminescent rim of the regional dolomite generation.

E) The base of a cavity containing pyrite (P), saddle dolomite, and clear equant calcite (plane-polarized light). The pyrite appears to have nucleated on a barite (B) crystal. The barite has dissolved and a void remains. Famennian marginal-slope facies, Fossil Downs Station drill-hole FD 15 171.4 m. Scale bar = 0.5 mm. Billiton sample no. 106726

F) Same area in E under cathodoluminescence. The paragenetic sequence is — barite, pyrite (P), saddle dolomite (SD), bright-luminescent calcite (BC), dull-luminescent calcite (DC), late bright-luminescent calcite (LB), and late brightly banded-luminescent (BB) calcite.

G) Fenestral pores in a peloidal grainstone filled by clear equant calcite cement (plane-polarized light). Pyrite (P) occurs in a fracture in the host limestone, Frasnian back-reef subfacies, Fossil Downs Station drill-hole FD 10 113.3 m. Scale bar = 1 mm. Billiton no. 106768

H) Same area in G under cathodoluminescence. The fenestral pores were almost entirely filled with non-luminescent (N) calcite. A fracture filled with bright-luminescent (B) calcite cuts through the limestone and contains pyrite (P). The "horsetail" character of the fracture may indicate the fracture was produced by hydraulic pressures.



Generally sphalerite is transparent and displays distinctive colour zonation. However, where galena occurs as a replacement phase within the sphalerite, the sphalerite is opaque. The change from well zoned, transparent sphalerite to opaque sphalerite occurs laterally in colloform sphalerite. This lateral change indicates that the opaque sphalerite is a product of subsequent alteration of the well zoned sphalerite. The opaque sphalerite often corresponds to areas where galena inclusions occur. The development of opaque sphalerite is most likely due to an increase in the iron content. The cause of the alteration of well-zoned sphalerite to opaque sphalerite is not known.

Sulphur Isotopes.—Sulphur isotope analyses were performed on two samples of galena (Table 10). The first sample, from the Fossil Downs Station area, has a $\delta^{34}\text{S}$ value of +6.5‰. The second sample is from the Cadjebut Mine and has a $\delta^{34}\text{S}$ value of +9.2‰.

Marcasite.

Marcasite is generally the last sulphide phase in the mineralization event. It occurs as rectangular to rhombic euhedra, that grew in open pores as interlocking crystals at the base of pores (Figures 15F, 15G, 15H). In grainstones that have disseminated sphalerite, marcasite may occur as a rim around the sphalerite by replacement or dissolution of the host limestone. In some samples two generations of marcasite, separated by a second sphalerite generation, were observed. The second sphalerite/marcasite generation is volumetrically less important than the first sphalerite/marcasite generation.

Possible Barite Pseudomorphs

In some of the thin sections examined, a number of lath-shaped molds were observed (Figures 16C, 16D, 16E, 16F). While some of these lath-shaped molds were voids others contained clear equant calcite. These lath-shaped pseudomorphs and molds are closely associated with mineralization and often appear to have been nucleation sites for the mineralization. Both gypsum and barite have a blade-shaped-crystal morphology. However, at the temperatures indicated by fluid inclusions for the mineralization event (90°C), gypsum would most likely have converted to anhydrite. Minor amounts of barite occur in the Blendevalle deposit, although the barite formed as a late stage in respect to the mineralization (Ringrose, 1989).

Parageneisi of Mineralization Relative to Host-carbonate Diagenesis

Fossil Downs Station and Brooking Springs Station areas.—The mineralization from the Fossil Downs Station and Brooking Springs Station areas occurs within the bright-luminescent calcite cement zone (Figures 15A, 15B). In the bright-luminescent calcite cement zone the mineralization occurs directly after the first bright-yellow band of this zone (Figures 9E, 9F). There is evidence that some calcite cementation occurred during the mineralization event, with calcite occurring between pyrite mineralization and later sphalerite. However this calcite cementation is small relative to total clear calcite cementation of the pores. Mineralization was not observed within the dull-luminescent calcite cement zone.

Sulphide mineralization is commonly observed within fractured limestone. A sample from within the Fossil Downs atoll (FD 10 113.30 m; Figures 16G, 16H) shows some minor iron sulphide within a fracture. The fenestral porosity of this sample had been almost entirely occluded by the non-luminescent calcite generation, so that the porosity and permeability of

this lithology after burial diagenesis would have been minimal. However, as the photograph clearly shows, hydraulic fracturing created porosity and permeability within this limestone. A small amount of iron sulphide and bright-luminescent calcite precipitated in the fracture. It is most likely that sulphide mineralization, bright-luminescent calcite and fracturing were part of the same event.

In dolomitized lithologies, mineralization post-dates the regional dolomite and occurs within the early part of the saddle-dolomite generation (Figures 14E, 14F). The main stage of mineralization (pyrite) occurs within the bright-luminescent zone in the saddle dolomite. Minor sphalerite precipitated slightly later than the main stage of mineralization and is observed at the contact between the bright-luminescent and the later dull banded-luminescent zones of the saddle dolomite.

Horse Spring Range.—Sulphides occur mainly within Famennian marginal-slope facies in samples from Horse Spring Range. Unlike the banded nature of the bright-luminescent cement in the Fossil Downs Station area, the bright-luminescent cement at Horse Spring Range is relatively uniform. Sphalerite occurs within this bright-luminescent calcite cement (Figure 17A, 17B).

Pillara Range.—The calcite cements in pores containing mineralization in samples from the Pillara Range (near the Blendevale deposit) have been neomorphosed (so that zonation is destroyed) and the cements now have a uniform bright luminescence. Pyrite in these pores is in direct contact with the host carbonate (Pillara Limestone). A thin generation of clear equant calcite cement separates the pyrite generation from the later sphalerite generation (Figures 17C, 17D). The occurrence of pyrite directly in contact with the host carbonate suggests that mineralization occurred early in relation to the clear equant calcite cement sequence in this area.

Figure 17. Thin-section photomicrographs of sulphide mineralization within calcite cements in other areas of the Lennard Shelf.

A) A cement-filled cavity lined by microcrystalline (M) marine cement and filled with clear equant calcite (plane-polarized light). Sphalerite (S) and a dolomite (D) rhomb occur within the clear equant calcite cement. Famennian marginal-slope facies, Horse Spring Range drill-hole HD 9 270.7m. Scale bar = 0.5 mm. Billiton no. 106779

B) Same area in A under cathodoluminescence. The microcrystalline (M) marine cement is predominantly non-luminescent and is overgrown by non-luminescent (N) scalenohedral calcite cement. The bright-luminescent (B) cement, which overgrows the non-luminescent cement, contains sphalerite (S) and dolomite (D) in its outer zones. The dolomite does not have the same luminescence character as the regional dolomite phase. The bright-luminescent cement is overgrown by uniform dull-luminescent (DC) cement.

C) A pore lined by pyrite (P) and sphalerite (S) and filled by clear equant calcite (plane-polarized light). Clear calcite occurs between the pyrite and sphalerite generations. Frasnian back-reef subfacies, Pillara Quarry (Pillara Range). Scale bar = 0.5 mm. Billiton no. 106812

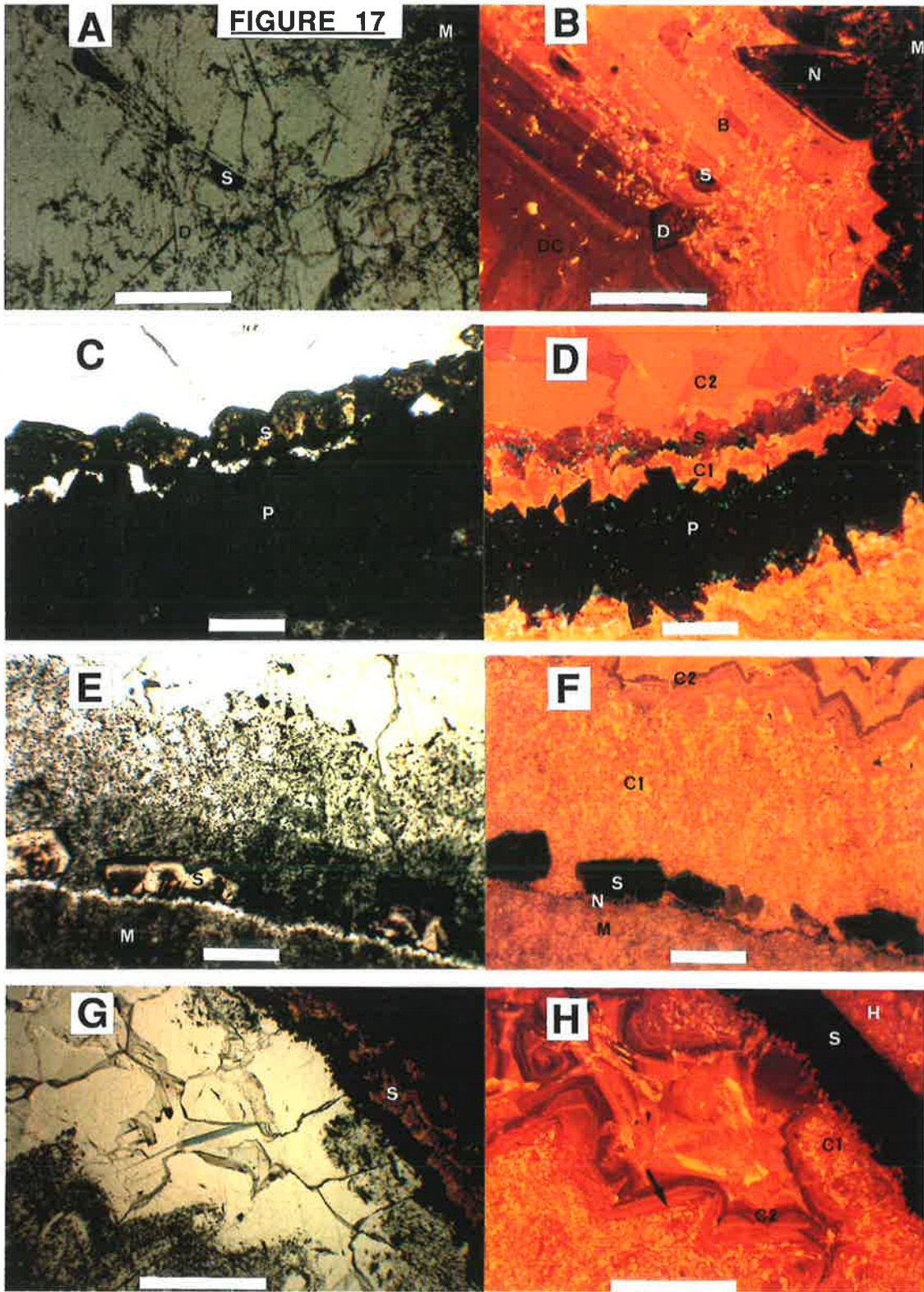
D) Same area as C under cathodoluminescence. The host limestone has a mottled bright-luminescent character. A generation of patchy bright-luminescent calcite overgrew the pyrite (P) before the sphalerite (S) precipitated. The remaining clear equant cement has a patchy bright- and dull-luminescence (C2). The absence of growth banding within the clear equant calcite suggest recrystallization has occurred.

E) A pore lined by microcrystalline (M) marine cement and filled with inclusion-rich calcite cement and clear equant calcite cement (plane-polarized light). Sphalerite (S) is separated from the marine cement by a thin zone of clear calcite cement. Windjana Limestone, Wagon Pass prospect, drill-hole NRD 96 27.3 m. Scale bar = 0.5 mm. Billiton no. 106851

F) Same area in E under cathodoluminescence. The microcrystalline (M) marine cement has a mottled bright- and dull-luminescence. A thin zone of patchy non-luminescent (N) calcite overgrew the marine cement. Sphalerite (S) precipitated on the non-luminescent cement. The inclusion-rich calcite (C1), which overgrew the sphalerite, has a patchy bright- and dull-luminescent character. Banded bright- and dull-luminescent (C2) calcite filled the remaining pore space.

G) A sphalerite (S) lined intracrystalline pore filled by clear and inclusion-rich calcite cements (plane-polarized light). The inclusion-rich cement is not isopachous, unlike the marine cements. Windjana Limestone, Wagon Pass prospect, drill-hole NRD 96 30.1 m. Scale bar = 1 mm. Billiton no. 106852

H) Same area in G under cathodoluminescence. The sphalerite (S) is in direct contact with the host limestone (H). The inclusion-rich calcite (C1) cement, which overgrew the sphalerite, has a patchy bright- and dull-luminescence. Although the inclusion-rich cement has been recrystallized it retains its growth form (arrow). The inclusion-rich cement is overgrown by banded bright- and dull-luminescent calcite (C2) cement.



Napier Range.—Sulphides occur within Frasnian and Famennian marginal-slope facies and Famennian reef facies (Windjana Limestone) in the Napier Range. Samples from the Wagon Pass prospect display sphalerite either with a thin layer of clear calcite cement separating the sphalerite from the marine cement (Figures 17E, 17F) or in direct contact with marine calcite (Figures 17G, 17H). The thin layer of clear calcite cement has a patchy bright- and non-luminescence. Postdating the sphalerite is an inclusion rich calcite cement that has a mottled bright-luminescent character. This cement is not isopachous and staining reveals its strong ferroan nature. Younger calcite cement generations in the pores display banded moderate to bright-luminescence. Stable isotope analyses were not performed on these calcite cement generations and their relationship to the cement generations of the Fossil Downs Station area is unclear.

Oscar Range.—Hurley and Lohmann (1989) illustrated (their Figures 14D and 14E) a stromatactis void that contained pyrite from the Famennian Napier Formation, in the northwest Oscar Range (Borehole MD-1, depth 36.0 m). The stromatactis void was partially filled with internal sediment and lined with isopachous fibrous cement. The isopachous fibrous cement is probably of marine origin. The mottled, bright-luminescent nature of this cement and the slightly lower $\delta^{18}\text{O}$ values relative to the marine signature (Hurley and Lohmann's Figure 17) suggest that this marine cement has been recrystallized. Pyrite formed as an isopachous lining on the fibrous calcite and is postdated by a mottled, bright-luminescent scalenohedral calcite cement (similar to the altered, inclusion rich calcite from the Napier Range). Based on the texture, Hurley and Lohmann assigned this altered layer to the marine/eogenetic cement generation. Hurley and Lohmann considered the alteration may have occurred during the Late Carboniferous

uplift event. The altered calcite, which precedes the pyrite, is most likely marine calcite that was recrystallized during the mineralization event.

KARSTIFICATION AND SUBAERIAL EXPOSURE.

MVT deposits are commonly emplaced in carbonate breccias suggested to be either associated with paleokarst or induced by a slightly earlier phase of dissolution by the ore solutions (Sangster 1988). The meteoric karst hypothesis is generally favoured, due to the usual presence of an overlying unconformity, similarity of the ore-bearing breccia zones to known paleokarst solution collapse breccias, solution-thinned strata below the breccia zone, and the relative scarcity of wallrock alteration (Sangster 1988). The Devonian reefs of the Lennard Shelf have been subjected to Late Carboniferous meteoric karsting, and mineralization is commonly present within brecciated host carbonates (e.g. the Cadjebut deposit). However, no direct link has been identified between karsting and the occurrence of mineralization for the carbonates of the Lennard Shelf.

Frasnian-Famennian Subaerial Exposure.—During the growth history of the reef complexes, emergence of the platforms did not produce any major subaerial exposure surfaces (Playford *et al.* 1989). The disconformity on the platform, that marked the regression at the Frasnian-Famennian boundary in the northern Oscar Range, is the only identified period of platform emergence of real significance (Playford *et al.* 1989; Hurley and Lohmann 1989). Hurley and Lohmann (1989) did not identify any evidence that indicated a significant period of exposure occurred at the Frasnian-Famennian boundary.

Late Carboniferous Karstification.—The most significant karstification event that affected the Devonian reefs of the Lennard Shelf was at the Late Carboniferous unconformity. Late Carboniferous-Early Permian sandstones of the Grant Group unconformably overlie the karst surface created during uplift

and erosion in the Late Carboniferous. Grant Group sandstones occur in sinkholes within the Devonian carbonates in many locations on the Lennard Shelf. These areas include the Fossil Downs Station, Geikie Gorge, Horse Spring Range, and Oscar Range areas. Hurley (1986) identified sandstones of the Grant Group that had filled sinkholes to depths of 210 m in the southeast Oscar Range.

North of Brooking Springs homestead, ferroan calcite cement filled a large cavern that has a gossanous contact with the host limestone. Ferroan calcite is formed in a reducing environment and therefore generally associated with formation in the burial diagenetic environment. Primary fluid inclusions indicate this ferroan calcite cement precipitated from an almost fresh pore fluid at temperatures of more than 80°C. Apart from the present karstification there is no evidence for a karsting event younger than the Late Carboniferous-Early Permian on the Lennard Shelf.

In the drill cores from the Fossil Downs Station and Brooking Springs Station areas features relating to meteoric fluids can be seen at depths of more than 200 m (FD 16) below the present level of erosion. These features include oxidized sulphide mineralization, dissolution of the carbonate host, dedolomitization, and sediment and calcite spar filling large (greater than 1 metre) caverns. Orange sediments and orange, black or white calcite spars line some fractures and fill large cavities. The host limestone at the edges of these fractures and cavities have undergone dissolution. It is unlikely that the present-day karst could have produced the thick (several metres) calcite spars that fill the caverns. Immediately below the present-day surface, caves have been encountered during drilling. These caves are considered to be a result of present-day karsting. The dedolomite and oxidized sulphide mineralization could also be explained by the modern meteoric fluids. However, many of the gossans observed in the outcropping limestones contain sandstones of the Grant Group and/or large quantities of calcite spar (of burial origin). It is evident

that meteoric fluids (both at present and in the Late Carboniferous) exploited the sulphide mineralization during karstification.

Possible Pre-Fairfield Karst.—In the Wagon Pass area (Napier Range), Billiton geologists (Michael Clifford and Rick Berg) have identified a possible karst event that has not been previously documented. Dissolution features in the Windjana Limestone occur in drill core (NRD 91) at depths of at least 26 m and possibly extend to 60 m. Most of the dissolution cavities have been filled by sediment (Figure 16B). The sediments are fine grained calcareous sandstones and siltstones and contain small fragments of limestone that are similar in colour to the host limestone. The cavity-filling sediment ranges in colour from brown to green-grey. In one sample, layering in the sediment is defined by different coloured sediment. Importantly, mineralization occurs both in the host limestone and within the sediment filling the cavities. A sample of the sediment infilling the cavities was processed for microfossil analysis. This sample (NRD 91-24.20 m) was a green-grey calcareous siltstone and contained crinoid ossicle fragments. The sample also contained spores of the Retispora lepidophyta Assemblage (late Famennian-Strunian in age). Playford (1976) documented this assemblage and noted that it was the typical assemblage of the lower portion of the Fairfield Group and ?Napier Formation (in BMR 2 Laurel Downs). The assemblage is dominated by spores with only a minor (< 1%) acritarch component. Acritarchs were also rare in the lower Fairfield Formation assemblages documented by Playford (1976). He suggested that the low acritarch distribution may reflect some sort of preservation winnowing, as their organic walls in the samples studied are less durable than most of the spore exines and therefore more susceptible to preferential removal. The occurrence of crinoid ossicles and acritarchs is indicative of open marine conditions when these sediments were deposited.

ORIGIN OF DOLOMITES AND MINERALIZATION

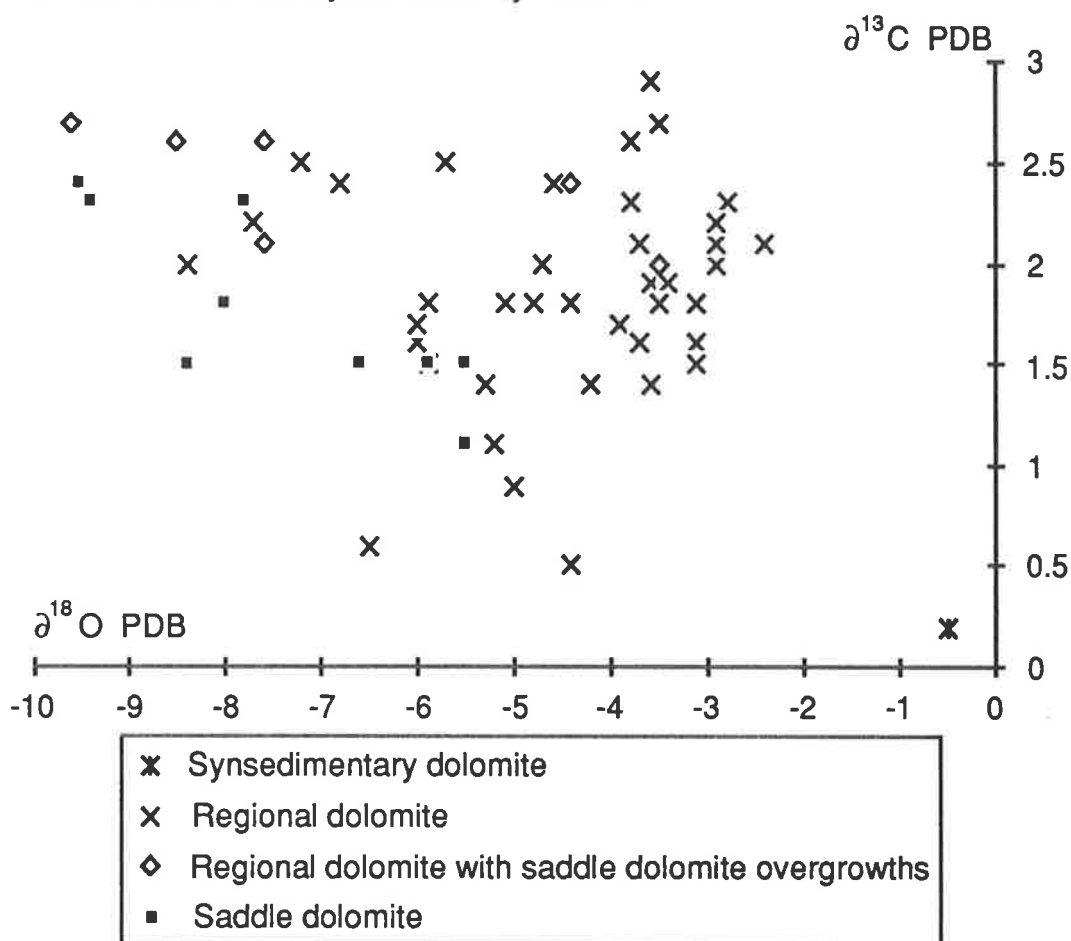
Synsedimentary Dolomite.

A synsedimentary origin for the dolomite in the basal Pillara Limestone of the Emanuel Range is supported by: (a) the restricted distribution of the fine-grained, fabric-mimicking dolomite to the peritidal environment; (b) the fine-grained nature of the dolomite crystals; and (c) the heavy oxygen isotopic composition of the dolomite. The $\delta^{18}\text{O}$ value of the synsedimentary dolomite is 1.9‰ more positive than the heaviest value for the regional dolomites (Figure 18). The relatively high $\delta^{18}\text{O}$ value (-0.5‰) for the synsedimentary dolomite is within the range of values of Upper Devonian synsedimentary supratidal dolomites on the Barbwire Terrace (Wallace 1990). Wallace (1990) suggested the relatively high $\delta^{18}\text{O}$ values for the sabka dolomite of the Barbwire Terrace were due to precipitation of dolomite from highly evaporated waters. Wallace proposed a $\delta^{18}\text{O}$ value for Upper Devonian "normal marine dolomite" of approximately -2‰ (PDB), based on the lowest value of the sabka dolomites.

Regional Dolomite.

In contrast to the synsedimentary dolomite, the regional dolomite has a much more diverse distribution. The regional dolomite occurs in both Frasnian (platform and marginal-slope facies) and Famennian (marginal-slope facies) lithologies. The occurrence of regional dolomite along stylolites indicates dolomitization was at least partially concurrent with stylolitization. Playford (1984), Kerans (1985) and Wallace *et al.* (in press) conclude the regional dolomite formed from basinal brines that were expelled by sediment compaction from the Fitzroy Trough. Wallace *et al.* (in press) suggested that the high $\delta^{18}\text{O}$ values of the regional dolomite, relative to other examples of Devonian burial dolomites, may be due to the dolomitizing brines having heavier $\delta^{18}\text{O}$ compositions.

Figure 18. Carbon and oxygen isotope compositions of regional dolomite, saddle dolomite and synsedimentary dolomite.



A basinal brine model is consistent with the timing, distribution, and geochemistry of the regional dolomite. The regional dolomite formed directly after the non-luminescent calcite cement generation and preceded all but the earliest part of the bright-luminescent calcite cement. As discussed previously, the change from non-luminescent calcite to bright-luminescent calcite cementation corresponded to an increase in the temperature and salinity, and a decrease in Eh of the pore fluids.

The regional dolomite formed from fluids that were rich in radiogenic strontium compared to Late Devonian seawater. Strontium isotope analyses of the carbonate generations, from the Fossil Downs Station area, display a progressive increase in the $^{87}\text{Sr}/^{86}\text{Sr}$ ratio in younger generations. Radiogenic strontium may be inherited from silicate minerals and/or derived from postdepositional decay of ^{87}Rb (Veizer 1989). The strontium isotope values of

the regional dolomite are best explained as part of the evolving pore fluids in the burial diagenetic environment. Radiogenic strontium indicates a strontium source outside the carbonate, probably derived from interaction of pore fluids with basinal shales (or Precambrian basement). The pore fluids that precipitated the younger carbonate generations had a longer period of contact with the shales and also incorporated radiogenic strontium derived from ^{87}Rb decay. The regional dolomite represents the earlier part of this pore fluid evolution.

Oxygen and carbon isotope analyses indicate relatively uniform $\delta^{18}\text{O}$ and $\delta^{13}\text{C}$ values (Figure 18) for the regional dolomite across the Lennard Shelf. However, a small number of samples of regional dolomites have low $\delta^{18}\text{O}$ values. Figures 19 and 20 show the carbon and oxygen (respectively) isotope values for regional dolomite samples from the Fossil Downs Station and Geikie Gorge areas. The carbon isotope values (Figure 19) are relatively uniform and do not display any regional trend in values. The oxygen isotope values (Figure 20) are variable and a distinct trend in the values is discernible. The regional dolomite in the areas near Fossil Downs and Brooking Springs homesteads have oxygen values that are more negative than the values for the regional dolomites to the north. The samples with lighter oxygen isotope values correspond to areas in which significant mineralization occurs, and probably represent recrystallization of the regional dolomite by the warmer and more saline mineralizing fluids.

The distribution of the regional dolomite appears to have been controlled by the porosity and permeability of the limestones as well as the flow path of the basinal brines. North of the Copley Valley (Figure 20), the non-luminescent calcite cemented most of the back-reef subfacies. Regional dolomitization occurred in the back-reef lithologies that had not been totally cemented by the non-luminescent calcite. Wallace *et al.* (in press) illustrated that the regional dolomite has totally dolomitized a narrow zone of back-reef

subfacies immediately behind the reef flat. The marginal-slope facies, east of Geikie Gorge and in the Fossil Downs and Brooking Springs Stations areas, contain some lithologies that were strongly dolomitized. In contrast, the platform and marginal-slope facies, west of Copley Valley, do not contain any dolomite. This distribution pattern suggests that the dolomitizing fluids may have migrated from the south or south-east (from the Fitzroy Trough). Figure 20 illustrates the possible westerly extent of a dolomitizing front.

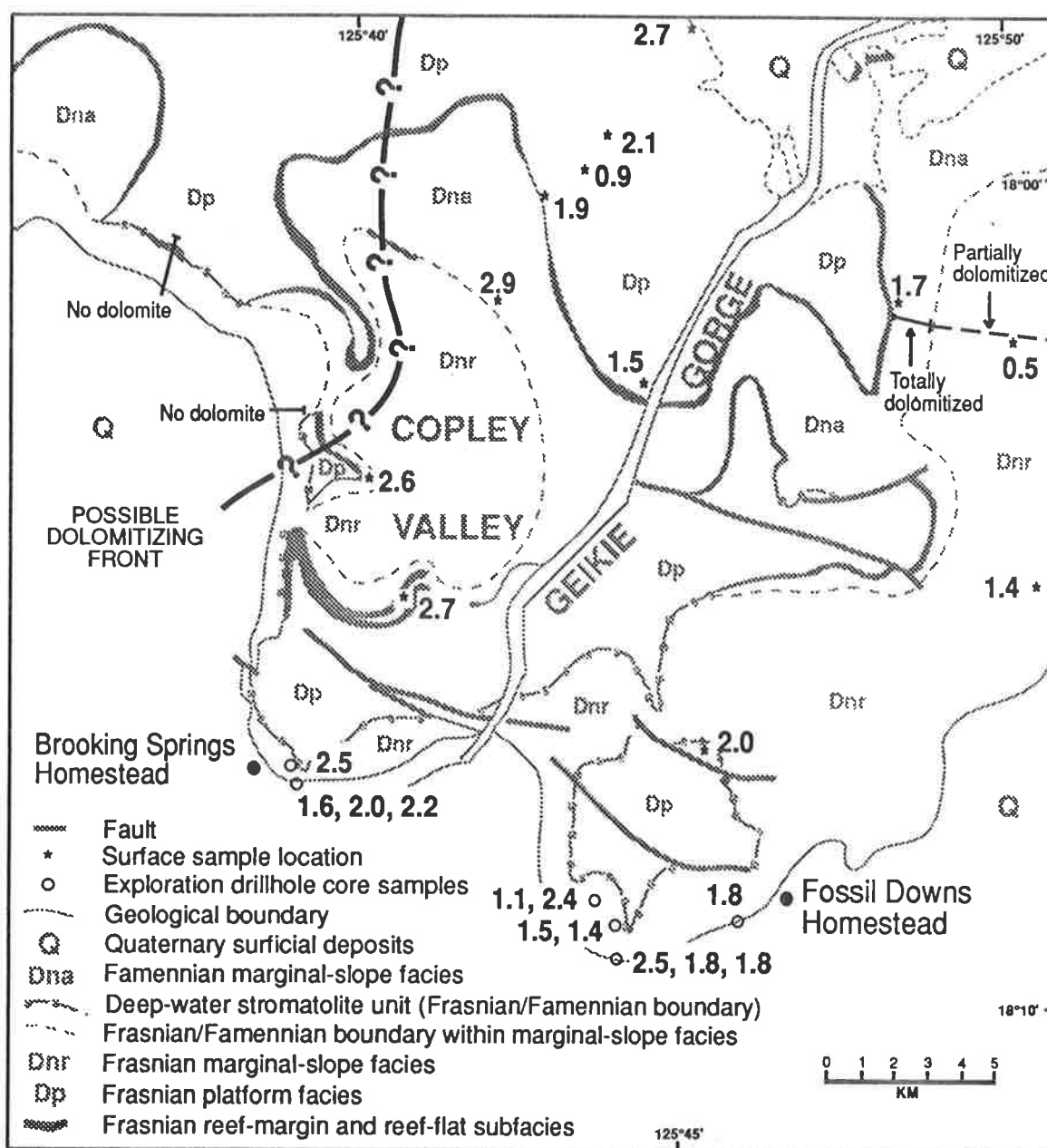


Figure 19.—Distribution of carbon isotope values of regional dolomites. Geological map modified from Wallace (1987).

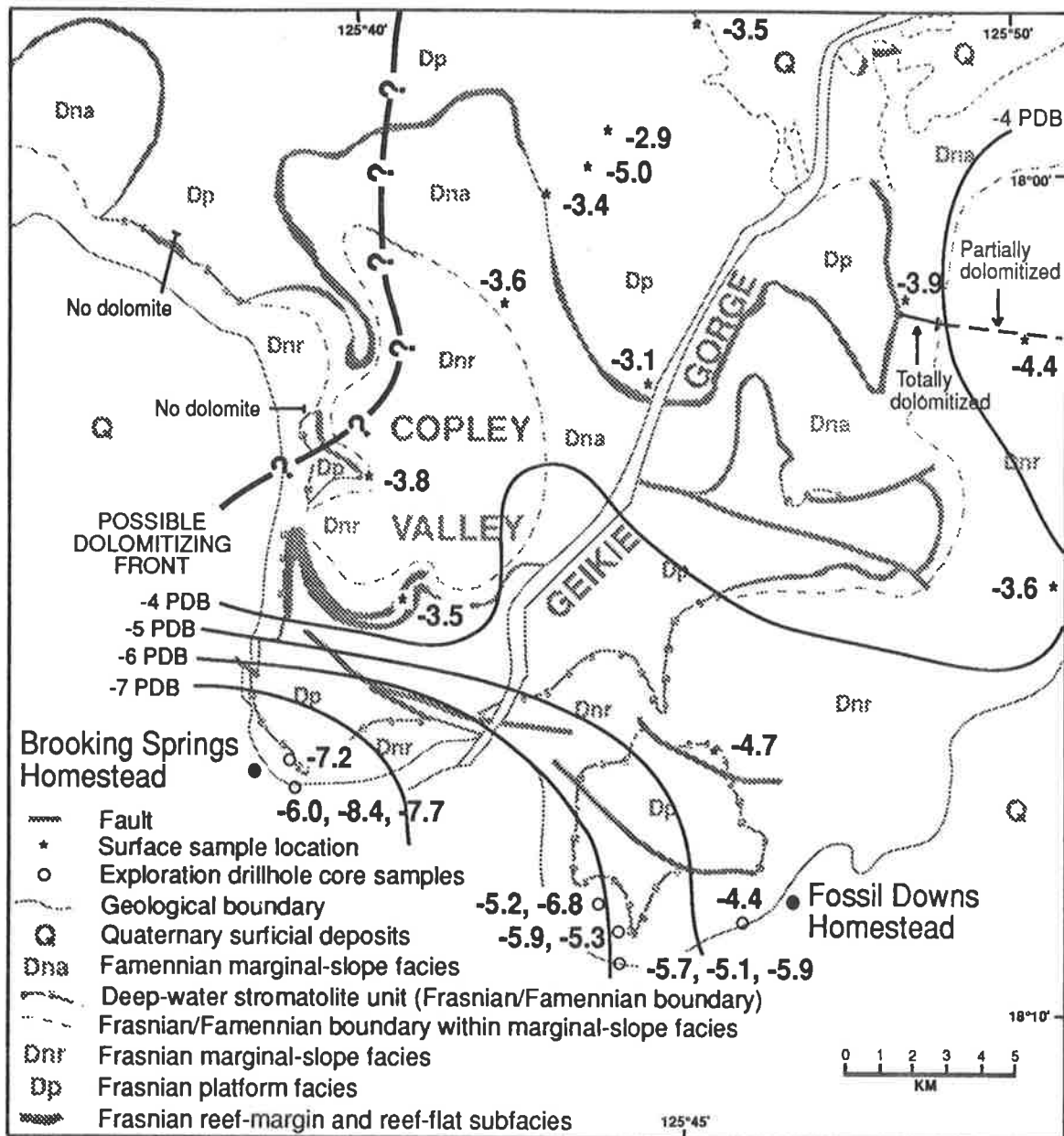


Figure 20. Distribution of oxygen isotope values of regional dolomites. Geological map modified from Wallace (1989). (Variations in the oxygen isotope values in this area are illustrated by contour lines).

Dolomite in the Oscar Range is most extensive in the Frasnian back-reef lithologies immediately adjacent to the Precambrian core (Hurley 1986). In the Oscar Range the non-luminescent calcite is not a dominant cement generation. Unlike the lithologies north of Copley Valley, the back-reef subfacies of the Oscar Range were relatively porous and permeable at the time of dolomitization.

The regional dolomitizing event produced important secondary porosity. The best secondary porosity was within totally dolomitized lithologies where

moldic and intercrystalline porosity developed. Later calcite precipitation was not as effective in occluding the secondary porosity in the dolomite as it was in occluding the primary porosity of the host limestone. The difficulty of calcite to nucleate on dolomite may be the most likely reason why the porosity in dolomites remained. As a consequence of this , primary porosity of the host limestone was almost totally occluded by the Late Carboniferous in the Fossil Downs Station area, but some porosity remained in the dolomites.

Saddle Dolomite.

The occurrence of saddle dolomite ("secondary dolomite"; Anderson 1983) is a common feature of many MVT deposits. Anderson (1983) showed that the formation of saddle dolomite may be linked to sulphate reduction at or near the ore deposit site. This process could explain why saddle dolomite occurs closely associated with sulphide mineralization in the Fossil Downs Station, Brooking Springs Station and Horse Spring Range areas. The close association of the saddle dolomite and mineralization suggests that the pore fluids of these phases were similar.

With sulphate reduction, either calcite or dolomite may be precipitated, depending upon the relevant supply of Ca^{2+} and Mg^{2+} . Alternation in growth of the saddle dolomite and calcite cements is a common feature of the saddle dolomites of the Lennard Shelf. Microprobe analyses indicate zinc occurs within the saddle dolomite and bright-luminescent calcite cements. Anderson and Garven (1987) predict that if aqueous metals are present at or near the site of sulphate reduction, dolomite dissolution and sulphide precipitation occurs. The occurrence of aqueous zinc at the site of the precipitation of dolomite and calcite suggests sulphate reduction may have been intermittent. Sulphate reduction requires a reductant, usually organic matter. But if organic matter was present, a negative $\delta^{13}\text{C}$ value in the carbonates that precipitated at that time would be expected. The saddle dolomite does not seem to have negative $\delta^{13}\text{C}$

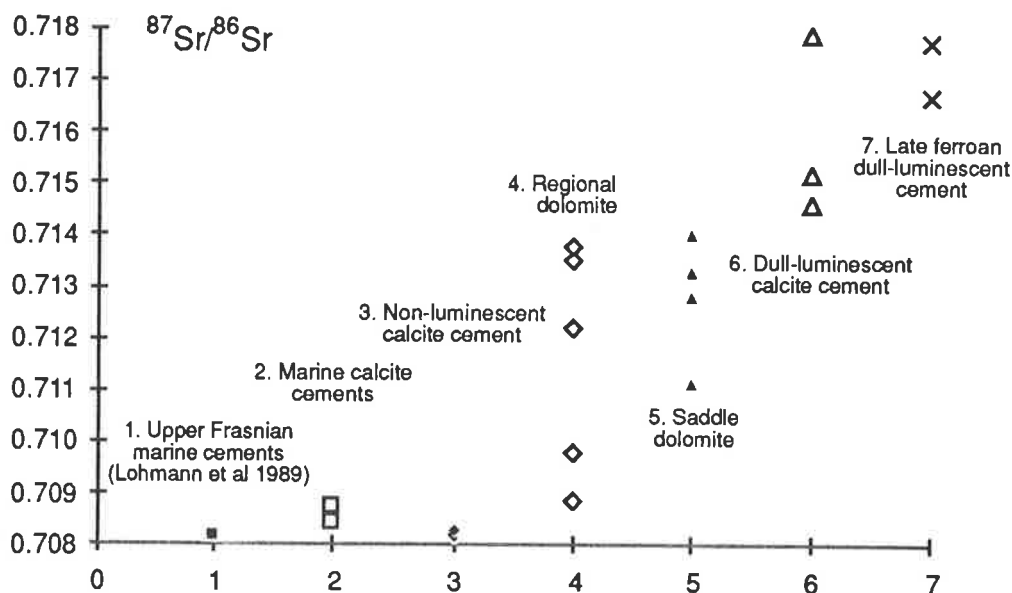
values and therefore, sulphate reduction may not have occurred near the site of mineralization.

Oxygen and carbon isotope values for saddle dolomites and regional dolomites display an overlap (Figure 18). The carbon isotope values for both dolomite types are relatively uniform. However the average $\delta^{18}\text{O}$ composition for the saddle dolomites is 3‰ lighter than the average $\delta^{18}\text{O}$ composition for the regional dolomite. The lower $\delta^{18}\text{O}$ values of the saddle dolomite compared to the regional dolomite are due to formation at elevated temperatures (confirmed by fluid inclusion homogenization temperatures in the saddle dolomite). The overlap in oxygen isotope values for the dolomites is probably due to recrystallization of the regional dolomite by the mineralizing fluids.

Friedman and O'Neil's (1977) fractionation curve was used to determine the original isotopic composition of the saddle dolomite fluids. Oxygen isotope values from saddle dolomite samples were used with the homogenization temperatures from a single saddle dolomite sample. An equilibrium value for $\Delta^{18}\text{O}$ ($\delta^{18}\text{O}$ dolomite - $\delta^{18}\text{O}$ calcite) of 3‰ (Land 1980) was used. The $\delta^{18}\text{O}$ water (SMOW) values for the saddle dolomites were 0 to 5‰ heavier than the corresponding value calculated for Devonian seawater. This difference in isotopic composition is consistent with the evolution of basin-derived pore fluids.

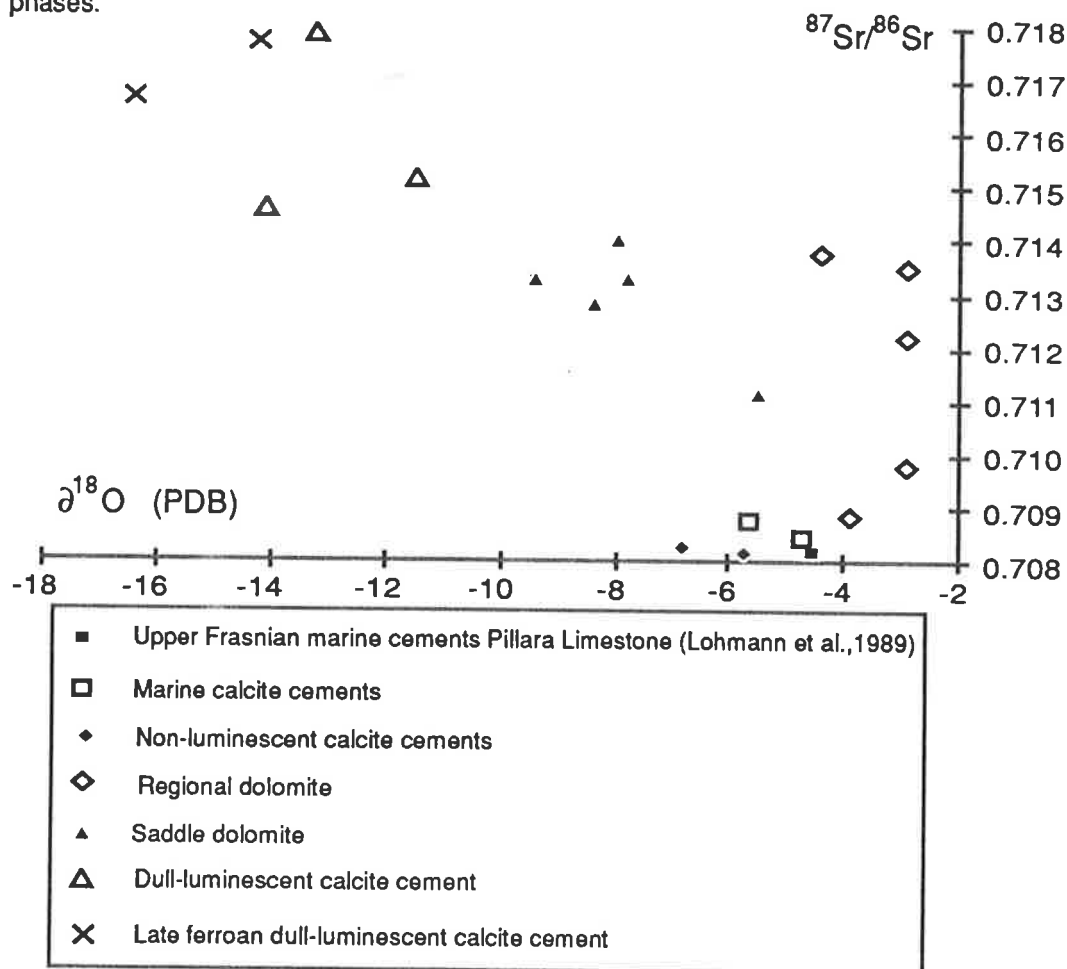
The strontium isotope values of the saddle dolomite overlap with the more radiogenic regional dolomite values (Figure 21). The distribution of the saddle dolomite is consistent with their formation by processes closely linked to the mineralization event. Dissolution of the regional dolomite, and precipitation nearby as saddle dolomite, was the most likely process. In this process, the component that dissolved (the regional dolomite), as well as the fluids that caused the dissolution (basinal brines), would control the strontium isotope composition of the saddle dolomite. The saddle dolomite displays lighter oxygen compared to the regional dolomite reflecting the higher precipitation

Figure 21.— Strontium isotopic composition of calcite and dolomite diagenetic phases.



temperature of the saddle dolomite. While the strontium values of the saddle dolomite are relatively uniform, the regional dolomite have a range of strontium values (Figure 22).

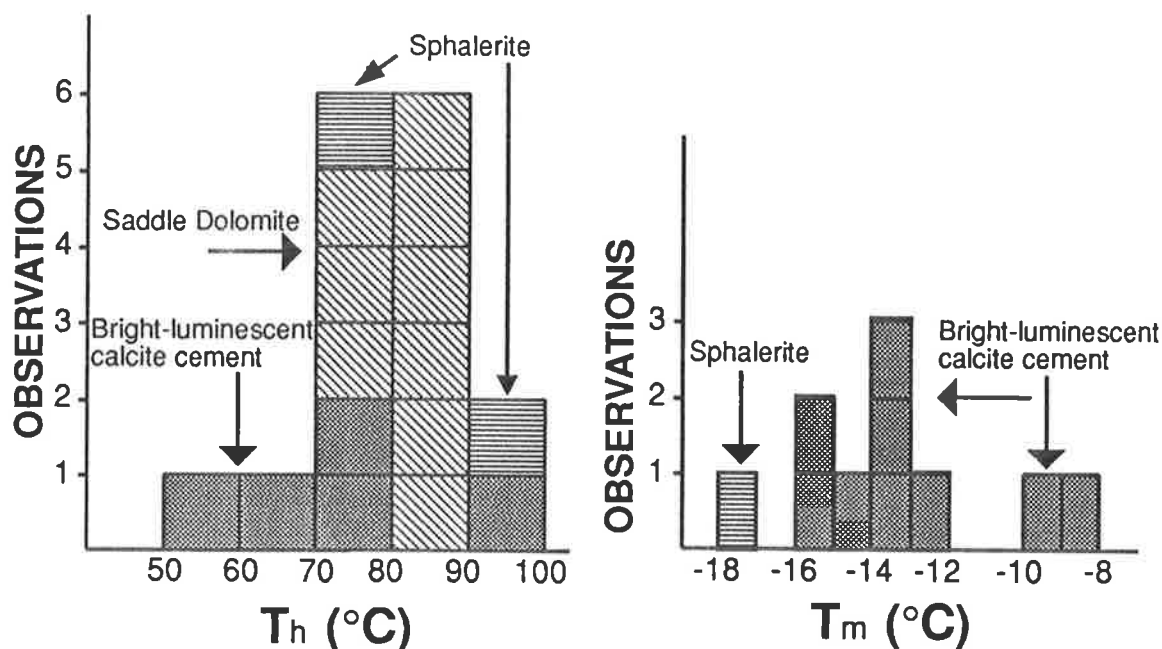
Figure 22.— Strontium and oxygen isotopic compositions of calcite and dolomite diagenetic phases.



- Upper Frasnian marine cements Pillara Limestone (Lohmann et al., 1989)
- Marine calcite cements
- ◆ Non-luminescent calcite cements
- ◇ Regional dolomite
- ▲ Saddle dolomite
- △ Dull-luminescent calcite cement
- × Late ferroan dull-luminescent calcite cement

The homogenization temperatures of fluid inclusions in the saddle dolomite (75.8 to 89.1°C) are similar to those in sphalerite inclusions (73.7 and 90.9°C) (Figure 23). These homogenization temperatures for the saddle dolomite and sphalerite are within the range of those for sphalerite from the Blendevalde deposit (70 and 100°C; Lambert and Etminan 1987).

Figure 23.— Fluid inclusion homogenization (T_h) and last melt (T_m) temperatures from sphalerite and diagenetic phases that are closely associated with sulphide mineralization.



In the Wagon Pass and Narlarla deposits, the saddle dolomite generation does not occur. An inclusion-rich calcite cement directly overgrew the sulphides and may represent a saddle dolomite equivalent for these deposits. Although this inclusion-rich cement displays a mottled luminescence (suggesting that it has been recrystallized) the cement exhibits variable inclusion density that may reflect the preservation of original growth zonation (Figures 17E and 17G).

Mineralization.

The transport and precipitation processes of the base metals and sulphur in MVT deposits remains a problem. The two main models used to explain the transport and precipitation problem are - metals and sulphur transported together (Barton 1967; Barnes 1983; and Sverjensky 1981) and metals and sulphur transported separately and deposited when they mix (Anderson 1983). In the case of the hypothesis that metals and sulphur were transported together, there are a number of alternative models proposed by which this process may occur. However, no definite conclusions regarding the transport and precipitation mechanisms of the MVT mineralization on the Lennard Shelf can be drawn as a result of this study. Nevertheless, some important revelations, as to the nature of the fluids that precede and succeed mineralization, can be made.

Temporally, the sulphide mineralization was essentially the same across the Lennard Shelf, although deposition probably occurred in pulses. Sulphide mineralization occurred early in the burial diagenetic history of the Devonian reef complexes. The occurrence of mineralization within latest Devonian shale (microfossil evidence from the Wagon Pass deposit), provides a maximum age for the mineralization event. The sulphides precipitated within the bright-luminescent calcite cement generation (that predates the Late Carboniferous unconformity) and is considered to be of Late Devonian/Early Carboniferous burial origin.

During the Early Carboniferous a north-west prograding delta resulted in the rapid deposition of up to 2500 metres of sediment in the Fitzroy Trough (Brown *et al.* 1984). Middleton (1984) noted a major period of movement of the Pinnacle Fault to have occurred during the Middle Carboniferous. Middleton suggested the movement of the Pinnacle Fault at that time was probably a result of increasing sediment load in the Fitzroy Trough. Compaction, overpressuring and episodic release of warm basinal brines may have been

produced by the rapid sedimentation in the Fitzroy Trough during the Early Carboniferous. The interaction of the basinal pore fluids with the trough sediments was the probable source of the zinc and lead of the MVT deposits on the Lennard Shelf.

The detection of zinc (by microprobe analysis) within the carbonate cements closely associated with the occurrence of sulphides, indicates that the metal concentrations of the pore fluids peaked during the mineralization event. The occurrence of relatively high concentrations of metals corresponds to high temperatures (at least 75 to 90°C) and high salinities (20 wt.% NaCl equivalent) in the pore fluids.

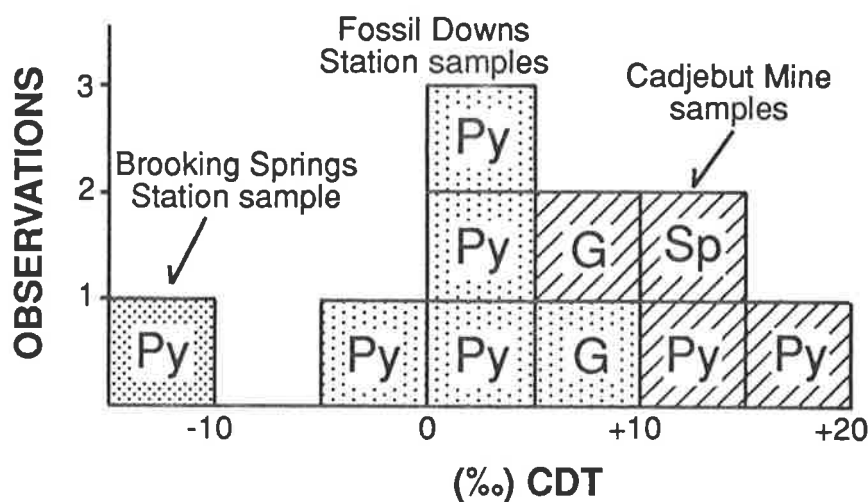
The Cadjebut deposit occurs beside the northern margin of the Fitzroy Trough. Warm, metalliferous, basinal brines, expelled from the Fitzroy Trough during a fluid expulsion event, were probably directed up the Pinnacle Fault and associated Cadjebut Fault onto the Lennard Shelf. However mineralization in other areas of the Lennard Shelf *lies* up to 100 kilometres from the Fitzroy Trough. A number of possible conduits existed to transport basinal brines from the Fitzroy Trough to deposition sites on the Lennard Shelf. These conduits include Devonian conglomerates and sandstone, Ordovician sediments, faults, and the basement contact. It is possible the fluids used more than one of these conduits. The Devonian conglomerates and sandstones interfinger with the marginal-slope facies and were possibly the most important aquifer in the Fossil Downs and Brooking Springs Station areas.

In the Fossil Downs and Brooking Springs Stations areas, the mineralization is best developed in marginal-slope facies along faults, fractures, and in dolomites. The mineralization occurs in lithologies that had available porosity at the time of the mineralizing event. But the mineralizing fluids also created porosity through brecciation and it is in this porosity that most of the sulphide mineralization occurs. Although the platform facies in the Fossil Downs atoll is not strongly mineralized, the mineralizing fluids were able

to penetrate lithologies that were essentially tight (Figure 15F). Hydraulic fracturing appears to have been the dominant process that produced the brecciation observed in the mineralized carbonates.

Sulphur isotope data from the Fossil Downs and Brooking Springs Station areas and Cadjebut Mine display distinct isotopic compositions (Figure 24). The sulphides from the Cadjebut Mine have relatively high $\delta^{34}\text{S}$ values and suggest that the sulphur was derived from seawater or evaporites.

Figure 24.— Sulphur isotope composition of sulphide mineralization from Cadjebut Mine and the Fossil Downs Prospect (Py=pyrite, Sp=sphalerite, G= Galena).



The Fossil Downs Station sulphides have $\delta^{34}\text{S}$ values close to 0‰ and the one sulphide sample from Brooking Springs Station has a $\delta^{34}\text{S}$ value of -12‰. The relatively low sulphur isotope compositions of the Fossil Downs Station and Brooking Springs Station areas suggest that the sulphur may have had a sedimentary source. Although based on a small number of samples, the distinct sulphur isotopic compositions between the Cadjebut Mine and the Fossil Downs area indicate that these areas had a different source of sulphur. If the reduced sulphur was transported with the metalliferous brines, it would be expected that the sulphur isotope values would reflect more homogeneous fluids. Barite displays a close association with sulphide mineralization and in some cases appears to have been a nucleation site for the sulphides. This

occurrence of barite and the detection of zinc within calcite immediately preceding sulphide precipitation, suggest reduced sulphur was not always freely available in the carbonates. An abundant sulphur source may be critical to large scale mineralization.

CONCLUSIONS

The cement stratigraphy described in this study is consistent with the results of previous diagenetic studies (Figure 25) by Kerans (1985) and Wallace *et al.* (in press). After marine cementation the Late Devonian/Early Carboniferous burial processes were the most important porosity occluding events in the Fossil Downs Station area (Figure 26). The first burial cement generation was the non-luminescent calcite cement. This cement generation is the dominant porosity occluding cement generation, after marine cementation, in the platform lithologies in the Geikie Gorge, Fossil Downs and Pillara Range areas. However, the non-luminescent calcite is not well-developed in the northern Oscar Range area. Connate Devonian seawater and, to a lesser extent, connate meteoric water, probably provided the pore fluids from which the non-luminescent calcite precipitated. Conglomerates that interfingered with the marginal-slope facies may have provided migration paths for connate Devonian seawater and meteoric fluids to flow through the platform lithologies.

Regional dolomitization, from basinal brines, occurred after non-luminescent calcite cementation. The regional dolomite occurs across the Lennard Shelf, but it is generally not extensive. Where the lithologies have been totally dolomitized secondary porosity is sometimes developed. As with the non-luminescent calcite cement, the regional dolomite distribution was controlled by the porosity and permeability of the lithologies and also the flow paths of the dolomitizing fluids.

Following dolomitization, warmer and more saline basinal brines were driven from the Fitzroy Trough by sediment compaction. Bright-luminescent calcite cements precipitated. The banded luminescent nature of this cement probably reflects the episodic nature of the expulsion of basinal brines. MVT mineralization occurs within the bright-luminescent calcite cement generation.

DIAGENETIC ENVIRONMENT		Kerans (1985)	Hurley (1986) and Hurley and Lohmann (1989)	Wallace (1987) and Wallace <i>et al.</i> (in press)	This Study
MARINE-BURIAL	DEVONIAN	Scalenohedral and bladed (Non-luminescent)	Scalenohedral calcite	Scalenohedral calcite	Scalenohedral calcite
		(Frasnian carbonates) Non-ferroan blocky calcite (Non-luminescent to banded-luminescent)	Non-ferroan blocky calcite (Banded bright luminescent)	Non-luminescent calcite	Non-luminescent calcite
BURIAL	? CARBONIFEROUS	Dolomite	Dolomite	Bright-luminescent calcite	Regional dolomite
		(Famennian carbonates) Ferroan blocky spar (Homogenous luminescence)	Pressure solution Non-ferroan blocky calcite (Non-luminescent)	Dolomite	Saddle dolomite
UPLIFT-RELATED	PERMIAN	Non-ferroan poikilitic calcite (Irregular, largely non-luminescent)	Non-ferroan blocky calcite (Moderate luminescent)	Dull-luminescent calcite	Bright-luminescent calcite
			Dedolomite, poikilitic calcite		Dull-luminescent calcite
BURIAL	PERMIAN		Sinkholes Calcrete crusts Vertical solution tubes	Banded-luminescent calcite	Late bright-luminescent calcite
			Pressure solution Non-ferroan blocky calcite (Bright or moderate luminescent)	Karstification	Karstification
			Ferroan blocky calcite (Dull or non-luminescent)	Late dull-luminescent calcite	Late (ferroan) dull-luminescent calcite
				Pressure solution	

Figure 25. Comparison of diagenetic studies of the Devonian reef complexes of the Lennard Shelf.

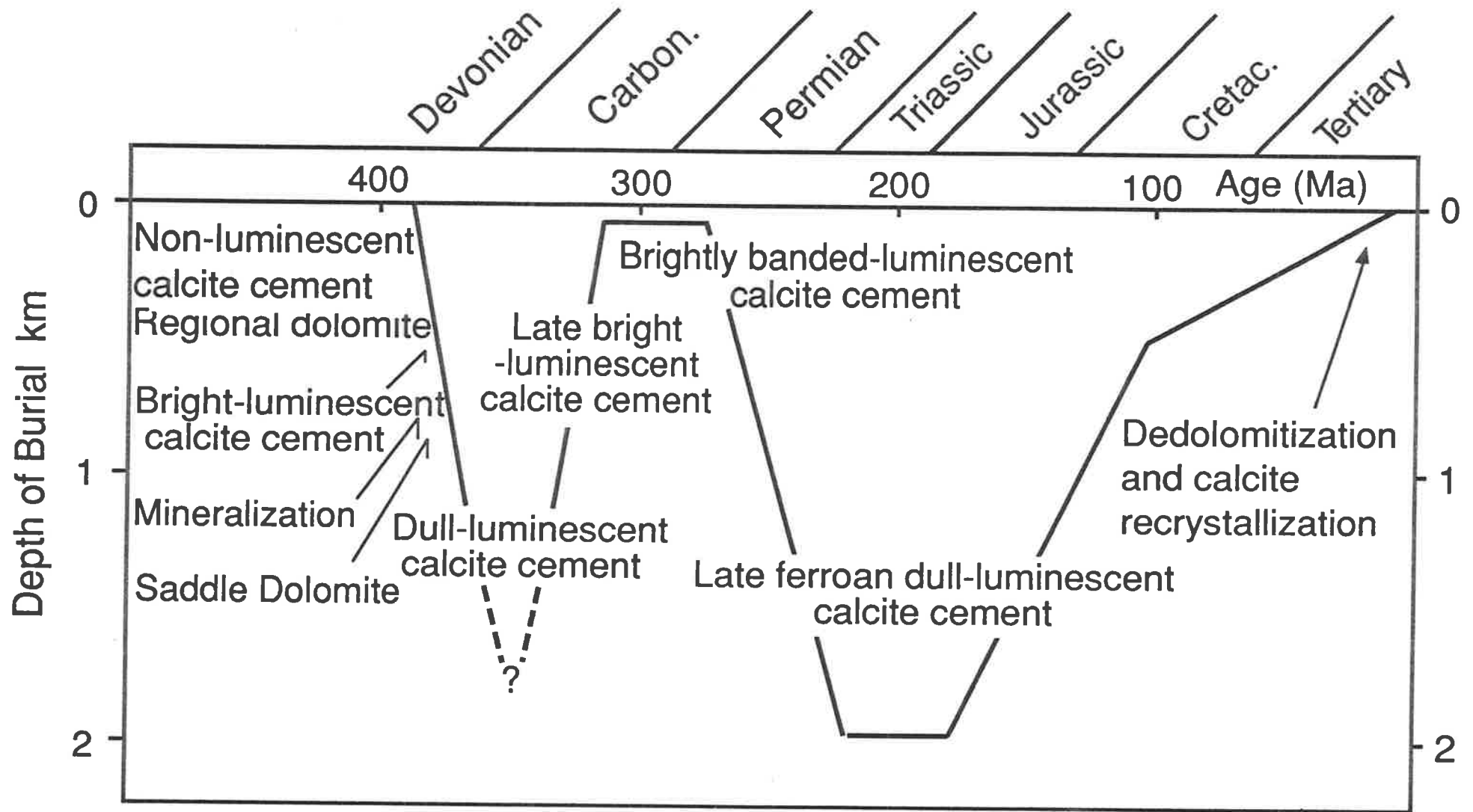


Figure 26.— Burial history of the Lennard Shelf reef complexes, illustrating the timing of the diagenetic phases (modified from Arne et al. 1989). 56

Sulphides precipitated during the same event across the Lennard Shelf. Saddle dolomite precipitation is closely associated with the mineralization event. There was alternation in the precipitation between the later stages of the regional dolomite, sulphides, saddle dolomite, and the early part of the bright-luminescent calcite cement. Although the mineralization filled primary pores in limestone and secondary pores in dolomitized lithologies, the mineralization event produced much of its own porosity by hydraulic fracturing.

The dull-luminescent cement contains radiogenic strontium which reflects the continued derivation of pore fluids from the basin sediments during the precipitation of this cement generation. The dull-luminescent calcite cement occluded most of the remaining porosity in limestones of the Fossil Downs and Geikie Gorge areas. In contrast, some limestones of the northern Oscar Range area still contained primary porosity by the end of dull-luminescent cementation. This difference in porosity occlusion between the two areas during Late Devonian/Early Carboniferous burial of the reef complexes indicates the influence of the basinal brines that were expelled into the carbonates in the Fossil Downs/Geikie Gorge area.

Following burial in the Late Devonian/Early Carboniferous, the reef complexes were uplifted and karstified at the Late Carboniferous unconformity. The uplift event was recorded by the precipitation of the late bright-luminescent calcite cement. This cement generation is of little importance in the porosity occlusion of the carbonates but reflects the more oxidizing conditions of the pore fluids as a result of the erosion event. During the Late Carboniferous karsting event, deep sink holes were produced in the limestones. The meteoric fluids exploited the sulphide mineralization and some sink holes have developed along pre-existing mineralized fractures. In some pores, the late brightly banded-luminescent calcite cement precipitated on iron oxide sediments, illustrating the oxidizing conditions during karstification.


Permian/Late Triassic burial of the reef complexes resulted in the precipitation of the late ferroan dull-luminescent calcite cement. The late ferroan dull-luminescent cement was precipitated from warm, fresh pore fluids. Burial depth of up to 3 km is inferred from fluid inclusion homogenization temperatures.

The Late Triassic/Early Jurassic Fitzroy Movement resulted in uplift and erosion, so that the reefs were again exposed and karstified.

- Anderson, G. M., 1975, Precipitation of Mississippi Valley-type ores: *Economic Geology*, v. 70, p. 937-942.
- Anderson, G. M., 1978, Basinal brines and MVT ore deposits: Episodes, v. 2, p. 15-19.
- Anderson, G. M., 1983, Some geochemical aspects of sulfide precipitation in carbonate rocks, *in* Kisvarsanyi, G., Grant, S. K., Pratt, W. P., and Koenig, J. W., eds., International Conference on Mississippi Valley-Type Lead-Zinc Deposits, Proceedings volume: Rolla, Missouri, University of Missouri-Rolla, p. 61-76.
- Anderson, G. M. and Garven, G., 1987, Sulfate-sulfide-carbonate associations in Mississippi Valley-type lead-zinc deposits: *Economic Geology*, v. 82, p. 482-488.
- Arne, D. C., Green, P. F., Duddy, I. R., Gleadow, A. J. W., Lambert, I. B. and Lovering, J. F., 1989, Regional thermal history of the Lennard Shelf, Canning Basin, from apatite fission track analysis: Implications for the formation of Pb-Zn ore deposits: *Australian Journal of Earth Sciences*, v. 36, p. 495-513.
- Barnes, H. L., 1983, Ore-depositing reactions in Mississippi Valley-type deposits, *in* Kisvarsanyi, G., Grant, S. K., Pratt, W. P., and Koenig, J. W., eds., International Conference on Mississippi Valley-Type Lead-Zinc Deposits, Proceedings volume: Rolla, Missouri, University of Missouri-Rolla press, p. 77-85.
- Barton, P. B., 1967, Possible role of organic matter in the precipitation of the Mississippi Valley ores: *Economic Geology Monograph* 3, p. 371-378.
- Beales, F. W., 1975, Precipitation mechanisms for Mississippi Valley-type ore deposits: *Economic Geology*, v. 70, p. 943-948.
- Botten, P., 1984, Uranium exploration in the Canning Basin, a case study, *in* Purcell, P. G., ed., The Canning Basin, W. A.: (Proceedings, Geological Society of Australia/ Petroleum Exploration Society of Australia symposium): Perth, Geological Society of Australia, p. 485-502.
- Brown, J. S., 1970, Mississippi Valley-type lead-zinc ores: *Mineral Deposita* v. 5, p. 103-119.

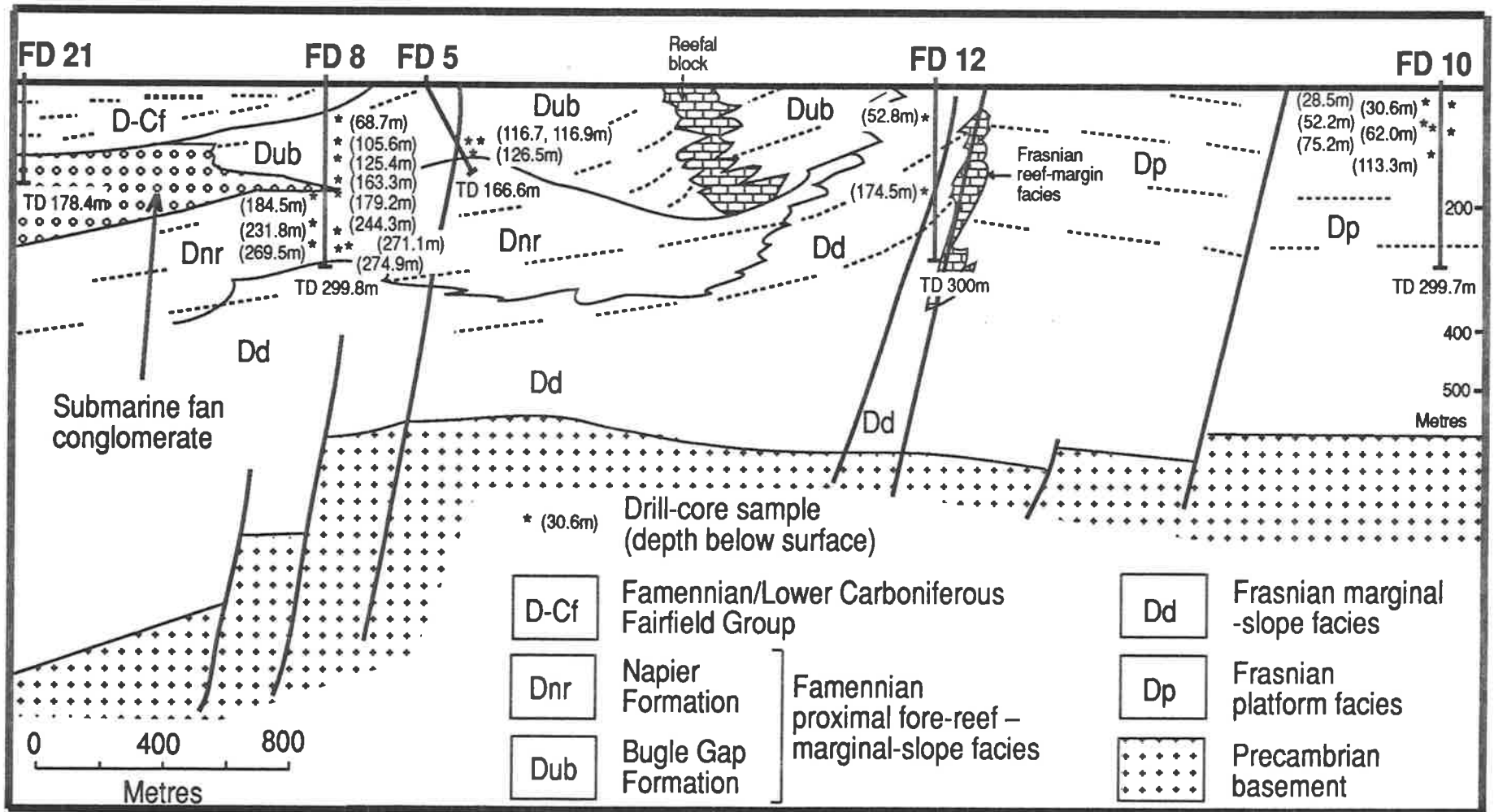
- Brown, S. A., Boserio, I. M., Jackson, K. S. and Spence, K. W., 1984, The Geological Evolution of the Canning Basin — Implications for Petroleum Exploration, *in* Purcell, P. G., ed., The Canning Basin, W. A.: (Proceedings, Geological Society of Australia/ Petroleum Exploration Society of Australia symposium): Perth, Geological Society of Australia, p. 85-96.
- Carpenter, A. B., Trout, M. L. and Pickett, E. E., 1974, Preliminary report on the origin and chemical evolution of the lead- and zinc-rich oil field brines in central Mississippi: *Economic Geology*, v. 69, p. 1191-1206.
- Cathles, L. M. and Smith, A. T., 1983, Thermal constraints on the formation of Mississippi Valley-type lead-zinc deposits and their implications for episodic basin dewatering and deposit genesis: *Economic Geology*, v. 78, p. 983-1002.
- Choquette, P. W. and James, N. P., 1987, Diagenesis #12. Diagenesis in limestones— 3. The deep burial environment: *Geoscience Canada*, v. 14, p. 3-35.
- Coplen, T. B., Kendall, C. and Hopple, J., 1983, Comparison of stable isotope reference samples: *Nature*, v. 302, p. 236-238.
- Craig, H., 1957, Isotopic standards for carbon and oxygen and correction factors for mass-spectrometric analysis of carbon dioxide: *Geochemica et Cosmochimica Acta*, v. 12, p. 133-149.
- Dickson, J. A. D., 1966, Carbonate identification and genesis as revealed by staining: *Journal of Sedimentary Petrology*, v. 36, p. 491-505.
- Etminan, H. and Hoffmann, C. F., 1989, Biomarkers in fluid inclusions: a new tool in constraining source regimes and its implications for the genesis of Mississippi Valley-type deposits: *Geology*, v. 17, p. 19-22.
- Forman, D. J. and Wales, D. W., 1981, Geological evolution of the Canning Basin, Western Australia: Australian Bureau of Mineral Resources Bulletin, v. 210, 91p.
- Frank, J. R., Carpenter, A. B. and Oglesby, T. W., 1982, Cathodoluminescence and composition of calcite cement in the Taum Sauk Limestone (Upper Cambrian), southeast Missouri: *Journal of Sedimentary Petrology*, v. 52, p. 631-638.

- Friedman, I. and O'Neil, J. R., 1977, Compilation of stable isotope fractionation factors of geochemical interest, *in* Fleischer, M., ed., Data of Geochemistry: United States Geological Survey Professional Paper 440K, 12 p.
- Grover, J. R. and Read, J. F., 1983, Paleoaquifer and deep burial related cements defined by regional cathodoluminescence patterns, Middle Ordovician carbonates, Virginia: American Association of Petroleum Geologists, v. 67, p. 1275-1303.
- Hemming, N. G., Meyers, W. J. and Grams, J. C., 1989, Cathodoluminescence in diagenetic calcites: the role of Fe and Mn as deduced from electron probe and spectrophotometric measurements: *Journal of Sedimentary Petrology*, v. 59, p. 404-411.
- Heyl, A. V., 1967, Some aspects of genesis of strataform lead-zinc-barite-fluorite deposits in the United States, *Genesis of Strataform lead-zinc-barite-fluorite deposits: Economic Geology Monograph 3*, p. 20-32.
- Hurley, N. F., 1986, Geology of the Oscar Range Devonian Reef complex, Canning Basin, Western Australia (Unpublished Ph. D. dissertation): Michigan, U.S.A., University of Michigan, 269p.
- Hurley, N. F. and Lohmann, K. C., 1989, Diagenesis of Devonian reefal carbonates in the Oscar Range, Canning Basin, Western Australia: *Journal of Sedimentary Petrology*, v. 59, p. 127-146.
- Kerans, C., 1985, Petrology of Devonian and Carboniferous carbonates of the Canning and Bonaparte Basins, Western Australia: Western Australian Mining and Petroleum Research Institute: Report No. 12, 302p.
- Kerans, C., Hurley, N. F. and Playford, P. E., 1986, Marine diagenesis in Devonian reef complexes of the Canning Basin Western Australia: *in* Schroeder, J. H., and Purser, B. H., eds., Reef Diagenesis: Heidelberg, Springer-Verlag, p. 357-380.
- Lambert, I. B., and Etminan, H., 1987, Biochemistry and origins of sediment-hosted base-metal sulphide deposits, in Bladon, G. M., ed., Yearbook of the Bureau of Mineral Resources: Canberra, Australian Government Publishing Service, p. 89-93.

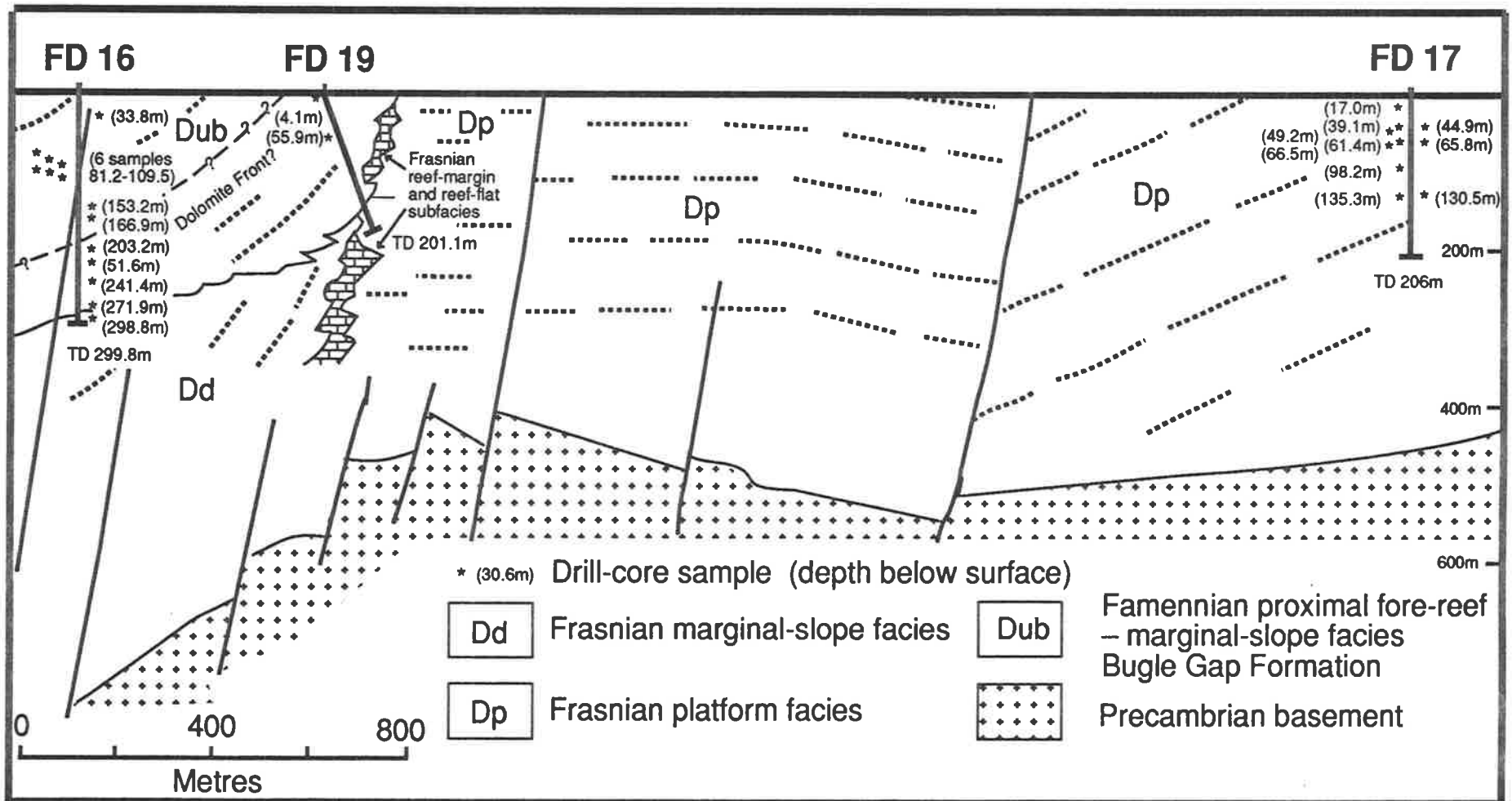
- 
- Land, L. S., 1980, The isotopic and trace element geochemistry of dolomite: the state of the art., *in* Zenger, D.H., Dunham, J. B., and Ethington, R. L., eds., Concepts and Models of Dolomitization: Society of Economic Paleontologists and Mineralogists Special Publication 28, p. 87-110.
- Lohmann, K. C., Carpenter, S. J., Opdyke, B. N., Dunn, P. A., Hurley, N. P., and Halliday, A. N., 1989, Global correlation of $^{87}\text{Sr}/^{86}\text{Sr}$, $\delta^{18}\text{O}$, and $\delta^{13}\text{C}$ values of Late Devonian Marine cements from the Alberta, Dinant, and Canning Basins, in Geological Society of America 1989 Annual Meeting, Abstracts: St. Louis, Missouri.
- Machel, H., 1985, Cathodoluminescence in calcite and dolomite and its chemical interpretation: *Geoscience Canada*, v. 12, p. 139-147.
- Meyers, W. J., 1974, Carbonate cement stratigraphy of the Lake Valley Formation (Mississippian), Sacramento Mountains, New Mexico: *Journal of Sedimentary Petrology*, v. 44, p. 837-861.
- Middleton, M. F., 1984, Seismic geohistory analysis: a case history from the Canning Basin, Western Australia: *Geophysics*, v. 49, p. 333-343.
- Ohle, E. L., 1980, Some considerations in determining the origin of ore deposits of Mississippi Valley-type: *Economic Geology*, v. 75, p. 161-172.
- Ohle, E. L., 1985, Breccias in Mississippi Valley-type deposits: *Economic Geology*, v. 80, p. 1736-1752.
- Playford, G., 1976, Plant microfossils from the Upper Devonian and Lower Carboniferous of the Canning Basin, Western Australia: *Palaeontographica*, Abt. B, v. 158, p. 1-78.
- Playford, P. E., 1980, Devonian "Great Barrier Reef" of Canning Basin, Western Australia: *American Association of Petroleum Geologists Bulletin*, v. 64, p. 814-840.
- Playford, P. E., 1984, Platform-margin and marginal-slope relationships in Devonian reef complexes of the Canning Basin, *in* Purcell, P. G., ed., *The Canning Basin, W. A.: (Proceedings, Geological Society of Australia/ Petroleum Exploration Society of Australia symposium): Perth, Geological Society of Australia*, p. 189-214.
- Playford, P. E., Hurley, N. F., Kerans, C. and Middleton, M. F., 1989, Reefal platform development, Devonian of the Canning Basin, Western Australia, *in* ,eds., *Controls on Carbonate Platform and Basin Development: The Society of Economic Paleontologists and Mineralogists Special Publication 44*, p. 187-202.

- Playford, P. E. and Lowry, D. C., 1966, Devonian reef complexes of the Canning Basin, Western Australia: Western Australia Geological Survey Bulletin 118, 150 p.
- Potter II, R. W., 1977, Pressure corrections for fluid-inclusion homogenization temperatures based on the volumetric properties of the system NaCl—H₂O: Journal of Research, United States Geological Survey, v. 5, p. 603-607.
- Radke, B. M. and Mathis, R. L., 1980, On the formation and occurrence of saddle dolomite: Journal of Sedimentary Petrology, v. 50, p. 1149-1168.
- Ringrose, C. R., 1984, The geology and genesis of the Narlarla lead-zinc deposit, Napier Range, Western Australia, *in* Purcell, P. G., ed., The Canning Basin, W. A.: (Proceedings, Geological Society of Australia/ Petroleum Exploration Society of Australia symposium): Perth, Geological Society of Australia, p. 455-462.
- Ringrose, C. R., 1989, Studies of selected carbonate-hosted lead-zinc deposits in the Kimberley region: Geological Survey of Western Australia, Report 24, 103 p.
- Roedder, E., 1968, Temperature, salinity, and origin of the ore-forming fluids at Pine Point, Northwest Territories, Canada, from fluid inclusion studies: Economic Geology, v. 63, p. 439-450.
- Roedder, E., 1971, Fluid-inclusion evidence on the environment of formation of mineral deposits of the Southern Appalachian Valley: Economic Geology, v. 66, p. 777-791.
- Roedder, E., 1984, Fluid inclusions. Reviews in Mineralogy, Vol. 12. Mineralogical Society of America : 644 p.
- Sangster, D. F., 1983, Mississippi Valley-type deposits: a geological melange., *in* Kisvarsanyi, G., Grant, S. K., Pratt, W. P., and Koenig, J. W., eds., International Conference on Mississippi Valley-Type Lead-Zinc Deposits, Proceedings volume: Rolla, Missouri, University of Missouri-Rolla press, p. 7-19.
- Sangster, D. F., 1988, Breccia-hosted lead-zinc deposits in carbonate rocks, *in* James, N. P. and Choquette, P. W., eds., Paleokarst: New York, Springer-Verlag, p. 104-116.
- Stueber, A. M., Pushkar, P. and Hetherington, E. A., 1984, A strontium isotopic study of Smackover brines and associated solids, southern Arkansas: Geochemica et Cosmochimica Acta, v. 48, p. 1637-1649.

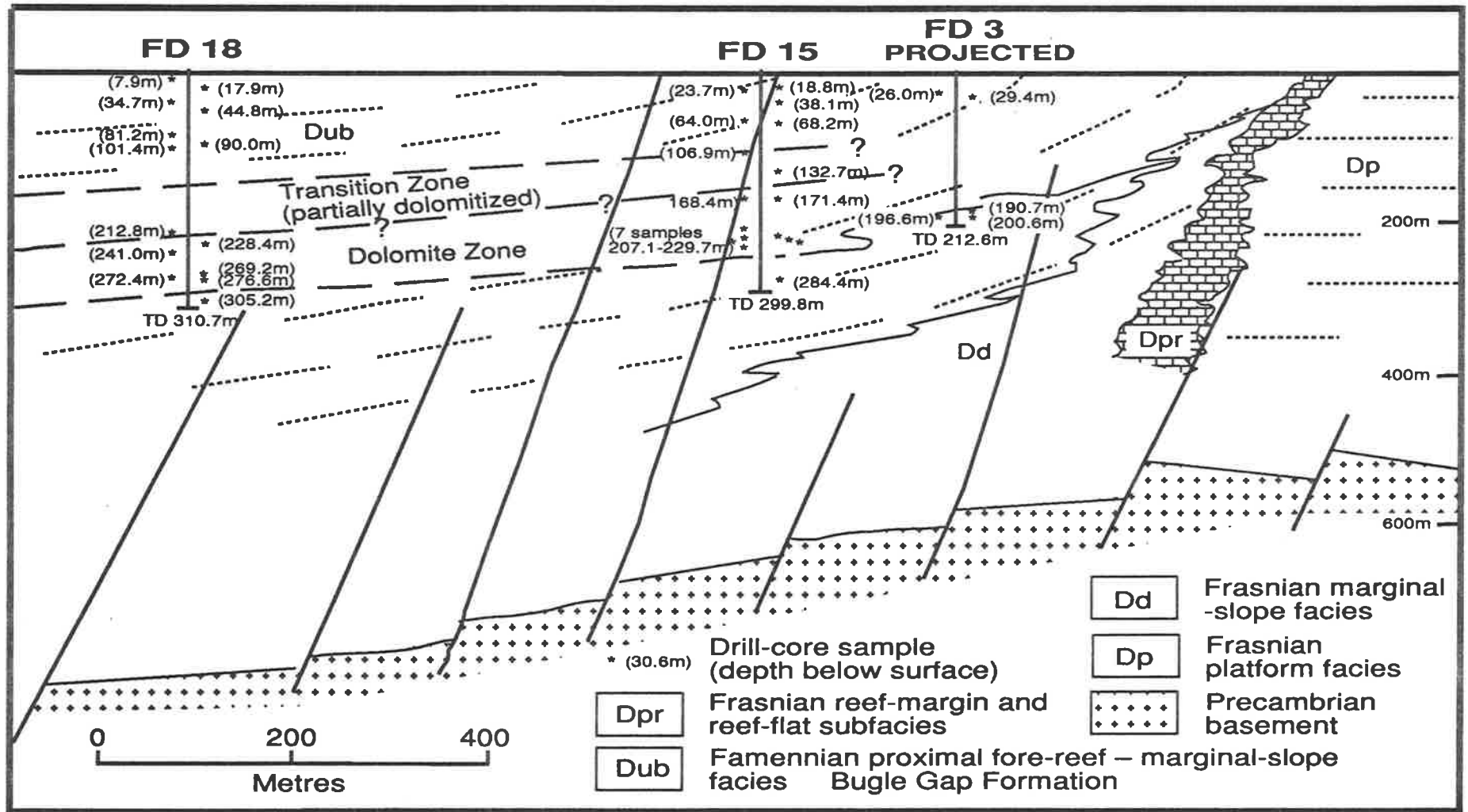
- Sverjensky, D. A., 1981, The origin of a Mississippi Valley-type deposit in the Viburnum Trend, southeast Missouri: *Economic Geology*, v. 76, p. 1848-1872.
- Sverjensky, D. A., 1986, Genesis of Mississippi Valley-type lead-zinc deposits: *Annual Review of Earth and Planetary Sciences*, v. 14, p. 177-199.
- Towner, R. R. and Gibson, D. L., 1983, Geology of the onshore Canning Basin, Western Australia: Australian Bureau of Mineral Resources, Bulletin 215, 51 p.
- Veizer, J., 1989, Strontium isotopes in seawater through time: *Annual Review of Earth and Planetary Sciences.*, v. 17, p. 141-167.
- Wallace, M. W., 1987, Sedimentology and diagenesis of Upper Devonian carbonates, Canning Basin, Western Australia: (Unpublished Ph. D. dissertation), Hobart, Tasmania, University of Tasmania, 184p.
- Wallace, M. W., 1990, Origin of dolomitization in the Devonian carbonates on the Barbwire Terrace, Canning Basin, Western Australia: *Sedimentology*
- Wallace, M. W., Playford, P. E., Kerans, C., and McManus, A. P., in press, Diagenesis in the Upper Devonian reef complexes of the Geikie Gorge region, Canning Basin, Western Australia: *American Association of Petroleum Geologists Bulletin*.
- White, D. L., 1968, Environments of generation of some base metal deposits: *Economic Geology*, v. 63, p. 301-335.
- Yeates, A. N., Gibson, D. L., Towner, R. R. and Crowe, R. W. A., 1984, Regional geology of the onshore Canning Basin, Western Australia, *in* Purcell, P. G., ed., *The Canning Basin, W. A.: (Proceedings, Geological Society of Australia/ Petroleum Exploration Society of Australia symposium)*: Perth, Geological Society of Australia, p. 23-25.



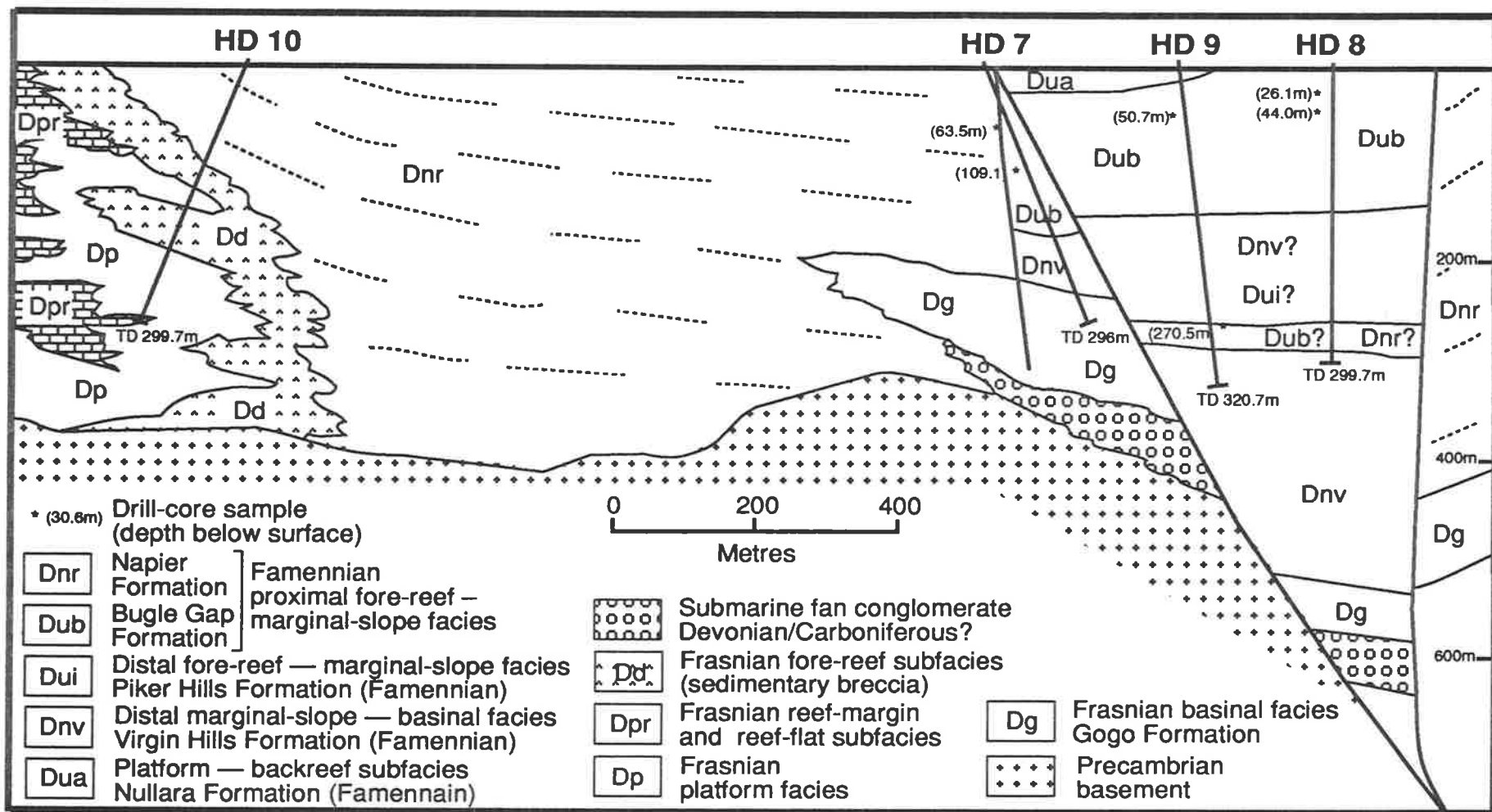
APPENDIX A. Geological cross-section through the Fossil Downs atoll illustrating exploration drill holes, facies and sample locations. (modified from Billiton Australia Ltd. unpublished sections)



APPENDIX B. Geological cross-section through the Geikie Gorge/Brooking Springs atoll illustrating exploration drill holes, facies and sample locations. (modified from Billiton Australia Ltd. unpublished sections)



APPENDIX C. Geological cross-section through the Fossil Downs atoll illustrating exploration drill holes, facies and sample locations. (modified from Billiton Australia Ltd. unpublished sections)



APPENDIX D. Geological cross-section through the Horse Spring Range area illustrating exploration drill holes, facies and sample locations. (modified from Billiton Australia Ltd. unpublished sections)

APPENDIX E

Uni. of Adelaide sample no.	Billiton sample no.	Drill Hole/ Location no.	Depth/Location	Diagenetic phase sampled for isotope analysis	$\delta^{18}\text{O}$ (PDB)	$\delta^{13}\text{C}$ (PDB)	$\delta^{34}\text{S}$ (CDT)	Sr87/Sr86
955001	106701	FH1	Findlay Hill	Regional dolomite with overgrowths	-8.53	2.63		
				Regional dolomite with overgrowths	-4.4	2.43		
955002	106705	FD18	228.4-228.55	Saddle dolomite	-8.43	1.53		0.711133
955003	106706	FD18	240.95-241.50	Regional dolomite	-5.69	2.46		
955004	106707	FD18	272.40-272.50	Regional dolomite	-5.12	1.79		
				Pyrite			-2	
955005	106708	FD18	276.60-276.90	Saddle dolomite	-6.62	1.5		
				Regional dolomite	-5.88	1.78		
955009	106709	FD18	305.15-305.25					
955010	106713	FD18	44.80-44.95	Recrystallized calcite	-5.67	-3.68		
				Pyrite			0	
955011	106718	FD15	18.82-19.00	Marine calcite	-5.72	0.81		
				Recrystallized calcite	-13.79	-3.19		
955012	106719	FD15	38.10-38.20	Bright- and dull-lum. calcite	-6.97	1.04		
				Late brightly banded-lum. calcite	-9.28	-4.04		
955013	106721	FD15	63.95-64.05	Recrystallized calcite	-13.24	-10.07		
				Late brightly banded-lum. calcite	-9.69	-5.35		
955014	106722	FD15	168.40-168.50	Saddle dolomite	-7.79	2.29		0.713294
955015	106723	FD15	106.90-107.00	Bright- and dull-lum. calcite	-11.37	0.97		
				Late bright-lum. calcite	-13.03	-3.29		
955016	106725	FD15	225.86-225.92	Saddle Dolomite	-7.97	1.77		0.714028
				Pyrite			0.9	
955017	106726	FD15	171.40-172.00	Late brightly banded-lum. calcite	-9.5	-2.97		
				Bright- and dull-lum. calcite	-10.94	0.91		
955018	106728	FD15	223.49-223.59	Regional dolomite	-5.29	1.35		
955019	106729	FD15	220.00-220.14	Regional dolomite	-5.86	1.47		
				Pyrite			0.6	
955020	106734	FD8	105.64-105.76	Dull-luminescent calcite	-12.94	1.53		
				Bright- and dull-lum. calcite	-5.71	-0.56		
				Dull-luminescent calcite	-14.13	0.99		0.714621
955021	106735	FD8	68.72-68.84	Dull-luminescent calcite	-13.19	0.67		0.717883
955022	106737	FD8	179.24-179.39					
955023	106740	B1/FD16	Brooking Springs Station	Regional dolomite with overgrowths	-9.62	2.67		
955024	106742	FD8	269.54-269.66	Recrystallized calcite	-10.76	-18.01		
				Pyrite			2.5	
955025	106744	FD16	271.85-272.07	Saddle Dolomite	-9.46	2.42		
				Regional dolomite	-7.68	2.22		

APPENDIX E

Uni. of Adelaide sample no.	Billiton sample no.	Drill Hole/ Location no.	Depth/Location	Diagenetic phase sampled for isotope analysis	$\delta^{18}\text{O}$ (PDB)	$\delta^{13}\text{C}$ (PDB)	$\delta^{34}\text{S}$ (CDT)	Sr87/Sr86
955026	106747	FD16	241.43-241.54	Regional dolomite	-5.96	1.6		
				Regional dolomite	-6.05	1.7		
				Regional dolomite	-5.43	1.65		
955027	106751	FD16	166.88-167.05	Regional dolomite	-8.35	2.05		
955028	106752	FD16	203.15-203.25	Saddle dolomite	-9.4	2.3		0.71328
955029	106754	FD16	153.15-153.20	Pyrite			-12.2	
955030	106760	FD17	66.50-66.62					
955031	106764	FD17	16.98-17.10					
955032	106767	FD10	75.22-75.32					
955033	106768	FD10	113.30-113.44					
955034	106772	FD10	28.50-28.60	Dull-luminescent calcite	-11.47	-0.19		0.715168
955035	106775	HD7	109.10-109.30	Regional dolomite	-3.67	1.55		
955036	106776	HD7	63.54-63.67					
955037	106777	HD9	50.70-50.80	Regionaldolomite	-3.49	1.83		
955038	106779	HD9	270.53-270.67					
955039	106780	HD8	44.02-44.12	Regional dolomite	-2.93	2.17		0.713493
955040	106781	FD8	274.90-275.00	Saddle dolomite	-5.89	1.52		
				Galena			6.5	
955041	106782	FD19	55.90-56.05	Regional dolomite	-7.25	2.52		
955042	106784	FD3	200.60-200.83	Regional dolomite	-6.75	2.45		
955043	106787	FD12	52.79-52.94	Marine calcite	-5.62	2.37		0.708758
955044	106790	FD5	116.86-117.00					
955045	106793	B1A/FD16	Brooking Springs Station	Regional dolomite with overgrowths	-7.59	2.09		
955046	106795	HSR1	Horsespring Range	Regional dolomite	-2.89	1.97		0.712192
955047	106796	C1	Cadjebut Mine	Galena			9.2	
955048	106797	C2	Cadjebut Mine	Pyrite			18.2	
				Sphalerite			13	
955049	106798	C3	Cadjebut Mine	Pyrite			11.9	
955050	106799	85.53	Geikie Gorge	Regional dolomite	-3.72	2.13		
955051	106800	85.112	Geikie Gorge	Regional dolomite	-3.13	1.78		
955052	106801	MW1	Geikie Gorge	Regional dolomite	-6.53	0.63		
				Dull-luminescent calcite	-13.58	-0.03		
955053	106802	F3	Fossil Downs Station	Brachiopod shell (marine calcite)	-4.7	1.77		0.708411
955054	106803	85.33	Geikie Gorge	Non-luminescent calcite	-5.71	1.66		0.708149
955055	106804	F9	Fossil Downs Station	Regional dolomite	-4.72	1.98		
955056	106805	C4	Cadjebut Mine	Recrystallized calcite	-9.48	-7.61		
955057	106807	GK	Glenister Knolls	Regional dolomite	-4.25	1.39		
955058	106811	M GAP	Menyous Gap					
955059	106812	PQ	Pillara Quarry					

APPENDIX E

Uni. of Adelaide sample no.	Billiton sample no.	Drill Hole/ Location no.	Depth/Location	Diagenetic phase sampled for isotope analysis	$\delta^{18}O$ (PDB)	$\delta^{13}C$ (PDB)	$\delta^{34}S$ (CDT)	Sr87/Sr86
955060	106813	DG	Dingo Gap	Late ferroan dull-lum. calcite	-15.62	-4.72		
955061	106814	EB1	Elimberrie bioherm No.1	Regional dolomite	-4.8	1.75		
955062	106815	EB2	Elimberrie bioherm No.2					
955063	106817	OR1	Nth-west Oscar Range					
955064	106819	WG	Windjana Gorge	Regional dolomite	-4.65	2.36		
955065	106820	FH90	Findlay Hill	Regional dolomite with overgrowths	-3.54	1.97		
				Regional dolomite with overgrowths	-7.6	2.58		
955066	106821	HDD1	Horsespring Range	Regional dolomite	-3.09	1.61		
955067	106823	HD7	Horsespring Range	Regional dolomite	-2.38	2.07		
955068	106824	FD1	Fossil Downs	Regional dolomite	-3.57	1.45		
955069	106825	FD2	Fossil Downs	Regional dolomite	-4.42	0.47		
				Late ferroan dull-lum. calcite	-14.23	-2.38		0.717703
955070	106826	FD3	Fossil Downs	Regional dolomite	-3.87	1.7		0.708857
955071	106827	BS1	Brooking Springs Station	Regional dolomite	-3.78	2.58		
955072	106828	BS2	Brooking Springs Station	Regional dolomite	-3.63	2.92		
				Dull-luminescent calcite	-9.9	2.1		
955073	106829	BS3	Brooking Springs Station	Regional dolomite	-3.4	1.91		
955074	106830	BS4	Brooking Springs Station	Regional dolomite	-5.05	0.86		
				Non-luminescent calcite	-6.83	0.9		0.708254
955075	106831	BS5	Brooking Springs Station	Regional dolomite	-2.87	2.08		0.709778
955076	106832	BS6	Brooking Springs Station					
955077	106833	BS7	Brooking Springs Station	Non-luminescent calcite	-6.95	2.01		
955078	106834	BS8	Brooking Springs Station	Regional dolomite	-3.49	2.7		
955079	106836	BS10	Brooking Springs Station	Late ferroan dull-lum. calcite	-16.45	-1.07		0.716663
955080	106837	BS11	Brooking Springs Station	Dull-luminescent calcite	-10.6	0.27		
955081	106838	BS12	Brooking Springs Station	Regional dolomite	-3.51	2.71		
955082	106839	NPS	Nth. Pandanus Springs	Regional dolomite	-2.84	2.32		
955083	106840	GG1	Geikie Gorge	Regional dolomite	-3.07	1.46		
955084	106842	NAR	Narlara	Regional dolomite	-3.95	1.92		
955085	106843	NAP	Napier Downs	Regional dolomite	-3.8	2.32		
955086	106845	NRD 91	25.5-25.8					
955087	106850	NRD 91	24.2					
955088	106851	NRD 96	27.30-27.55					
955089	106852	NRD 96	30.1-30.4					
955090	106854	FD8	231.8	Regional dolomite	-4.42	1.79		0.713755
955091	106855	FD8	271.1	Saddle dolomite	-5.48	1.11		0.711133
955092	106856	FD3	26	Saddle dolomite	-5.53	1.49		
955093	106857	FD3	29.4	Regional dolomite	-5.22	1.12		
955094	106858	NWG	No Way Gossan	Synsedimentary dolomite	-0.5	0.23		